

FIPS 204-Compatible Threshold ML-DSA via Shamir Nonce DKG

Leo Kao 

Codebat Technologies Inc., Taipei, Taiwan

Abstract. We present the first threshold ML-DSA (FIPS 204) scheme achieving *statistical share privacy (no computational assumptions)* with arbitrary thresholds while producing standard 3.3KB signatures (ML-DSA-65, NIST Level 3) verifiable by unmodified implementations. Our primary technique is *Shamir nonce DKG*: parties jointly generate the signing nonce via a distributed key generation protocol, so that both the nonce and the long-term secret are degree- $(T-1)$ Shamir sharings. This achieves *statistical nonce share privacy (no computational assumptions)*: the honest party’s nonce share has conditional min-entropy exceeding $5\times$ the secret key entropy for $|S| \leq 17$ (tightest case: $5.02\times$ at $|S| = 17$; *statistical* here means a min-entropy bound requiring no computational assumptions, not closeness to uniform in statistical distance—the bounded nonce range makes $SD \approx 0.9926$ from uniform inevitable). Key privacy of the aggregated signature—whether σ reveals the signing key beyond the public key—follows under the same assumption as single-signer ML-DSA, which remains an open problem in the broader literature. In coordinator-based profiles (P1, P3+), this eliminates the two-honest requirement for nonce share privacy ($|S| \geq T$ suffices); in the fully distributed profile (P2), $|S \setminus C| \geq 2$ is required for commitment and r0-check mask-hiding (nonce share privacy itself holds at $|S| \geq T$ in P2 as well). As a secondary technique, we introduce pairwise-canceling masks ($|S \setminus C| \geq 2$) for commitment and r0-check values, addressing the three challenges unique to lattice-based threshold signing: the $\|\mathbf{z}\|_\infty$ rejection sampling check, secure evaluation of the r0-check without leaking cs_2 , and EUF-CMA security under the resulting Irwin-Hall nonce distribution.

We instantiate these techniques in three deployment profiles with complete UC proofs. Profile P1 uses a TEE coordinator (3 online rounds plus 1 offline preprocessing round, 5.8 ms for 3-of-5). Profile P2 eliminates hardware trust via MPC (5 rounds, 22ms for small thresholds). Profile P3+ uses lightweight 2PC with semi-asynchronous signing (2 logical rounds, 22ms), where signers precompute nonces offline and respond within a time window. Our Rust implementation scales from 2-of-3 to 32-of-45 thresholds with sub-100ms latency (P1 and P3+) and success rates of $\approx 21\text{--}45\%$, comparable to single-signer ML-DSA. A direct shift-invariance analysis (Corollary 8) shows the per-session EUF-CMA security loss from the Irwin-Hall nonce distribution is < 0.007 bits for $|S| \leq 17$ and < 0.013 bits for $|S| \leq 33$; over q_s signing sessions the total loss is $< 0.013 \cdot q_s$ bits (Corollary 1), eliminating the scalability gap found in prior work.

Keywords: threshold signatures · ML-DSA · post-quantum cryptography · lattice-based cryptography · FIPS 204

1 Introduction

The imminent arrival of cryptographically relevant quantum computers poses an existential threat to currently deployed public-key cryptography. In response, the National Institute

E-mail: leo@codebat.ai (Leo Kao)

of Standards and Technology (NIST) has completed a multi-year standardization process, culminating in the release of FIPS 204 [Nat24b], which specifies ML-DSA (Module-Lattice-Based Digital Signature Algorithm) as the primary post-quantum signature standard. As organizations worldwide begin transitioning to ML-DSA, there is an urgent need for threshold variants that enable distributed signing while maintaining compatibility with the standard.

1.1 Motivation: The Threshold Gap

Threshold signatures allow a group of N parties to collectively sign messages such that any subset of T or more parties can produce a valid signature, while any coalition of fewer than T parties learns nothing about the secret key. This primitive is essential for protecting keys by distributing signing authority across multiple servers, enforcing multi-party authorization in financial systems, and building robust PKI infrastructure through distributed certificate authorities.

For classical ECDSA and Schnorr signatures, efficient threshold protocols have been extensively studied and deployed [GG18, CGG⁺20, Lin21, KG21]. More recently, Lyu et al. [LLZD25] achieved two-round threshold ECDSA in the threshold-optimal multi-party setting. However, the lattice-based structure of ML-DSA presents new challenges. The core difficulty lies in the *Fiat-Shamir with Aborts* paradigm: signatures are only valid when the response vector $\mathbf{z} = \mathbf{y} + c\mathbf{s}_1$ satisfies $\|\mathbf{z}\|_\infty < \gamma_1 - \beta$, where \mathbf{y} is a masking vector, c is a sparse challenge, and \mathbf{s}_1 is the secret key. This rejection sampling step complicates the threshold setting.

The State of Affairs. Current approaches to threshold ML-DSA can be categorized as follows:

1. **Short-coefficient secret sharing** [dPN25]: Uses carefully constructed linear secret sharing schemes (LSSS) where reconstruction coefficients remain small. This approach produces standard-size signatures and has been demonstrated for $T \leq 8$. Two separate arguments constrain scaling: (a) the Ball-Çakan-Malkin bound [BÇMR21] shows that $\{0, 1\}$ -LSSS for threshold T requires share size $\Omega(T \log T)$, a communication complexity lower bound; (b) for ML-DSA specifically, the reconstruction coefficients of dPN25’s construction are binomial coefficients $\binom{T}{k}$, which exceed $q = 8,380,417$ when $T \geq 26$ (since $\binom{25}{12} = 5,200,300 < q$ but $\binom{26}{13} = 10,400,600 > q$; see Corollary 9), providing a tighter practical ceiling for this specific approach.
2. **Noise flooding** [BKP13]: Masks the large Lagrange coefficients with overwhelming statistical noise. This works for arbitrary thresholds but produces signatures approximately $5\times$ larger than standard ML-DSA, breaking FIPS 204 compatibility.
3. **Specialized constructions** [BKL⁺25]: Ringtail and similar schemes modify the underlying signature algorithm to be threshold-friendly, achieving good efficiency but producing signatures incompatible with the FIPS 204 standard.

This leaves a gap: for $T \in [9, 32]$, there is no known scheme that simultaneously achieves standard signature size, practical success rates, and FIPS 204 compatibility. This range is precisely where many real-world applications fall (organizations typically require 16-of-32 or similar thresholds for robust multi-party control).

1.2 Our Contribution

We present **Masked Threshold ML-DSA**, the first threshold signature scheme for ML-DSA that achieves *statistical share privacy (no computational assumptions)* with arbitrary

thresholds $T \leq N$ while producing standard-size signatures (≈ 3.3 KB for ML-DSA-65) syntactically identical in format to single-signer ML-DSA. Unlike prior pairwise-mask schemes that require a two-honest assumption ($|S| \geq T + 1$), our protocol achieves *nonce share privacy* with signing sets of size $|S| \geq T$ (the minimum required by Shamir’s (T, N) threshold property for reconstruction) in coordinator-based profiles (P1, P3+), where individual masked commitments \mathbf{W}_i are sent only to the coordinator rather than broadcast (Remark 11); commitment and r0-check mask hiding retains $|S \setminus C| \geq 2$ (Lemma 2), which applies to P2’s broadcast model. This addresses the threshold gap for $T \in [9, 32]$ while remaining practical for configurations such as (3, 5), (11, 15), and (16, 21).

The scheme achieves practical success rates overlapping with single-signer ML-DSA (theoretical single-signer baseline ≈ 20 – 25% ; observed threshold range ≈ 21 – 45% (see Table 5); the higher end is due to the Irwin-Hall distribution’s greater concentration near zero, placing more nonces within the $\|\mathbf{z}\|_\infty < \gamma_1 - \beta$ acceptance region relative to the uniform single-signer nonce) and is fully verifier-compatible with FIPS 204. The aggregated nonce follows an Irwin-Hall distribution rather than uniform, introducing a quantifiable security cost. We provide two analyses:

Conservative bound (Raccoon-style Rényi, Theorem 4): The per-session multiplicative advantage blowup is $\sqrt{R_2^{\text{vec}}} \approx 2^{2.7}$ for $|S| \leq 17$, equivalent to an additive ≈ 2.7 bits of per-session security loss in bits (the advantage bound blows up by a factor $(R_2^{\text{vec}})^{q_s/2}$, which corresponds to a linear $q_s \times 2.7$ bit loss when expressed in bits). This bound becomes vacuous for $q_s \geq 36$ queries and should not be used for concrete security estimates. At $|S| = 33$, the per-session Rényi blowup satisfies $\log_2 \sqrt{R_2^{\text{vec}}} \approx 37.5$ bits; starting from the 96-bit post-Cauchy–Schwarz proof baseline (half the 192-bit ML-DSA-65 security parameter, arising from the Rényi-to-probability conversion), the provable security bound drops to ≈ 58 bits after a *single* signing session and is formally vacuous at $q_s = 3$ ($96 - 3 \times 38 < 0$). This is not a weakness of the scheme itself, but a fundamental limitation of the Raccoon-style bounding technique: the per-session Rényi divergence scales as $|S|^4$, making the proof unable to certify any security level for practical signing volumes at large T . This failure directly motivates the direct shift-invariance analysis introduced below.

Direct shift-invariance bound (Corollary 8): Using the Irwin-Hall distribution’s shift-invariance property, the per-session EUF-CMA loss is < 0.007 bits for $|S| \leq 17$ and < 0.013 bits for $|S| \leq 33$. Over q_s sessions the total loss is $< 0.013 \cdot q_s$ bits (additive), remaining non-vacuous for any polynomial q_s and bounded below 1 bit per session for all $|S| \leq 2584$. This bound is $\approx 440\times$ tighter than the conservative bound and is the one used throughout this paper for security claims.

Our approach is based on two techniques. The primary technique is *Shamir nonce DKG*: parties jointly generate the signing nonce via a distributed key generation protocol, producing a degree- $(T-1)$ Shamir sharing of \mathbf{y} that matches the structure of the long-term secret \mathbf{s}_1 . Each party then computes $\mathbf{z}_i = \mathbf{y}_i + c \cdot \mathbf{s}_{1,i}$ without applying the Lagrange coefficient, and the combiner reconstructs $\mathbf{z} = \sum_i \lambda_i \mathbf{z}_i = \mathbf{y} + c\mathbf{s}_1$. Because the adversary observes only $T - 1$ evaluations of the honest party’s degree- $(T - 1)$ polynomial, the remaining degree of freedom provides an approximate one-time pad: the honest party’s nonce share \mathbf{y}_h has conditional min-entropy exceeding $5\times$ the secret key entropy (for $|S| \leq 17$), requiring no computational assumptions (Theorem 3; **proved**).

Key privacy given the public signature is a distinct, open question: it is conjectured to hold computationally under the same Module-LWE assumption that secures ML-DSA itself, but a formal reduction from key privacy to Module-LWE remains unavailable for FIPS 204 ML-DSA specifically (with its HighBits/hint-vector structure), unresolved even in the single-signer FIPS 204 setting (**open problem**).

The secondary technique is *pairwise-canceling masks*, adapted from ECDSA [CGG+20] to the lattice setting. These masks are used for the commitment values \mathbf{W}_i and the r0-check shares \mathbf{V}_i (which contain $\lambda_i \cdot c \cdot \mathbf{s}_{2,i}$), hiding individual contributions while preserving

correctness in the sum. Unlike ECDSA, ML-DSA presents additional challenges: the r0-check leaks cs_2 which enables key recovery, and the Irwin-Hall nonce distribution must preserve EUF-CMA security. We address both with complete UC proofs.

Performance. Our Rust implementation achieves practical signing times: 5.8ms (P1-TEE), 21.5ms (P2-MPC), 22.1ms (P3+-Async) for (3,5)-threshold on commodity hardware (per valid signature, 3–4 expected attempts; (2, 3) achieves 4ms for P1 and 17ms for P3+, see Table 5). P1 and P3+ remain under 100ms *per attempt* for all configurations up to (32,45); P2 trades higher latency (~ 130 – 194 ms per attempt for $T \geq 16$, non-monotone due to rejection-sampling variance) for eliminating hardware trust. Communication cost: ≈ 12.3 KB per party per attempt.

Security. We prove security in the random oracle model. Unforgeability reduces to the Module-SIS problem, matching the security of single-signer ML-DSA. Nonce share privacy is statistical (no computational assumptions) via the Shamir nonce DKG, with conditional min-entropy exceeding $5\times$ the secret key entropy for $|S| \leq 17$; key privacy given the public signature is conjectured to hold computationally under Module-LWE (open problem, unproven even for single-signer FIPS 204). Commitment and r0-check privacy reduce to PRF security.

Deployment Profiles. We define three deployment profiles with different trust assumptions, all with complete security proofs:

Profile P1 (TEE-Assisted): A TEE/HSM coordinator performs the r0-check and hint generation inside a trusted enclave, achieving optimal 3-round signing. We prove EUF-CMA security under Module-SIS (Theorem 2), with statistical nonce share privacy (Theorem 3) and PRF-based mask privacy (Lemma 2).

Profile P2 (Fully Distributed): A fully untrusted coordinator where the r0-check is computed via an MPC subprotocol using SPDZ [DPSZ12] and edaBits [EGK⁺20]. Using combiner-mediated commit-then-open and constant-depth comparison circuits, we achieve **5 online rounds** (reduced from 8). We prove UC security against *static* malicious adversaries corrupting up to $N - 1$ parties (Theorem 7).

Profile P3+ (Semi-Async 2PC): Designed for human-in-the-loop authorization. Two designated Computation Parties (CPs) jointly evaluate the r0-check via 2PC, but signers participate *semi-asynchronously*: they precompute nonces offline and respond within a time window (e.g., 5 minutes) rather than synchronizing for multiple rounds. This achieves **2 logical rounds** (1 signer step + 1 server round). We prove UC security against *static* adversaries under the assumption that at least one CP is honest (Theorem 8). The “Async” column in Table 1 distinguishes our work from concurrent approaches, which require synchronous multi-round signer participation.

1.3 Technical Overview

Protocol Overview. A trusted dealer creates Shamir shares of $\mathbf{sk} = (\mathbf{s}_1, \mathbf{s}_2)$ and establishes pairwise seeds via ML-KEM. Before each signing attempt, parties execute a Shamir nonce DKG to jointly generate degree- $(T-1)$ shares of the nonce \mathbf{y} (this can be preprocessed offline). The 3-round online signing protocol then has parties (1) commit to their DKG nonce shares, (2) exchange masked commitments to derive challenge c , and (3) send responses $\mathbf{z}_i = \mathbf{y}_i + c \cdot \mathbf{s}_{1,i}$ (no Lagrange coefficient, no mask). The combiner applies Lagrange coefficients during aggregation: $\mathbf{z} = \sum_i \lambda_i \mathbf{z}_i = \mathbf{y} + c\mathbf{s}_1$, and outputs $\sigma = (\tilde{c}, \mathbf{z}, \mathbf{h})$ if $\|\mathbf{z}\|_\infty < \gamma_1 - \beta$.

Key algebraic observation. The correctness of this construction rests on the fact that the partial response $\mathbf{z}_i = \mathbf{y}_i + c\mathbf{s}_{1,i}$ is \mathbb{Z}_q -linear in the Shamir evaluation. Because \mathbf{y} and \mathbf{s}_1 are both degree- $(T-1)$ Shamir polynomials over the same evaluation points, Lagrange interpolation distributes over addition:

$$\sum_{i \in S} \lambda_i \mathbf{z}_i = \sum_{i \in S} \lambda_i \mathbf{y}_i + c \sum_{i \in S} \lambda_i \mathbf{s}_{1,i} = \mathbf{y} + c\mathbf{s}_1.$$

This allows each signer to transmit the *unscaled* response \mathbf{z}_i —without pre-multiplying by the Lagrange coefficient $\lambda_i \in \mathbb{Z}_q$ —so that $\|\mathbf{z}_i\|_\infty \leq \lceil \gamma_1/|S| \rceil + \beta$ holds at the individual level. The combiner applies $\{\lambda_i\}$ only at aggregation, where Lagrange interpolation recovers a valid $\mathbf{z} = \mathbf{y} + c\mathbf{s}_1$ satisfying $\|\mathbf{z}\|_\infty < \gamma_1 - \beta$ via standard rejection sampling. By contrast, approaches based on generic LSSS with large reconstruction coefficients $\lambda_i \sim q$ must either pre-scale partial responses—producing individual norms $\|\lambda_i \mathbf{z}_i\|_\infty \sim q\gamma_1$, which universally violate the rejection bound and cause every signing attempt to abort—or employ noise flooding to mask the large shares, sacrificing FIPS 204 signature-size compatibility.

1.4 Comparison with Prior and Concurrent Work

Table 1 summarizes threshold ML-DSA schemes, comparing arbitrary threshold support, dishonest-majority security, round complexity, and FIPS 204 compatibility.

Three concurrent works address threshold ML-DSA with FIPS 204 compatibility. Bienstock et al. [BdCE⁺26] achieve arbitrary T with UC security, but require honest-majority and 23–79 communication rounds (range reflects threshold configurations from $T = 2$ to $T = N$; per their protocol analysis). Borin et al. [BCdP⁺25] and Celi et al. [CdPE⁺26] (the latter extending the former) achieve dishonest-majority with 6 rounds, but are limited to $T \leq 6$ by the constraints of their short-coefficient LSSS construction (the Ball-Çakan-Malkin bound [BÇMR21] establishes an asymptotic $\Omega(T \log T)$ lower bound on LSSS share size; their specific construction further requires small Lagrange reconstruction coefficients, limiting T to single digits in practice). Trilithium [DKLS25] is UC-secure but restricted to 2 parties in a server-phone architecture.

Profile P2 combines arbitrary thresholds, dishonest-majority security, constant rounds (5 rounds), UC security, and FIPS 204 compatibility, a combination not achieved by prior work. Profile P3+ achieves UC security (Theorem 8) under the 1-of-2 CP honest assumption, with semi-asynchronous signer participation (2 logical rounds).

We contribute: (1) Shamir nonce DKG for threshold ML-DSA, achieving statistical nonce share privacy (no computational assumptions) and in coordinator-based profiles (P1, P3+), eliminating the two-honest requirement for response shares ($|S| \geq T$ suffices; see Remark 11)—to our knowledge, the first threshold lattice-based signature achieving both: (i) statistical nonce share privacy (no computational assumptions), and (ii) $|S| = T$ signing sets in coordinator-based form. (Raccoon [dPEK⁺24] achieves statistical nonce privacy via sum-of-uniform nonces without computational assumptions, but requires $|S| \geq T + 1$ (not $|S| = T$) for nonce share privacy in its coordinator model, and targets Dilithium (not FIPS 204-compatible ML-DSA). Our improvement is specifically on the $|S| = T$ threshold; both schemes are non-computational for nonce privacy.); (2) Pairwise-canceling masks adapted to the lattice setting for commitment and r0-check values, addressing rejection sampling and r0-check key leakage; (3) Three deployment profiles (P1-TEE, P2-MPC, P3+-2PC) with different trust/performance trade-offs, including the novel semi-async model for P3+; (4) Complete security proofs, with unforgeability reducing to Module-SIS, statistical privacy via Shamir nonce DKG (Theorem 3), and UC security proofs for all profiles; (5) A reference implementation with benchmarks from (2, 3) to (32, 45) threshold configurations. Key generation currently assumes a trusted dealer for Shamir share distribution; a fully decentralized DKG achieving verifiable short-coefficient shares is an open problem discussed in Section 6.

Table 1: Comparison of threshold ML-DSA schemes. \checkmark = supported, \times = not supported. “Dishon.” = dishonest-majority *unforgeability* (tolerates $N - 1$ corruptions for EUF-CMA; for P2, commitment/r0-check privacy additionally requires $|S \setminus C| \geq 2$, see \bullet); Bienstock et al. require honest majority. “Privacy” column: **Stat.** = statistical nonce share privacy (no computational assumptions, conditional min-entropy $\geq 5 \times$ secret key entropy) for nonce shares \mathbf{y}_i *conditioned on the DKG view only*; key privacy given the public signature σ is an *open problem* for this work (conjectured computational under M-LWE; unproven even for single-signer FIPS 204; see §4). Comp. for prior work = computational privacy guarantee per each scheme’s respective analysis (specifics vary: may cover nonce shares, response shares, or key leakage from the signature). Commitment/r0-check privacy for this work uses PRF-based masks ($|S \setminus C| \geq 2$ for P2). “(TEE)” = dishonest-majority via TEE trust (not purely cryptographic); “(1/2 CP)” = via 1-of-2 computation-party honest assumption. *P3+ = 1 signer step + 1 server round. \dagger P1 UC assumes ideal TEE (Theorem 5)—a hardware trust assumption, not a cryptographic guarantee; P2’s dishonest-majority UC (Theorem 7) is purely cryptographic. \ddagger Rounds shown as online+offline; the +1 offline nonce-DKG preprocessing round is structurally necessary to prevent rewinding and is amortizable over batches of signing sessions. \bullet P2 achieves dishonest-majority *unforgeability* (tolerates $N - 1$ corruptions); commitment and r0-check *privacy* additionally requires $|S \setminus C| \geq 2$ (Lemma 2). At $T = N$ with $N - 1$ corruptions, mask hiding does not hold in P2; P1 and P3+ retain nonce-share privacy at $|S \setminus C| = 1$ via coordinator-only communication. \S UC proofs for this work (Theorems 5–8) are against *static* adversaries (corruption set fixed before execution); adaptive adversary security is an open problem. ^aRound count for Bienstock et al. as reported in [BdCE⁺26]; exact range depends on protocol variant and threshold T .

Scheme	T	Size	Rnd	FIPS	Dishon.	UC	Async	Privacy
del Pino-Niot [dPN25]	≤ 8	3.3 KB	3	\checkmark	\checkmark	\times	\times	Comp.
Noise Flooding [BKP13]	∞	17 KB	3	\times	\checkmark	\times	\times	Comp.
Ringtail [BKL ⁺ 25]	∞	13 KB	2	\times	\checkmark	\times	\times	Comp.
<i>Concurrent Work (2025–2026)</i>								
Bienstock et al. [BdCE ⁺ 26]	∞	3.3 KB	23–79 ^a	\checkmark	\times	\checkmark	\times	Comp.
Celi et al. [CdPE ⁺ 26]	≤ 6	3.3 KB	6	\checkmark	\checkmark	\times	\times	Comp.
Trilithium [DKLS25]	2	3.3 KB	14	\checkmark	\times	\checkmark	\times	Comp.
This work (P1)	∞	3.3 KB	$3+1^{\ddagger}$	\checkmark	(TEE)	$\checkmark^{\dagger\S}$	\times	Stat.
This work (P2)	∞	3.3 KB	$5+1^{\ddagger}$	\checkmark	\checkmark^{\bullet}	\checkmark^{\S}	\times	Stat.
This work (P3+)	∞	3.3 KB	2*	\checkmark	(1/2 CP)	\checkmark^{\S}	\checkmark	Stat.

1.5 Paper Organization

Section 2 provides background; Sections 3–4 present the protocol and security analysis; Section 5 gives benchmarks; Sections 6–7 discuss extensions and conclude.

2 Preliminaries

2.1 Notation

We use bold lowercase letters (e.g., \mathbf{s}) for vectors and bold uppercase letters (e.g., \mathbf{A}) for matrices. For an integer q , we write $\mathbb{Z}_q = \mathbb{Z}/q\mathbb{Z}$ for the ring of integers modulo q . We define the polynomial ring $R_q = \mathbb{Z}_q[X]/(X^n + 1)$ where n is a power of 2.

For a polynomial $f \in R_q$, we write $\|f\|_\infty = \max_i |f_i|$ for its infinity norm, where coefficients are represented in $(-q/2, q/2]$. For a vector $\mathbf{v} = (v_1, \dots, v_k) \in R_q^k$, we define $\|\mathbf{v}\|_\infty = \max_i \|v_i\|_\infty$.

We write $a \stackrel{\$}{\leftarrow} S$ to denote sampling a uniformly at random from a set S . We write $\text{negl}(\kappa)$ for a negligible function in the security parameter κ .

2.2 Lattice Problems

Our security relies on the hardness of the Module-SIS and Module-LWE problems [Reg09, LPR10].

Definition 1 (Module-SIS). The $\text{M-SIS}_{n,k,\ell,q,\beta}$ problem is: given a uniformly random matrix $\mathbf{A} \stackrel{\$}{\leftarrow} R_q^{k \times \ell}$, find a non-zero vector $\mathbf{z} \in R_q^\ell$ such that $\mathbf{A}\mathbf{z} = \mathbf{0} \pmod{q}$ and $\|\mathbf{z}\|_\infty \leq \beta$, where $\|\cdot\|_\infty$ denotes the ℓ^∞ norm computed with polynomial coefficients centered in $(-q/2, q/2]$.

Remark 1 (Notation: β disambiguation). The parameter β in the M-SIS definition above is a generic norm bound following standard lattice notation [LPR10]. The ML-DSA signing parameter $\beta = \tau\eta = 196$ (see parameters below) is a distinct, concrete value: the SIS norm bound instantiated for our unforgeability proof is $\gamma_1 - \beta_{\text{sign}} = 2^{19} - 196 \approx 524,092$ (Remark 2). No clash arises because the SIS definition is parameterized generically and the ML-DSA $\beta = 196$ is always used in the signing context.

Remark 2 (SelfTargetMSIS). The security reduction in Theorem 2 extracts a solution to the *inhomogeneous SelfTargetMSIS* variant [KLS18]: given $[\mathbf{A} | -\mathbf{t}_1 \cdot 2^d]$, find a short $(\mathbf{v}, \Delta c)$ with $\|\mathbf{v}\|_\infty < \gamma_1 - \beta$ such that $[\mathbf{A} | -\mathbf{t}_1 \cdot 2^d] \begin{bmatrix} \mathbf{v} \\ \Delta c \end{bmatrix} = 2\gamma_2 \mathbf{w}_1 + \mathbf{r}_0$ where \mathbf{w}_1 is a known target and $\|\mathbf{r}_0\|_\infty \leq \gamma_2$ (the `LowBits` residual from `HighBits` rounding). By [KLS18], `SelfTargetMSIS` hardness follows from M-SIS hardness under a standard parameter embedding; we therefore state Theorem 2 in terms of M-SIS.

Definition 2 (Module-LWE). The $\text{M-LWE}_{n,k,\ell,q,\chi}$ problem is to distinguish between:

- $(\mathbf{A}, \mathbf{A}\mathbf{s} + \mathbf{e})$ where $\mathbf{A} \stackrel{\$}{\leftarrow} R_q^{k \times \ell}$, $\mathbf{s} \stackrel{\$}{\leftarrow} \chi^\ell$, $\mathbf{e} \stackrel{\$}{\leftarrow} \chi^k$
- (\mathbf{A}, \mathbf{u}) where $\mathbf{u} \stackrel{\$}{\leftarrow} R_q^k$

where χ is a distribution over R_q with small coefficients.

For ML-DSA-65 parameters ($n = 256$, $q = 8380417$, $k = 6$, $\ell = 5$), both problems are believed to be hard at the 192-bit security level.

2.3 ML-DSA (FIPS 204)

ML-DSA [Nat24b], based on the CRYSTALS-Dilithium design [DKL⁺18], is a lattice-based digital signature scheme using the Fiat-Shamir with Aborts paradigm [Lyu12, PS00]. Security in the quantum random oracle model follows from [KLS18]. We summarize the key algorithms.

Parameters. For ML-DSA-65 (NIST Security Level 3):

- $n = 256$: polynomial degree
- $q = 8380417 = 2^{23} - 2^{13} + 1$: modulus
- $k = 6, \ell = 5$: matrix dimensions
- $\eta = 4$: secret key coefficient bound
- $\gamma_1 = 2^{19}$: masking range
- $\gamma_2 = (q - 1)/32$: rounding parameter
- $\tau = 49$: challenge weight (number of ± 1 entries)
- $\beta = \tau \cdot \eta = 196$: signature bound
- $\omega = 55$: hint weight bound (max number of 1-entries in hint \mathbf{h})
- $d = 13$: dropping bits in Power2Round ($\mathbf{t} = \mathbf{t}_1 \cdot 2^d + \mathbf{t}_0$)

Key Generation.

1. Sample seed $\rho \xleftarrow{\$} \{0, 1\}^{256}$ and expand to matrix $\mathbf{A} \in R_q^{k \times \ell}$
2. Sample short secrets $\mathbf{s}_1 \xleftarrow{\$} \chi_\eta^\ell$ and $\mathbf{s}_2 \xleftarrow{\$} \chi_\eta^k$ with coefficients in $[-\eta, \eta]$
3. Compute $\mathbf{t} = \mathbf{A}\mathbf{s}_1 + \mathbf{s}_2$ and decompose $\mathbf{t} = \mathbf{t}_1 \cdot 2^d + \mathbf{t}_0$
4. Output $\text{pk} = (\rho, \mathbf{t}_1)$ and $\text{sk} = (\rho, \mathbf{s}_1, \mathbf{s}_2, \mathbf{t}_0)$

Signing. Sample nonce $\mathbf{y} \xleftarrow{\$} \{-\gamma_1 + 1, \dots, \gamma_1\}^{n\ell}$, compute $\mathbf{w}_1 = \text{HighBits}(\mathbf{A}\mathbf{y}, 2\gamma_2)$, derive challenge $c = H(\mu \| \mathbf{w}_1)$, and set $\mathbf{z} = \mathbf{y} + c\mathbf{s}_1$. If $\|\mathbf{z}\|_\infty \geq \gamma_1 - \beta$, restart (rejection sampling). Compute hint \mathbf{h} and output $\sigma = (\tilde{c}, \mathbf{z}, \mathbf{h})$.

Verification. Expand c from \tilde{c} , compute $\mathbf{w}'_1 = \text{UseHint}(\mathbf{h}, \mathbf{A}\mathbf{z} - c\mathbf{t}_1 \cdot 2^d)$, and verify $\|\mathbf{z}\|_\infty < \gamma_1 - \beta$ and $\tilde{c} = H(\mu \| \mathbf{w}'_1)$.

The z-bound check and r0-check together yield ≈ 20 – 25% per-attempt success (4–5 expected attempts). This is inherent to Fiat-Shamir with Aborts [Lyu12], not threshold-specific. *Note:* In our threshold protocol, the aggregated nonce follows an Irwin-Hall distribution (sum of $|S|$ bounded uniform variables) rather than a single uniform draw. The Irwin-Hall distribution has greater density near zero, shifting more nonces into the acceptance region $\|\mathbf{z}\|_\infty < \gamma_1 - \beta$. As a result, observed threshold signing success rates of 21–45% are consistent with (and can slightly exceed) the single-signer baseline; see Table 5.

2.4 Shamir Secret Sharing

Shamir’s (T, N) -threshold secret sharing [Sha79] allows a secret $s \in \mathbb{Z}_q$ to be distributed among N parties such that any T parties can reconstruct s , but any $T - 1$ parties learn nothing. For vector (module) secrets $\mathbf{s} \in R_q^\ell$, sharing is applied coordinate-by-coordinate over \mathbb{Z}_q .

Sharing. To share secret s :

1. Sample random polynomial $f(X) = s + r_1X + \dots + r_{T-1}X^{T-1} \in \mathbb{Z}_q[X]$
2. Give share $s_i = f(i)$ to party i for $i \in [N]$

Reconstruction. Given shares from set S with $|S| \geq T$:

$$s = f(0) = \sum_{i \in S} \lambda_i \cdot s_i \pmod{q}$$

where the **Lagrange coefficients** are:

$$\lambda_i = \prod_{j \in S, j \neq i} j \cdot (j - i)^{-1} \pmod{q}$$

Remark 3 (Lagrange Coefficient Magnitude). For the standard evaluation points $\{1, 2, \dots, T\}$, Lagrange coefficients satisfy $\lambda_i = (-1)^{i-1} \binom{T}{i}$, growing as $\approx 2^T / \sqrt{\pi T/2}$ (by Stirling’s formula). For $T \leq 8$, coefficients remain small ($\binom{8}{4} = 70$), enabling short-coefficient schemes [dPN25]. For $T \geq 26$, coefficients exceed $q = 8,380,417$ (since $\binom{25}{12} = 5,200,300 < q$ but $\binom{26}{13} = 10,400,600 > q$), aligning with the Ball-Çakan-Malkin bound [BÇMR21]. For *short-coefficient LSSS* designs [dPN25, BÇMR21] that require Lagrange products $\lambda_i \cdot \mathbf{z}_i$ to remain short *before* modular reduction, this is a binding obstacle: the product has norm $O(q \cdot \gamma_1) \gg \gamma_1 - \beta$. When $|S| > T$, the maximum Lagrange coefficient magnitude grows as $\binom{|S|}{\lfloor |S|/2 \rfloor}$ (larger than for $|S| = T$), so the constraint on T is the binding one in practice. In our construction, shares $\mathbf{z}_i \in \mathbb{Z}_q^\ell$ are large, but the aggregate satisfies $\sum_i \lambda_i \mathbf{z}_i = \mathbf{y} + \mathbf{cs}_1$ by the Shamir reconstruction identity; since $\|\mathbf{y} + \mathbf{cs}_1\|_\infty \leq \gamma_1 - \beta < q/2$, the computation in \mathbb{Z}_q yields the same result as integer arithmetic, and the z-bound check operates on the correct short value.

2.5 Security Definitions for Threshold Signatures

Definition 3 (Threshold Signature Scheme). A (T, N) -threshold signature scheme consists of algorithms:

- $\text{KeyGen}(1^\kappa, N, T) \rightarrow (\text{pk}, \{\text{sk}_i\}_{i \in [N]})$: Generates public key and secret key shares
- $\text{Sign}(\{\text{sk}_i\}_{i \in S}, \mu) \rightarrow \sigma$: Interactive protocol among parties in S (where $|S| \geq T$) to sign message μ
- $\text{Verify}(\text{pk}, \mu, \sigma) \rightarrow \{0, 1\}$: Deterministic verification

Remark 4 (Signing Set Size). With Shamir nonce DKG and coordinator-based communication (Remark 11), Profiles P1 and P3+ require only $|S| \geq T$ signers—the minimum required by Shamir’s (T, N) threshold property for reconstruction. This improves upon standard pairwise-mask schemes [CGG⁺20, CCL⁺23] that require $|S| \geq T + 1$. The nonce DKG provides statistical share privacy (no computational assumptions) even with a single honest party (see Theorem 3 and Remark 15). In P2’s broadcast model, $|S \setminus C| \geq 2$ is required for commitment privacy (Lemma 2).

Definition 4 (Unforgeability (EUFCMA)). A threshold signature scheme is EUFCMA secure if for any PPT adversary \mathcal{A} corrupting up to $T - 1$ parties:

$$\Pr[\text{EUFCMA}_{\Pi}^{\mathcal{A}}(\kappa) = 1] \leq \text{negl}(\kappa)$$

where in the security game:

1. $(\text{pk}, \{\text{sk}_i\}) \leftarrow \text{KeyGen}(1^\kappa, N, T)$
2. \mathcal{A} receives pk and $\{\text{sk}_i\}_{i \in C}$ for corrupted set C with $|C| < T$
3. \mathcal{A} can request signatures on messages of its choice (interacting with honest parties)

4. \mathcal{A} outputs (m^*, σ^*)
5. \mathcal{A} wins if $\text{Verify}(\text{pk}, m^*, \sigma^*) = 1$ and m^* was never queried

Definition 5 (Privacy (Informal)). A threshold signature scheme provides privacy if the view of any coalition C with $|C| < T$ can be efficiently simulated given only pk and the signatures produced.

Remark 5 (Informal vs. UC Privacy). Definition 5 is an informal stand-in. The full UC-level privacy guarantees, with explicit simulators and hybrid arguments, are established separately for each deployment profile: Theorem 5 (P1), Theorem 7 (P2), and Theorem 8 (P3+).

2.6 Pseudorandom Functions

Definition 6 (PRF Security). A function family $F : \mathcal{K} \times \mathcal{X} \rightarrow \mathcal{Y}$ is a secure PRF if for any PPT distinguisher \mathcal{D} :

$$\left| \Pr[\mathcal{D}^{F^k(\cdot)} = 1] - \Pr[\mathcal{D}^{R(\cdot)} = 1] \right| \leq \text{negl}(\kappa)$$

where $k \xleftarrow{\$} \mathcal{K}$ and $R : \mathcal{X} \rightarrow \mathcal{Y}$ is a truly random function.

In our construction, we instantiate the PRF with SHAKE-256, modeled as a random oracle in the security analysis.

3 Masked Threshold ML-DSA Protocol

We now present our masked threshold ML-DSA protocol in full detail. The protocol consists of a setup phase (key generation) and a signing phase (three-round interactive protocol).

3.1 Overview

The core challenge in threshold ML-DSA is handling the large Lagrange coefficients that arise in Shamir secret sharing over \mathbb{Z}_q . As noted in Remark 3, the Lagrange coefficients for standard evaluation points $\{1, \dots, N\}$ can be as large as $\binom{T}{\lfloor T/2 \rfloor} \approx 2^T / \sqrt{T}$ over \mathbb{Z} before modular reduction—for example, $\binom{16}{8} = 12870$ at $T = 16$ (see Lemma 21). When the naive reconstruction $\mathbf{z} = \sum_{i \in S} \lambda_i \mathbf{z}_i$ is computed, each response share $\mathbf{z}_i = \mathbf{y}_i + c \cdot \mathbf{s}_{1,i}$ is scaled by λ_i , inflating the ℓ_∞ -norm by up to $12870 \times$ (at $T = 16$)—far beyond the rejection-sampling bound $\gamma_1 - \beta = 524092$. For large T , the coefficient magnitude eventually exceeds q , causing aliasing in the modular reduction.

Our solution is based on two key techniques:

1. **Shamir nonce DKG:** Parties jointly generate the nonce \mathbf{y} via a Shamir-style distributed key generation, so that both \mathbf{y} and the long-term secret \mathbf{s}_1 are degree- $(T-1)$ Shamir sharings. Each party computes $\mathbf{z}_i = \mathbf{y}_i + c \cdot \mathbf{s}_{1,i}$ (without Lagrange coefficients), and the combiner reconstructs $\mathbf{z} = \sum_i \lambda_i \mathbf{z}_i = \mathbf{y} + c\mathbf{s}_1$. This achieves *statistical share privacy* (conditional min-entropy $\geq 5 \times$ secret key entropy for $|S| \leq 17$, requiring no computational assumptions), in coordinator-based profiles (P1, P3+), eliminates the two-honest requirement ($|S| \geq T$ suffices; see Remark 11), and requires no pairwise masks on the response \mathbf{z}_i .
2. **Pairwise-canceling masks:** For the commitment values \mathbf{W}_i and the r0-check shares \mathbf{V}_i , we add pairwise-canceling masks that hide individual contributions while preserving correctness in the sum.

3.2 Threat Model and Deployment Profiles

We consider a (T, N) -threshold setting where an adversary may corrupt up to $T - 1$ parties. Table 2 summarizes our three deployment profiles.

Table 2: Deployment Profiles: Trust Assumptions and Security Guarantees

Property	Profile P1	Profile P2	Profile P3+
Coordinator	TEE/HSM	Untrusted	2PC pair
Trust assumption	TEE integrity	None (MPC)	1-of-2 CP honest
r0-check location	Inside enclave	MPC subprotocol	2PC subprotocol
cs_2 exposure	Never leaves TEE	Never reconstructed	Split between CPs
Online rounds	3	5	2*
Signer sync	Multi-round	Multi-round	Semi-async
Latency	Low	Medium	Lowest
Complexity	Low	High	Medium
Common to all profiles:			
Adversary model	Static, malicious (up to $T - 1$ parties)		
Signing set size	$ S \geq T$		
Security goal	EUF-CMA under Module-SIS		
Privacy goal	Statistical share privacy (Theorem 3)		
Output format	FIPS 204-compatible signature		

*P3+ = 1 signer step (within time window) + 1 server round (2PC). Signers precompute nonces offline.

Profile P1 (Primary). A TEE/HSM coordinator aggregates masked contributions and performs the r0-check inside a trusted enclave. The value cs_2 is reconstructed inside the enclave and never exposed. This is our recommended deployment model, combining threshold distribution among parties with hardware-isolated aggregation.

Profile P2 (Fully Distributed). A fully distributed protocol where no single party learns cs_2 . The r0-check is computed via an MPC subprotocol using SPDZ [DPSZ12] and edaBits [EGK⁺20] (see Section 6). Using combiner-mediated commit-then-open and constant-depth comparison circuits, we achieve **5 online rounds** (optimized from 8). We prove UC security against malicious adversaries corrupting up to $N - 1$ parties in Theorem 7.

Profile P3+ (Semi-Async 2PC). Designed for human-in-the-loop authorization scenarios. Two designated *Computation Parties* (CPs) jointly evaluate the r0-check via lightweight 2PC. Each CP receives additive shares of cs_2 ; neither learns the complete value unless they collude.

The key innovation is *semi-asynchronous signer participation*: signers precompute nonces $(\mathbf{y}_i, \mathbf{w}_i, \text{Com}_i)$ offline at any time, then respond within a bounded time window (e.g., 5 minutes) after receiving the challenge. A client daemon handles the cryptographic operations transparently, completing the signing process in under 1 second.

This achieves **2 logical rounds** (1 signer step + 1 server round). The 2PC uses pre-garbled circuits for reduced online latency ($\sim 15\text{ms}$). Profile P3+ is suited for deployments requiring human authorization where signers cannot coordinate for multiple synchronous rounds.

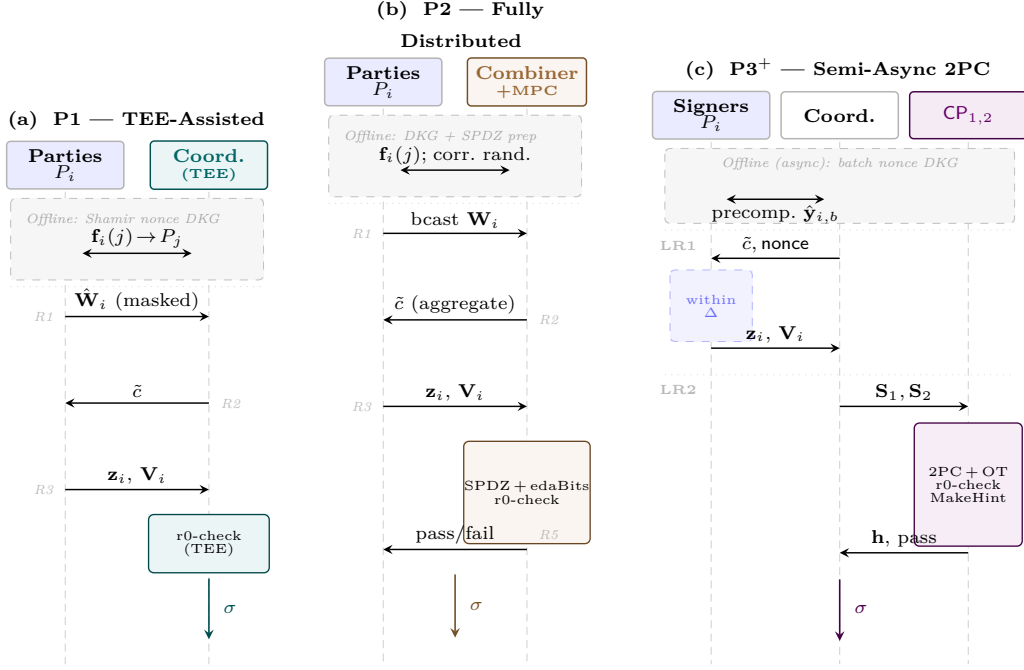


Figure 1: Protocol message flows for the three deployment profiles. Shaded top regions are offline preprocessing; dashed lines are actor lifelines. **(a) P1:** masked commitments \tilde{W}_i sent only to trusted TEE coordinator, enabling $|S \setminus C| = 1$. **(b) P2:** all values broadcast; dishonest-majority security via SPDZ+edaBits; r0-check computed inside MPC. **(c) P3⁺:** semi-async signers respond within window Δ ; two CPs run garbled-circuit 2PC for r0-check. LR = Logical Round; R = Protocol Round.

3.3 Setup Phase

Pairwise Seed Establishment. Before key generation, each pair of parties (i, j) with $i < j$ establishes a shared secret seed $\text{seed}_{i,j} \in \{0, 1\}^{256}$. This may be done via ML-KEM key exchange (each party generates a keypair; pairs perform encapsulation and decapsulation to derive the shared seed) or via pre-shared keys from a trusted setup.

Each party i stores seeds $\{\text{seed}_{\min(i,j), \max(i,j)}\}_{j \neq i}$ for all other parties.

Key Generation. The key generation can be performed by a trusted dealer or via a distributed key generation protocol. We present the trusted dealer version; see Section 6 for DKG.

Remark 6 (Key Generation Scope). Threshold key generation is an *application-layer* component outside the scope of FIPS 204. The resulting public key $\text{pk} = (\rho, \mathbf{t}_1)$ is byte-identical to a standard FIPS 204 ML-DSA-65 public key and is usable with any FIPS 204-compliant verification implementation without modification. The threshold secret key shares $\{\text{sk}_i\}$ are specific to this construction and replace the single-party FIPS 204 signing key; they do not affect the signature format or verifiability.

3.4 Shamir Nonce DKG

The primary technique enabling statistical share privacy is the *Shamir nonce DKG*: parties jointly generate the signing nonce \mathbf{y} as a degree- $(T-1)$ Shamir sharing, matching the

Algorithm 1 KeyGen($1^\kappa, N, T$): Threshold Key Generation

-
- 1: Sample seed $\rho \xleftarrow{\$} \{0, 1\}^{256}$
 - 2: Expand $\mathbf{A} = \text{ExpandA}(\rho) \in R_q^{k \times \ell}$
 - 3: Sample $\mathbf{s}_1 \xleftarrow{\$} \chi_\eta^\ell, \mathbf{s}_2 \xleftarrow{\$} \chi_\eta^k$ ▷ Short secret keys
 - 4: Compute $\mathbf{t} = \mathbf{A}\mathbf{s}_1 + \mathbf{s}_2$
 - 5: Decompose $(\mathbf{t}_1, \mathbf{t}_0) \leftarrow \text{Power2Round}(\mathbf{t}, d)$ ▷ FIPS 204 Alg. 29; $\mathbf{t} = \mathbf{t}_1 \cdot 2^d + \mathbf{t}_0$
 - 6: Set $\text{pk} = (\rho, \mathbf{t}_1)$
 - 7: **for** each secret polynomial s in \mathbf{s}_1 and \mathbf{s}_2 **do**
 - 8: Create Shamir sharing: $p_s(X) = s + a_1X + \dots + a_{T-1}X^{T-1}$, $a_j \xleftarrow{\$} R_q$
 - 9: Compute shares: $s_i = p_s(i)$ for $i \in [N]$
 - 10: **end for**
 - 11: **return** $\text{pk}, \{\text{sk}_i = (\mathbf{s}_{1,i}, \mathbf{s}_{2,i}, \{\text{seed}_{*,*}\})\}_{i \in [N]}$
-

structure of the long-term secret \mathbf{s}_1 . This is executed once per signing attempt and can be preprocessed offline.

Algorithm 2 NonceDKG(S): Distributed Nonce Generation

-
- Input:** Signing set S with $|S| \geq T$
- 1: **for** each party $i \in S$ in parallel **do**
 - 2: Sample secret contribution $\hat{\mathbf{y}}_i \xleftarrow{\$} \{-\lfloor \gamma_1/|S| \rfloor, \dots, \lfloor \gamma_1/|S| \rfloor\}^{n\ell}$
 - 3: Construct degree- $(T-1)$ polynomial over R_q^ℓ :

$$\mathbf{f}_i(x) = \hat{\mathbf{y}}_i + \mathbf{a}_{i,1}x + \dots + \mathbf{a}_{i,T-1}x^{T-1}$$
 where $\mathbf{a}_{i,k} \xleftarrow{\$} R_q^\ell$ for $k = 1, \dots, T-1$
 - 4: Send $\mathbf{f}_i(j)$ to each party $j \in S$ over a private channel ▷ Encrypted via pairwise ML-KEM seeds
 - 5: **end for**
 - 6: **for** each party $j \in S$ **do**
 - 7: Compute nonce share: $\mathbf{y}_j = \sum_{i \in S} \mathbf{f}_i(j)$
 - 8: **end for**
-

The combined polynomial is $\mathbf{F}(x) = \sum_{i \in S} \mathbf{f}_i(x)$, with $\mathbf{F}(0) = \sum_i \hat{\mathbf{y}}_i = \mathbf{y}$ (the nonce) and $\mathbf{F}(j) = \mathbf{y}_j$ (the shares). This is a valid degree- $(T-1)$ Shamir sharing of \mathbf{y} over R_q^ℓ .

Remark 7 (Why Uniform Higher-Degree Coefficients). The coefficients $\mathbf{a}_{i,k}$ for $k \geq 1$ are sampled uniformly over R_q^ℓ (not from a short distribution). This is essential: the adversary observes $T-1$ evaluations of \mathbf{f}_h (the honest party's polynomial), leaving exactly one degree of freedom. The uniform *prior* distribution of $\mathbf{a}_{h,T-1}$ ensures high entropy in this free parameter; combined with the bounded-nonce constraint, the honest party's share $\mathbf{f}_h(x_h)$ retains conditional min-entropy $\geq n\ell \cdot \log_2(2\lfloor \gamma_1/|S| \rfloor + 1)$ bits per session (the support of each per-party share coordinate is $\{-\lfloor \gamma_1/|S| \rfloor, \dots, \lfloor \gamma_1/|S| \rfloor\}$, a range of $2\lfloor \gamma_1/|S| \rfloor + 1$ values counting both endpoints; the approximation $\approx n\ell \cdot (20 - \log_2 |S|)$ bits holds to within 1 bit for $|S| \leq 17$). See Theorem 3 and Remark 19.

Remark 8 (Communication Cost). The nonce DKG requires $|S| \cdot (|S| - 1)$ point-to-point messages, each of size $n\ell \cdot \lceil \log_2 q \rceil$ bits (≈ 3.6 KB for ML-DSA-65; $256 \times 5 \times 23 = 29,440$ bits). For a $(3, 5)$ -threshold with $|S| = 3$, this is 6 messages totaling ≈ 22 KB; for $|S| = 32$, the DKG requires $32 \times 31 = 992$ messages totaling ≈ 3.6 MB. This $O(|S|^2)$ offline preprocessing cost does not appear in the online round complexity comparison; it is amortizable over batches of signing sessions (multiple nonce DKG rounds can be preprocessed during idle time) and is absent from the online communication cost (≈ 12.3 KB per party per online attempt). The DKG round is independent of the message to be

signed and can be executed offline as a preprocessing step, so online signing latency is unchanged.

Remark 9 (Why No VSS for the Nonce DKG). The *key* DKG uses Feldman commitments [Fel87] because the long-term secret \mathbf{s}_1 has short coefficients and parties must verifiably bind their contributions during a one-time setup. The *nonce* DKG has a different structure: the higher-degree polynomial coefficients are sampled R_q^ℓ -uniformly (by design, for entropy), and the constant term $\hat{\mathbf{y}}_i$ must remain hidden to preserve nonce privacy (Theorem 3). Feldman-style commitments publish g^{a_k} for each coefficient, which would not hide $\hat{\mathbf{y}}_i$ against a discrete-log adversary and would require a hiding commitment scheme instead—substantially complicating the offline round. We instead adopt an *optimistic* approach: shares are sent over private authenticated channels, and any cheating party is detectable *a posteriori* by the blame protocol (Section 6.1), which asks parties to reveal their full polynomials to the TEE. The TEE recomputes each share and verifies consistency with the submitted \mathbf{z}_i values. The optimistic threshold of $K = 33$ consecutive aborts ensures blame is triggered before a malicious party can cause meaningful disruption (honest probability $(0.75)^{33} < 10^{-4}$).

3.5 Pairwise-Canceling Masks

Pairwise-canceling masks are used to hide the commitment values \mathbf{W}_i (for challenge derivation) and the r0-check shares \mathbf{V}_i (which contain $\lambda_i \cdot c \cdot \mathbf{s}_{2,i}$). For any signing set S , each party $i \in S$ computes a mask \mathbf{m}_i such that $\sum_{i \in S} \mathbf{m}_i = \mathbf{0}$.

Definition 7 (Pairwise-Canceling Mask). For signing set S and PRF context $\text{ctx} \in \{0, 1\}^*$ (composed as $\text{ctx} = \text{nonce}^* \parallel \text{label}$, where nonce^* is the appropriate per-session identifier defined below, and label is a fixed domain tag), party i computes:

$$\mathbf{m}_i^{(\text{ctx})} = \sum_{j \in S: j > i} \text{PRF}(\text{seed}_{i,j}, \text{ctx}) - \sum_{j \in S: j < i} \text{PRF}(\text{seed}_{j,i}, \text{ctx})$$

where $\text{PRF} : \{0, 1\}^{256} \times \{0, 1\}^* \rightarrow R_q^k$ is instantiated with SHAKE-256 (here $k = 6$ is the module rank, not the dropping-bits parameter $d = 13$). The per-session nonce ensures masks are fresh in each signing session (see Mask Hiding, Lemma 2).

We use $\text{ctx} = \text{nonce}_0 \parallel \text{"comm"}$ for commitment masks $\mathbf{m}_i^{(w)} \in R_q^k$, where $\text{nonce}_0 = H(\text{"nonce0"} \parallel \text{Com}_{i_1} \parallel \dots)$ is the *pre-challenge* nonce derived at the start of Round 2 (before the challenge c is known). We use $\text{ctx} = \text{nonce} \parallel \text{"s2"}$ for r0-check masks $\mathbf{m}_i^{(s2)} \in R_q^k$, where nonce is the post-challenge per-session identifier.

Lemma 1 (Mask Cancellation). For any signing set S and nonce, $\sum_{i \in S} \mathbf{m}_i = \mathbf{0}$.

Proof. Each pair (i, j) with $i < j$ contributes $+\text{PRF}(\text{seed}_{i,j}, \text{nonce})$ from party i (since $j > i$) and $-\text{PRF}(\text{seed}_{i,j}, \text{nonce})$ from party j (since $i < j$); these cancel exactly in the sum, so $\sum_{i \in S} \mathbf{m}_i = \mathbf{0}$. \square

3.6 Signing Protocol

The signing protocol is a three-round interactive protocol among parties in the signing set S (where $|S| \geq T$), preceded by an offline nonce DKG preprocessing step (Algorithm 2). We assume a broadcast channel or a designated combiner (TEE/HSM in Profile P1).

Remark 10 (Commitment Model). The Round 1 commitments Com_i bind parties to their nonces before seeing others' values, preventing adaptive attacks. However, *we do not publicly verify these commitments during normal signing*—the masked values \mathbf{W}_i cannot be verified without revealing private mask seeds, and the responses \mathbf{z}_i are privacy-protected

Algorithm 3 Sign: Three-Round Threshold Signing Protocol

Public Input: Message μ , public key $\text{pk} = (\rho, \mathbf{t}_1)$, signing set S
Private Input: Party i holds $\text{sk}_i = (\mathbf{s}_{1,i}, \mathbf{s}_{2,i}, \{\text{seed}_{*,*}\})$

Preprocessing: Nonce DKG (offline)

- 1: Execute $\text{NonceDKG}(S)$ (Algorithm 2) to obtain nonce shares $\{\mathbf{y}_i\}_{i \in S}$

Round 1: Nonce Commitment

- 2: **for** each party $i \in S$ in parallel **do**
- 3: Compute $\mathbf{w}_i = \mathbf{A}\mathbf{y}_i$ ▷ Using DKG nonce share
- 4: Sample $r_i \xleftarrow{\$} \{0, 1\}^{256}$
- 5: Compute $\text{Com}_i = H(\text{"com"} \parallel \mathbf{y}_i \parallel \mathbf{w}_i \parallel r_i)$
- 6: Broadcast Com_i
- 7: Store $(\mathbf{y}_i, \mathbf{w}_i, r_i)$ as local state
- 8: **end for**

Round 2: Masked Reveal and Challenge

- 9: **Pre-round:** Derive preliminary nonce $\text{nonce}_0 = H(\text{"nonce0"} \parallel \text{Com}_{i_1} \parallel \dots \parallel \text{Com}_{i_{|S|}})$
where $(i_1, \dots, i_{|S|}) = \text{sort}(S)$
- 10: **for** each party $i \in S$ in parallel **do**
- 11: Compute Lagrange coefficient for reconstruction at point 0: $\lambda_i = \prod_{j \in S, j \neq i} \frac{j}{j-i} \bmod q$ ▷ Shamir interpolation at $x = 0$
- 12: Compute commitment mask $\mathbf{m}_i^{(w)} \in R_q^k$ using $\text{nonce}_0 \parallel \text{"comm"}$
- 13: Send $(\mathbf{W}_i = \lambda_i \cdot \mathbf{w}_i + \mathbf{m}_i^{(w)}, r_i)$ to coordinator ▷ NOT broadcast; see Remark 15
- 14: **end for**
- 15: **Coordinator:**
- 16: Aggregate $\mathbf{W} = \sum_{j \in S} \mathbf{W}_j = \sum_j (\lambda_j \mathbf{w}_j + \mathbf{m}_j^{(w)})$ ▷ Substitute definition of \mathbf{W}_j
- 17: = $\sum_j \lambda_j \mathbf{w}_j + \sum_j \mathbf{m}_j^{(w)} = \sum_j \lambda_j \mathbf{A}\mathbf{y}_j + \mathbf{0}$ ▷ Masks cancel (Lemma 1); $\mathbf{w}_j = \mathbf{A}\mathbf{y}_j$
- 18: = $\mathbf{A} \sum_j \lambda_j \mathbf{y}_j = \mathbf{A}\mathbf{y}$ ▷ Linearity of \mathbf{A} ; Lagrange reconstruction of \mathbf{y} from $\{\mathbf{y}_j\}_{j \in S}$
- 19: Set $\mathbf{w} \leftarrow \mathbf{W}$ ▷ $\mathbf{w} = \mathbf{A}\mathbf{y}$; used in r0-check and hint computation
- 20: Compute $\mathbf{w}_1 = \text{HighBits}(\mathbf{w}, 2\gamma_2)$
- 21: Compute $\tilde{c} = H_{\text{chal}}(\mu \parallel \mathbf{w}_1)$ and expand to challenge $c \in R_q$ ▷ FIPS 204 spec; no invertibility check needed
- 22: Derive $\text{nonce} = H(\text{"nonce"} \parallel \tilde{c} \parallel \mu \parallel \text{sort}(S))$
- 23: Broadcast $(\mathbf{w}_1, \tilde{c}, \text{nonce})$ to all parties ▷ Only HighBits; individual \mathbf{W}_i stay private

Round 3: Response

- 24: **for** each party $i \in S$ in parallel **do**
- 25: Compute response: $\mathbf{z}_i = \mathbf{y}_i + c \cdot \mathbf{s}_{1,i}$ ▷ No λ_i , no mask
- 26: Compute $\mathbf{V}_i = \lambda_i \cdot c \cdot \mathbf{s}_{2,i} + \mathbf{m}_i^{(s_2)}$ ▷ Masked, for r0-check
- 27: Send $(\mathbf{z}_i, \mathbf{V}_i)$ to combiner
- 28: **end for**

Aggregation and r0-Check (see Subsection 3.10)

- 29: Combiner computes $\mathbf{z} = \sum_{i \in S} \lambda_i \cdot \mathbf{z}_i \bmod q$ ▷ Lagrange at combiner
- 30: **if** $\|\mathbf{z}\|_\infty \geq \gamma_1 - \beta$ **then**
- 31: **return** \perp (z-bound abort, retry from Round 1)
- 32: **end if**
- 33: Combiner computes $\mathbf{cs}_2 \leftarrow \sum_{i \in S} \mathbf{V}_i = \sum_{i \in S} (\lambda_i \mathbf{cs}_{2,i} + \mathbf{m}_i^{(s_2)})$ ▷ Substitute definition of \mathbf{V}_i
- 34: = $c \sum_{i \in S} \lambda_i \mathbf{s}_{2,i} + \sum_{i \in S} \mathbf{m}_i^{(s_2)} = \mathbf{cs}_2 + \mathbf{0}$ ▷ Lagrange reconstruction of \mathbf{s}_2 from shares $\{\mathbf{s}_{2,i}\}_{i \in S}$ using same λ_i as Line 206; masks cancel (Lemma 1)
- 35: **r0-check:** Verify $\|\text{LowBits}(\mathbf{w} - \mathbf{cs}_2, 2\gamma_2)\|_\infty < \gamma_2 - \beta$
- 36: **if** r0-check fails **then**
- 37: **return** \perp (r0 abort, retry from Round 1)
- 38: **end if**
- 39: Compute $\mathbf{r} = \mathbf{A}\mathbf{z} - c\mathbf{t}_1 \cdot 2^d$ ▷ = $\mathbf{w} - \mathbf{cs}_2 + c\mathbf{t}_0$
- 40: Set $-c\mathbf{t}_0 \leftarrow \mathbf{w} - \mathbf{r} - \mathbf{cs}_2$ ▷ = $\mathbf{w} - (\mathbf{A}\mathbf{z} - c\mathbf{t}_1 \cdot 2^d) - \mathbf{cs}_2$
- 41: Compute hint $\mathbf{h} = \text{MakeHint}(-c\mathbf{t}_0, \mathbf{r}, 2\gamma_2)$
- 42: **if** $\text{weight}(\mathbf{h}) > \omega$ **then**

by the nonce DKG (Theorem 3). Instead, we follow an *optimistic* model: if signing fails (excessive aborts, invalid signatures), the TEE coordinator triggers a blame protocol where parties reveal their commitments for verification. This “commit always, open only on blame” approach minimizes latency on the normal path while enabling accountability. See Section 6.1 for details.

Remark 11 (Why \mathbf{W}_i Must Not Be Broadcast). Individual masked commitments $\mathbf{W}_i = \lambda_i \mathbf{A} \mathbf{y}_i + \mathbf{m}_i^{(w)}$ are sent *only to the coordinator*, not broadcast to all parties. This is critical for privacy when $|S \setminus C| = 1$: if \mathbf{W}_h were broadcast and the adversary controls all other parties in S , the pairwise mask $\mathbf{m}_h^{(w)}$ would be fully computable (all seeds are shared with corrupted parties), revealing $\lambda_h \mathbf{A} \mathbf{y}_h$.

Recovery of \mathbf{y}_h from $\mathbf{A} \mathbf{y}_h$ (when $k > \ell$). For ML-DSA-65, the public matrix $\mathbf{A} \in R_q^{k \times \ell}$ with $k = 6$, $\ell = 5$ (so $k > \ell$) is generated via the random oracle ExpandA. The Module-LWE assumption [LS15, ADPS16] requires that \mathbf{A} has full column rank ℓ with overwhelming probability over the random oracle sampling (see [Nat24b, Section 3.4] for ExpandA). When \mathbf{A} has full column rank and $k \geq \ell$, the left inverse $((\mathbf{A}^\top \mathbf{A})^{-1} \mathbf{A}^\top)$ exists over R_q (modulo invertibility of $\mathbf{A}^\top \mathbf{A}$, which holds with overwhelming probability for random \mathbf{A}), enabling recovery:

$$\mathbf{y}_h = (\mathbf{A}^\top \mathbf{A})^{-1} \mathbf{A}^\top \cdot (\lambda_h \mathbf{A} \mathbf{y}_h) / \lambda_h.$$

The scalar λ_h is invertible modulo q (as all Lagrange coefficients are, by construction). Thus, revealing $\mathbf{A} \mathbf{y}_h$ enables key extraction via $\mathbf{z}_h = \mathbf{y}_h + c \cdot \mathbf{s}_{1,h}$ (the adversary knows \mathbf{z}_h from the public signature and c from the challenge). This is a non-trivial lattice attack that does *not* rely on the high min-entropy of \mathbf{y}_h —it is a direct algebraic recovery, bypassing statistical privacy. Therefore, \mathbf{W}_i must remain coordinator-only.

The coordinator broadcasts only $(\mathbf{w}_1, \tilde{c})$, where $\mathbf{W} = \sum_i \mathbf{W}_i$ and $\mathbf{w}_1 = \text{HighBits}(\mathbf{W}, 2\gamma_2)$. Since \mathbf{w}_1 is implicit in any valid σ , this adds zero information to the adversary’s view. See Remark 15 for the full security argument.

In Profile P1, the TEE coordinator naturally keeps \mathbf{W}_i private. In Profile P3+, the combiner serves as coordinator. In Profile P2 (no designated coordinator), parties broadcast \mathbf{W}_i directly and rely on mask hiding (Lemma 2, requiring $|S \setminus C| \geq 2$) to protect individual contributions.

Remark 12 (Domain Separation). We use distinct domain tags (“com”, “nonce0”, “nonce”, “s2”, “comm”, “pairwise_seed”) for all hash function uses to ensure random oracle independence.

Remark 13 (Nonce Range Rounding and Asymmetry). When γ_1 is not divisible by $|S|$, rounding slightly reduces the nonce range. This has negligible impact: for ML-DSA-65 with $|S| = 17$, the range loss is $< 2 \times 10^{-5}$ per coordinate and does not affect the z-bound check since $|S| \cdot \lfloor \gamma_1 / |S| \rfloor \geq \gamma_1 - (|S| - 1) > \gamma_1 - \beta$ (holds for all $|S| \leq \beta = 196$, i.e., $|S| < 197$, covering all practical configurations). See Appendix G for details.

Additionally, the threshold protocol uses a *symmetric* per-party nonce range

$$\{-\lfloor \gamma_1 / |S| \rfloor, \dots, \lfloor \gamma_1 / |S| \rfloor\},$$

whereas FIPS 204 single-signer ML-DSA uses the slightly *asymmetric* range $\{-\gamma_1 + 1, \dots, \gamma_1\}$ (omitting $-\gamma_1$). The statistical distance between the symmetric range $\{-\gamma_1, \dots, \gamma_1\}$ and the FIPS 204 range is $1/(2\gamma_1 + 1) < 2^{-20}$ per coordinate, and the full-vector statistical distance over $n\ell = 1280$ coefficients is bounded by $1280/(2\gamma_1 + 1) \approx 1.22 \times 10^{-3} < 2^{-9}$. This difference is negligible and is absorbed into the ϵ_{H} term of Theorem 2; it does not affect the security argument or FIPS 204 compatibility of the output signature format.

3.7 Correctness

Theorem 1 (Correctness). *If all parties are honest and the protocol does not abort, then $\text{Verify}(\text{pk}, \mu, \sigma) = 1$.*

Proof. The aggregated response is $\mathbf{z} = \sum_{i \in S} \lambda_i \mathbf{z}_i = \sum_{i \in S} \lambda_i (\mathbf{y}_i + c \cdot \mathbf{s}_{1,i}) = \sum_{i \in S} \lambda_i \mathbf{y}_i + c \cdot \sum_{i \in S} \lambda_i \mathbf{s}_{1,i} = \mathbf{y} + c \mathbf{s}_1$. Both $\{\mathbf{y}_i\}$ and $\{\mathbf{s}_{1,i}\}$ are degree- $(T-1)$ Shamir shares of \mathbf{y} and \mathbf{s}_1 respectively, evaluated at the same set of points: KeyGen assigns $\mathbf{s}_{1,j} = p_{\mathbf{s}_1}(j)$ using party indices $j \in [N]$, and the nonce DKG assigns $\mathbf{y}_j = \mathbf{F}(j)$ using the same evaluation domain (Algorithm 2). Hence the Lagrange coefficients λ_i for the signing set S apply equally to both sharings, and reconstruction yields both correct secrets simultaneously. The masked commitment aggregation gives $\mathbf{W} = \sum_i \mathbf{W}_i = \sum_i (\lambda_i \mathbf{w}_i + \mathbf{m}_i^{(w)}) = \mathbf{A} \sum_i \lambda_i \mathbf{y}_i = \mathbf{A} \mathbf{y} = \mathbf{w}$, where mask cancellation follows from Lemma 1. Since $\mathbf{z} = \mathbf{y} + c \mathbf{s}_1$ and $\mathbf{w} = \mathbf{A} \mathbf{y}$, verification proceeds as in single-signer ML-DSA. \square

Remark 14 (Implementation Notes). (1) Each party computes $\mathbf{z}_i = \mathbf{y}_i + c \cdot \mathbf{s}_{1,i}$ without applying the Lagrange coefficient λ_i . The combiner applies λ_i during aggregation: $\mathbf{z} = \sum_i \lambda_i \mathbf{z}_i$. While individual $\lambda_i \mathbf{z}_i$ may have large coefficients, the sum $\mathbf{z} = \mathbf{y} + c \mathbf{s}_1$ is short ($< q/2$), so mod q reduction is correct. (2) Signatures are FIPS 204-compatible: same format, size (3309 bytes for ML-DSA-65), and pass unmodified verifiers. Signer-side differences (Irwin-Hall nonces, nonce DKG, interactive protocol) do not affect security or verification.

3.8 Nonce Distribution and Security

The aggregated nonce $\mathbf{y} = \sum_{i \in S} \hat{\mathbf{y}}_i$ (the sum of each party’s constant-term contribution from the nonce DKG) follows an Irwin-Hall distribution concentrated around zero. This equals the Lagrange reconstruction $\mathbf{y} = \sum_{i \in S} \lambda_i \mathbf{y}_i$ by the following two-step argument: letting $\mathbf{F}(x) = \sum_{k \in S} \mathbf{f}_k(x)$ be the combined degree- $(T-1)$ polynomial, we have $\mathbf{F}(0) = \sum_{k \in S} \mathbf{f}_k(0) = \sum_{k \in S} \hat{\mathbf{y}}_k$ (direct, by definition of the constant term), and also $\mathbf{F}(0) = \sum_{i \in S} \lambda_i \mathbf{F}(i) = \sum_{i \in S} \lambda_i \mathbf{y}_i$ (Lagrange interpolation at 0). This preserves EUF-CMA security: using smooth Rényi divergence bounds from [dPEK⁺24], we compute per-coordinate $R_{2,\text{coord}}^\epsilon \leq 1.003$ for $|S| \leq 17$. Since nonce coordinates are sampled independently, the full-vector divergence is $R_2^{\text{vec}} = (R_{2,\text{coord}}^\epsilon)^{1280} \leq (1.003)^{1280} \approx 2^{5.5}$ for $|S| \leq 17$ (≈ 3 -bit security loss; exact: $(1.00292)^{1280} \approx 2^{5.4}$). For $|S| = 33$, $R_2^{\text{vec}} \approx 2^{75}$ (≈ 38 -bit loss). See Theorem 4 and Appendix D.

3.9 Abort Probability

The per-attempt success probability is comparable to single-signer ML-DSA ($\approx 20\%$; empirically ≈ 21 – 45% due to Irwin-Hall concentration and configuration-dependent variance). Without masking, success degrades as $(0.2)^T$ —for $T = 16$, this is 6.6×10^{-12} . Our masked approach achieves constant success rate, a speedup of 10^5 – $10^{21} \times$ (Appendix F).

3.10 The r0-Check Subprotocol

A critical component of ML-DSA signing that requires careful treatment in the threshold setting is the *r0-check*: verifying that $\|\text{LowBits}(\mathbf{w} - c \mathbf{s}_2, 2\gamma_2)\|_\infty < \gamma_2 - \beta$. This check ensures that the hint \mathbf{h} correctly recovers $\mathbf{w}_1 = \text{HighBits}(\mathbf{w})$ during verification.

The Challenge. In single-signer ML-DSA, the signer has direct access to \mathbf{s}_2 and can compute $\mathbf{w} - c \mathbf{s}_2$ directly. In our threshold setting, \mathbf{s}_2 is secret-shared among the parties, and no single party (including the combiner) knows the complete \mathbf{s}_2 .

Our Approach: Masked Reconstruction of cs_2 . We extend the pairwise-canceling mask technique to reconstruct cs_2 at the combiner while preserving privacy of individual shares:

1. Each party i computes $\mathbf{V}_i = \lambda_i \cdot c \cdot \mathbf{s}_{2,i} + \mathbf{m}_i^{(s_2)}$, where $\mathbf{m}_i^{(s_2)} \in R_q^k$ is a pairwise-canceling mask using domain separator nonce $\|s_2$.
2. The combiner aggregates: $\sum_{i \in S} \mathbf{V}_i = c \cdot \sum_i \lambda_i \mathbf{s}_{2,i} + \sum_i \mathbf{m}_i^{(s_2)} = cs_2$
3. The combiner computes $\mathbf{w} - cs_2$ and performs the r0-check locally.

Computing ct_0 for Hints. The hint computation requires ct_0 where $\mathbf{t}_0 = \mathbf{t} - \mathbf{t}_1 \cdot 2^d$. Since $\mathbf{t} = \mathbf{A}\mathbf{s}_1 + \mathbf{s}_2$, we have:

$$ct_0 = ct - ct_1 \cdot 2^d = c(\mathbf{A}\mathbf{s}_1 + \mathbf{s}_2) - ct_1 \cdot 2^d$$

The combiner can compute this as follows. First, cs_2 is obtained from the masked reconstruction above. Second, since $\mathbf{A}\mathbf{z} = \mathbf{A}(\mathbf{y} + cs_1) = \mathbf{w} + c\mathbf{A}\mathbf{s}_1$, we have $c\mathbf{A}\mathbf{s}_1 = \mathbf{A}\mathbf{z} - \mathbf{w}$. Combining these, $ct_0 = (\mathbf{A}\mathbf{z} - \mathbf{w}) + cs_2 - ct_1 \cdot 2^d$.

Security Consideration. The combiner learns cs_2 during r0-check. Since virtually all ML-DSA challenges are invertible in R_q (Monte Carlo: 100% of 10^4 samples), an adversary with (c, cs_2) can recover $\mathbf{s}_2 = c^{-1}(cs_2)$. Thus cs_2 must be protected.

Resolution. We address this via three deployment profiles (Table 2). In Profile P1 (TEE), cs_2 is computed inside the enclave and never exposed; ct_0 is derived from the formula above, and the hint \mathbf{h} is computed inside the enclave before output. In Profile P2 (MPC), parties jointly evaluate the r0-check *without reconstructing cs_2* : the MPC circuit extends to also compute $ct_0 = (\mathbf{A}\mathbf{z} - \mathbf{w}) + cs_2 - ct_1 \cdot 2^d$ using the internally-held intermediate cs_2 , and outputs $\mathbf{h} = \text{MakeHint}(-ct_0, \mathbf{A}\mathbf{z} - ct_1 \cdot 2^d, 2\gamma_2)$ directly (since MakeHint is a bitwise comparison of bounded-norm vectors, it adds only $O(knd)$ comparison gates to the r0-check circuit); cs_2 is never exposed outside the MPC. In Profile P3+ (2PC), two CPs each hold an additive share of cs_2 , so neither learns the complete value; hint computation proceeds analogously within the 2PC. See Section 6 for P2/P3 details.

4 Security Analysis

We prove that our masked threshold ML-DSA protocol achieves EUF-CMA security and statistical share privacy. This section contains proofs for all main results; full UC proofs for P2 and P3+ appear in Appendix H.

4.1 Security Model

We consider a static adversary \mathcal{A} that corrupts a set $C \subset [N]$ with $|C| < T$ before execution. The adversary controls corrupted parties, observes all broadcasts, and adaptively chooses messages to sign.

Trust Assumptions. Profile P1 (Primary): The coordinator runs in a TEE/HSM. The adversary cannot observe values computed inside the enclave (specifically cs_2); only the final signature $\sigma = (\tilde{c}, \mathbf{z}, \mathbf{h})$ exits the enclave. We model the enclave as ideal; compromise of the TEE is out of scope. Our theorems target this profile.

Remark 15 ($|S| \geq T$ Suffices in Coordinator-Based Profiles). With Shamir nonce DKG, Profiles P1 and P3+ require only $|S| \geq T$. The adversary observes: (1) nonce shares \mathbf{y}_h with high conditional min-entropy (statistical, Theorem 3); (2) r0-check shares \mathbf{V}_i never broadcast, staying inside the TEE/2PC; (3) masked commitments \mathbf{W}_i sent only to the coordinator, which publishes only \mathbf{w}_1 (already implicit in σ). Individual \mathbf{W}_i must stay private: if broadcast with $|S \setminus C| = 1$, the adversary could recover \mathbf{y}_h from $\lambda_h \mathbf{A} \mathbf{y}_h$ via linear algebra (since \mathbf{A} is generically injective [Nat24b, LPR10]), then extract $\mathbf{s}_{1,h}$. In P2, mask hiding (Lemma 2) protects broadcast \mathbf{W}_i under the existing $|S \setminus C| \geq 2$ condition; note that mask hiding applies only to \mathbf{W}_i and \mathbf{V}_i (which do not appear in the signature) and does *not* contribute to nonce share privacy—the latter is provided purely by the statistical properties of the nonce DKG (Theorem 3). Additionally, P2’s blame protocol (Section 6.1) assumes challenge invertibility (c invertible in R_q ; empirically $> 99.9\%$ of ML-DSA-65 challenges are invertible [Nat24b]); this invertibility claim is heuristic and does not constitute a formal negligibility bound.

1. **Nonce share \mathbf{y}_h :** Statistical privacy via nonce DKG (Theorem 3). The nonce share has high conditional min-entropy (no computational assumptions), holding even with $|S \setminus C| = 1$. **Key privacy given the signature σ is computational and not formally reduced to Module-LWE in this work;** it remains an open problem to provide a tight security reduction for the bounded-distance decoding problem $\mathbf{z}_h = \mathbf{y}_h + c \cdot \mathbf{s}_{1,h}$ when c is a sparse challenge and \mathbf{y}_h has bounded (but not short) coefficients. We note that single-signer ML-DSA faces the identical question: FIPS 204 [Nat24b] does not formally reduce key privacy (given signatures) to Module-LWE either.
2. **r0-check shares \mathbf{V}_i :** Never broadcast—processed inside the TEE (P1), as MPC inputs (P2), or via 2PC (P3+). Even with $|S \setminus C| = 1$, the adversary does not observe individual \mathbf{V}_h .
3. **Masked commitments \mathbf{W}_i :** Sent only to the coordinator (not broadcast). The coordinator publishes only $\mathbf{w}_1 = \text{HighBits}(\mathbf{W}, 2\gamma_2)$, which is already implicit in the signature (verifiers reconstruct \mathbf{w}_1 from $(\mathbf{A}, \mathbf{z}, c, \mathbf{h})$). This adds zero information to the adversary’s view.

Why individual \mathbf{W}_i must stay private. If \mathbf{W}_h were broadcast with $|S \setminus C| = 1$, the pairwise mask $\mathbf{m}_h^{(w)}$ would be computable by the adversary (all seeds involve corrupted counterparties), exposing $\lambda_h \mathbf{A} \mathbf{y}_h$. Since $\mathbf{A} \in R_q^{k \times \ell}$ with $k > \ell$ is generically injective (the NTT isomorphism $R_q \cong \mathbb{Z}_q^n$ [Nat24b] decomposes \mathbf{A} into n independent $k \times \ell$ matrices over \mathbb{Z}_q ; we heuristically model each as uniformly random and apply the \mathbb{Z}_q full-rank bound of [LPR10, Lemma 2.1] componentwise, giving full column rank with probability $\geq 1 - q^{\ell-k}$; this is the same standard heuristic used in ML-DSA [DKL⁺18, Nat24b]), the adversary could recover \mathbf{y}_h via linear algebra—this is *not* a Module-LWE instance because \mathbf{y}_h has full-size (not short) coefficients (i.e., coefficients drawn from $[-\lceil \gamma_1/|S| \rceil, \lceil \gamma_1/|S| \rceil]$ with $\lceil \gamma_1/|S| \rceil \approx 2^{19}/|S| \gg \eta = 4$; the Module-LWE hardness assumption requires error terms with small coefficients). Combined with \mathbf{z}_h (extractable from the public signature), this would yield $\mathbf{s}_{1,h} = c^{-1}(\mathbf{z}_h - \mathbf{y}_h)$, a complete key recovery (assuming c is invertible in R_q ; empirically, $> 99.9\%$ of ML-DSA-65 challenges are invertible [Nat24b]). The coordinator-only communication model eliminates this attack vector entirely. *Caveat for Profile P2 blame path:* In P2, the distributed blame protocol (Section 6.1) also relies on c -invertibility to verify party responses without a coordinator. The claim that $> 99.9\%$ of challenges are invertible is an empirical estimate and does not yield a cryptographically negligible failure probability; this invertibility argument for P2 blame verification is therefore heuristic, not a formal negligibility bound.

Profile-specific analysis. In P1, the TEE coordinator naturally keeps individual \mathbf{W}_i private. In P3+, the combiner serves as coordinator (trusted for privacy under the 1-of-2 CP honest assumption). In P2 (no designated coordinator), parties broadcast \mathbf{W}_i directly; mask hiding (Lemma 2) protects individual values under the existing $|S \setminus C| \geq 2$ condition, which P2 already requires.

4.2 Unforgeability

Theorem 2 (Unforgeability). *If Module-SIS is hard and H is a random oracle, then the masked threshold ML-DSA scheme is EUF-CMA secure. Using the direct shift-invariance bound (Corollary 8, Theorem 30), the Irwin-Hall nonce distribution introduces at most $q_s \times 6.1 \times 10^{-3}$ bits of security loss for $|S| \leq 17$ ($q_s \times 0.013$ bits for $|S| \leq 33$), where q_s is the number of signing queries. For $q_s \leq 1,600$ queries with $|S| \leq 17$, this is ≤ 9.8 bits, yielding a proven security bound of ≈ 86 bits under MSIS ($= 96 - 9.8$; the 96-bit baseline is a proof-technique artifact from Cauchy-Schwarz halving the 192-bit NIST Level 3 MSIS hardness once, identical to single-signer ML-DSA). The following bound holds via Rényi divergence:*

$$\begin{aligned} \text{Adv}_{\Pi}^{\text{EUF-CMA}}(\mathcal{A}) &\leq (R_2^{\text{vec,shift}})^{q_s/2} \cdot \sqrt{q_H \cdot \epsilon_{\text{M-SIS}} + \binom{N}{2} \cdot \epsilon_{\text{PRF}}} \\ &\quad + \frac{(q_H + q_s)^2}{2^{256}} + q_s \cdot \epsilon_{\text{IH}} \end{aligned}$$

where q_H, q_s are random oracle and signing queries, $R_2^{\text{vec,shift}} = (1 + \chi_{\text{direct}}^2)^{n\ell}$ is the full-vector per-session Rényi divergence from the direct shift-invariance analysis (here $n = 256$ is the ring degree, $\ell = 5$, giving $n\ell = 1280$) with per-coordinate $\chi_{\text{direct}}^2 \approx 6.62 \times 10^{-6}$ for $|S| = 17$ (Corollary 8), giving $R_2^{\text{vec,shift}} \approx 1.0085$, and $\epsilon_{\text{IH}} < 10^{-30}$ (smooth Rényi tail parameter, Theorem 4; note the per-coordinate empirical tail probability from the FFT computation is 2.3×10^{-20} for $|S| = 17$, Corollary 8—these are distinct quantities: the former is the smooth Rényi parameter used in the formal framework, the latter is the direct tail probability). The $(R_2^{\text{vec,shift}})^{q_s/2}$ factor accounts for multi-session Rényi composition (Remark 28): each of the q_s signing sessions contributes one factor of $R_2^{\text{vec,shift}}$ to the joint divergence. The total security loss is $\approx 6.1 \times 10^{-3} \cdot q_s$ bits, giving a **proven security bound of $\geq 96 - 0.006 \cdot q_s$ bits** for $|S| \leq 17$ (non-vacuous for $q_s < 16,000$; the 96-bit figure assumes $q_H = 1$ —see Remark 17 for the general q_H -dependent form, which is identical to the single-signer FIPS 204 convention). Our threshold construction adds only ≤ 10 bits of additional EUF-CMA loss from the Irwin-Hall nonce distribution for $q_s \leq 1,600$. The conservative Raccoon-style analytical bound is given in Remark 16.

Corollary 1 (Irwin-Hall Nonce Security Loss). *Under the conditions of Theorem 2, using the direct shift-invariance bound (Theorem 30, Corollary 8), the EUF-CMA security loss from Irwin-Hall nonces is $< 0.007 \cdot q_s$ bits for $|S| \leq 17$ and $< 0.013 \cdot q_s$ bits for $|S| \leq 33$, where q_s is the number of signing queries (multi-session composition; Remark 28). For $q_s = 1$ (single session), the per-session loss is < 0.007 bits ($|S| \leq 17$) or < 0.013 bits ($|S| \leq 33$). The single-session bound first exceeds 1 bit only at $|S| = 2584$, fully eliminating scalability as a per-session security concern.*

Proof. We reduce to Module-SIS via a sequence of game hops. Let Game_i denote the i -th game and Win_i the event that \mathcal{A} produces a valid forgery in Game_i .

Game₀ (Real). The real EUF-CMA game. Challenger runs KeyGen honestly, gives \mathcal{A} the public key pk and corrupted shares $\{\text{sk}_i\}_{i \in C}$. Signing oracle queries may return \perp (rejection abort); \mathcal{A} may re-issue the same or different queries. Security bounds are in terms of query counts q_s ; each attempt succeeds with non-negligible probability $\epsilon_{\text{acc}} \in [21\%, 45\%]$

depending on $|S|$ (see Table 5; comparable to single-signer ML-DSA's $\approx 25\%$), so all q_s successful queries complete in expected $O(q_s/\epsilon_{\text{acc}}) = O(q_s)$ attempts.

Game₁ (Random Oracle). Replace H with a lazily-sampled random function. By the random oracle model: $|\Pr[\text{Win}_1] - \Pr[\text{Win}_0]| = 0$.

Game₂ (Programmed Challenges). During signing, sample challenge $c \xleftarrow{\$} \mathcal{C}$ uniformly before computing \mathbf{w}_1 , then program $H(\mu \parallel \mathbf{w}_1) := c$. This fails only on collision. By birthday bound: $|\Pr[\text{Win}_2] - \Pr[\text{Win}_1]| \leq (q_H + q_s)^2/2^{256}$, where 2^{256} is the hash output space size (SHAKE-256 gives 256-bit challenges; this is a conservative bound since $|\mathcal{C}| < 2^{256}$).

Game₃ (Simulated Shares). The adversary's view reveals no information about honest parties' key shares: by (T, N) -Shamir perfect hiding, the joint distribution of the $T - 1$ corrupted evaluations is statistically independent of the secret \mathbf{s}_1 (though the evaluations themselves are correlated as points on a shared polynomial).

Important clarification: The signing oracle does *not* change in this hop — it continues using the actual short key shares $\{\mathbf{s}_{1,j}, \mathbf{s}_{2,j}\}_{j \notin \mathcal{C}}$ internally. Replacing those shares with $\mathbf{s}_{1,j} \xleftarrow{\$} R_q^\ell$ would cause the z-bound check ($\|\mathbf{z}\|_\infty \geq \gamma_1 - \beta$ almost surely for large $\mathbf{s}_{1,j}$) and the r0-check to fail with overwhelming probability, breaking correctness. This argument is purely about what the adversary *observes*: because honest shares are never directly visible to the adversary (see profile-specific paragraph below), the adversary's view is limited to the $|\mathcal{C}| \leq T - 1$ corrupted shares $\{\mathbf{s}_{1,i}\}_{i \in \mathcal{C}}$ and $\{\mathbf{s}_{2,i}\}_{i \in \mathcal{C}}$. By Shamir's perfect hiding, $T - 1$ evaluations of a degree- $(T - 1)$ polynomial reveal *no information* about the secret $\mathbf{s}_1 = \mathbf{f}(0)$: the conditional distribution of $\mathbf{f}(0)$ given any $T - 1$ evaluations is identical to the prior (marginal) distribution of $\mathbf{f}(0)$ (**statistical distance zero**: no event in the adversary's view distinguishes Game 2 from Game 3). A simulator in Game 3 samples corrupted shares $\{\mathbf{s}_{1,i}\}_{i \in \mathcal{C}}$ from the conditional Shamir distribution given \mathbf{s}_1 (computed via Lagrange interpolation with $T - |\mathcal{C}|$ uniformly random high-degree coefficients), which is identically distributed to the real key generation. Hence the adversary's view in Game₃ is identically distributed to that in Game₂, giving $\Pr[\text{Win}_3] = \Pr[\text{Win}_2]$.

Profile-specific observability of \mathbf{z}_j . In Profiles P1 and P3+, individual signer responses \mathbf{z}_j are transmitted only to the TEE coordinator or the honest CP, respectively, and are never observed by the adversary; the game hop is trivial. In Profile P2, \mathbf{z}_j is contributed to $\mathcal{F}_{\text{SPDZ}}$ for aggregation, which provides input privacy: only the aggregate $\mathbf{z} = \sum_{j \in S} \lambda_j \mathbf{z}_j$ is revealed. Since $\mathcal{F}_{\text{SPDZ}}$ hides individual \mathbf{z}_j , the adversary gains no information about $\mathbf{s}_{1,j}$ through \mathbf{z}_j in any profile. The Shamir replacement is therefore valid across all deployment profiles.

Game_{3.5} (Uniform Nonces). Replace the Irwin-Hall nonce distribution with uniform nonces: in each signing session, sample $\mathbf{y} \xleftarrow{\$} \{-\gamma_1, \dots, \gamma_1\}^{n_\ell}$ uniform instead of $\mathbf{y} = \sum_{i \in S} \hat{\mathbf{y}}_i$ (Irwin-Hall). The q_s signing sessions use independent nonce DKGs, so the per-session nonce distributions are i.i.d. copies of the Irwin-Hall distribution (convolution of $|S|$ uniform shares). By the *product rule* for Rényi-2 divergence (where $R_2(P||Q) = \sum_x P(x)^2/Q(x)$ in the ratio-sum convention): for independent sessions,

$$R_2^{\text{joint}} = (R_2^{\text{vec,shift}})^{q_s},$$

since the joint divergence factors as a product of per-session divergences (see Remark 28 for explicit derivation). By the Rényi-2 security bound (Theorem 4 with $\alpha = 2$, applied to the q_s -session joint distribution):

$$\Pr[\text{Win}_3] \leq (R_2^{\text{vec,shift}})^{q_s/2} \cdot \sqrt{\Pr[\text{Win}_{3.5}]} + q_s \cdot \epsilon_{\text{IH}}$$

where $R_2^{\text{vec,shift}} = (1 + \chi_{\text{direct}}^2)^{n\ell}$ is the full-vector Rényi divergence *per session* from the direct shift-invariance analysis (Theorem 30), with per-coordinate $\chi_{\text{direct}}^2 \approx 6.62 \times 10^{-6}$ for $|S| = 17$ (Corollary 8, $n\ell = 1280$), giving $R_2^{\text{vec,shift}} \approx 1.0085$ for $|S| = 17$. The tail probability satisfies $\epsilon_{\text{IH}} < 10^{-30}$ for $|S| \leq 17$ (this bound is $|S|$ -dependent; see Theorem 4 for the general formula as a function of $|S|$, n , and γ_1). This is the only game hop that incurs the Irwin-Hall security loss; nonce shares \mathbf{y}_j have high min-entropy by Theorem 3 (statistical, no computational assumptions). *Note on ϵ_{IH} :* The value $\epsilon_{\text{IH}} < 10^{-30}$ above is the smooth Rényi tail parameter from Raccoon Lemma 4.2 (Theorem 4, formal analytical bound). The ϵ column in Corollary 8 (2.3×10^{-20} for $|S| = 17$) is the per-coordinate empirical tail probability $\Pr[|Y_{\text{coord}}| > \gamma_1 - \beta]$ from the Direct Shift FFT computation—a distinct, looser quantity; both are negligible for all practical q_s . See Remark 28 for the concrete multi-session security accounting. The conservative Raccoon-style alternative (Remark 16) gives $R_2^{\text{vec}} \approx 2^{5.4}$ via the analytical bound, which is vacuous at $q_s \gtrsim 36$.

Game₄ (Simulated Signatures). Starting from uniform nonces (Game 3.5), simulate signing without knowing \mathbf{s}_1 : sample $\mathbf{z} \stackrel{\$}{\leftarrow} \{-\gamma_1 + \beta + 1, \dots, \gamma_1 - \beta - 1\}^{n\ell}$, compute $\mathbf{r} = \mathbf{A}\mathbf{z} - \mathbf{c}\mathbf{t}_1 \cdot 2^d$, set $\mathbf{w}_1 = \text{HighBits}(\mathbf{r}, 2\gamma_2)$, program $H(\mu \parallel \mathbf{w}_1) := c$, and set hint $\mathbf{h} = \mathbf{0}$ (zero hint; since $\text{UseHint}(\mathbf{0}, \mathbf{r}, 2\gamma_2) = \text{HighBits}(\mathbf{r}, 2\gamma_2) = \mathbf{w}_1$, verification passes with hint-weight $\|\mathbf{h}\|_1 = 0 \leq \omega$).

Remark on the hint distribution. The simulated hint $\mathbf{h} = \mathbf{0}$ differs in distribution from the real hint $\mathbf{h}_{\text{real}} = \text{MakeHint}(-\mathbf{c}\mathbf{t}_0, \mathbf{r}, 2\gamma_2)$ in Game 3.5, which may carry up to $\omega = 55$ nonzero bits. This substitution does *not* increase the adversary’s forging advantage. In Game 3.5 the real hint encodes partial information about the secret key component \mathbf{t}_0 (specifically, the “carry” pattern of $\text{LowBits}(\mathbf{r}, 2\gamma_2)$ relative to $\pm\gamma_2$, which depends on $\mathbf{c}\mathbf{t}_0 - \mathbf{c}\mathbf{s}_2$); by contrast, $\mathbf{h} = \mathbf{0}$ reveals *nothing* about the key. The adversary’s oracle view in Game 4 is therefore *strictly less informative* about the secret key than in Game 3.5, giving $\Pr[\text{Win}_4] \leq \Pr[\text{Win}_{3.5}]$ with *no additional loss* from the hint distribution change. (This is a standard observation in Dilithium-family proofs [Nat24b]: replacing a real hint with $\mathbf{0}$ is a valid simulation that removes rather than adds key leakage.)

The masked values \mathbf{W}_j require separate treatment by profile. In P1 and P3+, individual \mathbf{W}_j are transmitted *only* to the TEE coordinator or CP respectively and are never observable by the adversary; the adversary’s view contains only the aggregate $\mathbf{w}_1 = \text{HighBits}(\sum_j \mathbf{W}_j, 2\gamma_2)$, which is already implicit in σ — so the simulator need not produce individual \mathbf{W}_j at all, and Lemma 2 is not invoked for these profiles. In P2, parties broadcast individual \mathbf{W}_j ; the simulator produces each as uniform by Lemma 2, which applies since $|S \setminus C| \geq 2$ is a stated requirement of P2. By PRF security: $|\Pr[\text{Win}_4] - \Pr[\text{Win}_{3.5}]| \leq \binom{N}{2} \cdot \epsilon_{\text{PRF}}$ (there are $\binom{N}{2}$ pairwise PRF seeds established at key generation; a union bound over all honest-honest seed pairs gives this term, independent of q_s since each domain-separated session ID yields a fresh PRF input; for P1 and P3+ this term is vacuously 0 as the adversary does not observe individual \mathbf{W}_j , so the bound is conservative for those profiles). The change in \mathbf{z} -distribution between Game 3.5 (truncated shifted uniform: $\mathbf{y} + \mathbf{c}\mathbf{s}_1$ conditioned on $\|\mathbf{y} + \mathbf{c}\mathbf{s}_1\|_\infty < \gamma_1 - \beta$) and Game 4 (direct uniform on $\{-\gamma_1 + \beta + 1, \dots, \gamma_1 - \beta - 1\}^{n\ell}$) is absorbed by the SelfTargetMSIS reduction [KLS18]: the adversary \mathcal{B} extracts a valid SIS solution from any forgery $(\mathbf{z}^*, c^*, \mathbf{h}^*)$ satisfying $\|\mathbf{z}^*\|_\infty < \gamma_1 - \beta$, and this norm check is enforced identically in both games regardless of which simulated distribution \mathbf{z} was drawn from.

Reduction to M-SIS. In Game₄, we construct a SelfTargetMSIS adversary \mathcal{B} [KLS18]. Given SelfTargetMSIS instance $(\mathbf{A}, \mathbf{t}_1)$ with $\mathbf{A} \in R_q^{k \times \ell}$ and $\mathbf{t}_1 \in R_q^k$, \mathcal{B} uses $(\mathbf{A}, \mathbf{t}_1)$ directly as the threshold scheme’s verification key components and runs \mathcal{A} in Game₄, answering ROM queries by programming H uniformly at random, and recording all query-response pairs. \mathcal{B} picks a uniformly random index $i^* \in [q_H]$ as the “target” ROM query. When \mathcal{A}

outputs a forgery $(\mu^*, \mathbf{z}^*, c^*, \mathbf{h}^*)$, \mathcal{B} checks whether c^* equals the response at query i^* ; if not, \mathcal{B} aborts (probability $1/q_H$ of success). When the guess is correct, verification gives:

$$\text{HighBits}(\mathbf{A}\mathbf{z}^* - c^* \mathbf{t}_1 \cdot 2^d, 2\gamma_2) = \mathbf{w}_1^*$$

The verification equation expands as:

$$[\mathbf{A} \mid -\mathbf{t}_1 \cdot 2^d] \cdot \begin{bmatrix} \mathbf{z}^* \\ c^* \end{bmatrix} = 2\gamma_2 \mathbf{w}_1^* + \mathbf{r}_0^*$$

where $\mathbf{r}_0^* = \text{LowBits}(\mathbf{A}\mathbf{z}^* - c^* \mathbf{t}_1 \cdot 2^d, 2\gamma_2)$ satisfies $\|\mathbf{r}_0^*\|_\infty \leq \gamma_2$. The solution vector satisfies $\|(\mathbf{z}^*, c^*)\|_\infty \leq \max(\gamma_1 - \beta, 1) < \gamma_1$, solving the SelfTargetMSIS instance (known target $2\gamma_2 \mathbf{w}_1^*$, LowBits residual \mathbf{r}_0^*) with the appropriate norm bound. This is the SelfTargetMSIS direct reduction used in the FIPS 204 security proof [KLS18]. Since $\Pr[\mathcal{B} \text{ succeeds}] \geq \Pr[\text{Win}_4]/q_H$, we have $\Pr[\text{Win}_4] \leq q_H \cdot \epsilon_{\text{M-SIS}}$.

Conclusion. Games 4 and the M-SIS reduction give $\Pr[\text{Win}_{3.5}] \leq q_H \cdot \epsilon_{\text{M-SIS}} + \binom{N}{2} \cdot \epsilon_{\text{PRF}}$. Composing with the Rényi hop (Game 3 \rightarrow 3.5, joint divergence $(R_2^{\text{vec,shift}})^{q_s}$) via Lemma 17 and the birthday bound (Game 1 \rightarrow 2):

$$\text{Adv}_{\Pi}^{\text{EUF-CMA}}(\mathcal{A}) \leq (R_2^{\text{vec,shift}})^{q_s/2} \cdot \sqrt{q_H \cdot \epsilon_{\text{M-SIS}} + \binom{N}{2} \cdot \epsilon_{\text{PRF}}} + \frac{(q_H + q_s)^2}{2^{256}} + q_s \cdot \epsilon_{\text{IH}}$$

For ML-DSA-65 with $|S| \leq 17$: $R_2^{\text{vec,shift}} = (1 + \chi_{\text{direct}}^2)^{1280} \approx 1.0085$ (direct shift-invariance, Corollary 8); $\epsilon_{\text{IH}} < 10^{-30}$ (smooth Rényi tail parameter, Theorem 4); SHAKE-256 yields negligible ϵ_{PRF} . The security loss is $\approx 6.1 \times 10^{-3} \cdot q_s$ bits, giving a proven security bound of $\geq 96 - 0.006 \cdot q_s$ bits for $|S| \leq 17$ (non-vacuous for $q_s < 16,000$; conservative bound in Remark 16; 96-bit figure assumes $q_H = 1$, see Remark 17). \square

Remark 16 (Conservative Raccoon-Style Rényi Bound). The analytical Raccoon-style formula (Lemma 4.2 of [dPEK⁺24]) upper-bounds the per-coordinate Rényi divergence using $R_2^{\epsilon, \text{coord}} \leq 1 + |S|^4 \beta^2 / (4\gamma_1^2) \leq 1.003$ for $|S| \leq 17$, giving full-vector $R_2^{\text{vec}} = (R_2^{\epsilon, \text{coord}})^{1280} \approx 2^{5.4}$ and a multi-session loss of $\approx 2.7 \cdot q_s$ bits. This bound is *vacuous* for $q_s \gtrsim 36$ signing queries. Theorem 2 instead uses the direct FFT computation (Corollary 8, Theorem 30), which gives $\chi_{\text{direct}}^2 \approx 6.62 \times 10^{-6}$ per coordinate for $|S| = 17$, yielding $R_2^{\text{vec,shift}} \approx 1.0085$ —an improvement of $\approx 440\times$. The conservative bound should not be used for concrete security estimates.

Remark 17 (The 96-Bit Baseline and q_H Dependence). The “96-bit baseline” in Theorem 2 arises from applying Cauchy-Schwarz to the Rényi transfer: $\sqrt{q_H \cdot \epsilon_{\text{M-SIS}}} = 2^{-96}$ when $\epsilon_{\text{M-SIS}} = 2^{-192}$ (NIST Level 3 hardness) and $q_H = 1$. For q_H random oracle queries the pre-Irwin-Hall security baseline is $\frac{1}{2}(192 - \log_2 q_H)$ bits—e.g. 66 bits for $q_H = 2^{60}$. This q_H dependence is a standard proof-technique artifact of ROM-based Fiat-Shamir proofs and is identical in the single-signer FIPS 204 security analysis [KLS18, Nat24b]; it is not specific to the threshold construction. The Irwin-Hall security loss of $0.006 \cdot q_s$ bits (Corollary 8) is independent of q_H and represents the *additional* cost introduced by the threshold nonce sharing above the single-signer baseline.

4.3 Privacy

Theorem 3 (Statistical Share Privacy). *With Shamir nonce DKG, for any signing set S with $|S| \geq T$ and any coalition $C \subset S$ with $|C| \leq T - 1$: each honest party’s nonce share \mathbf{y}_h has conditional min-entropy*

$$H_\infty(\mathbf{y}_h \mid \text{View}_C^{\text{DKG}}) \geq nl \cdot \log_2(2[\gamma_1/|S|] + 1)$$

where $\text{View}_C^{\text{DKG}}$ consists of: (1) the corrupted parties' key shares; (2) nonce DKG evaluations $\{\mathbf{f}_h(j)\}_{j \in C}$ of the honest party's polynomial at corrupted indices; and (3) cross-evaluations $\{\mathbf{f}_{j'}(i)\}$ (for $j' \in S \setminus C$, $j' \neq h$, $i \in C$) of other honest parties' polynomials. (Equivalently, as corrupted parties generate their own polynomials, the adversary's view includes $\{\mathbf{f}_j\}_{j \in C}$ completely; the formal statement in Theorem 28 uses this equivalent conditioning.) The cross-evaluations $\{\mathbf{f}_{j'}(i)\}$ from other honest parties to corrupted parties do not affect the min-entropy of $\mathbf{f}_h(x_h)$: by Shamir's security theorem, $|C| \leq T - 1$ evaluations of any other degree- $(T - 1)$ polynomial $\mathbf{f}_{j'}$ are independent of its (irrelevant) constant term, and none of these evaluations are of \mathbf{f}_h itself. Additionally, since each $j \in C$ is corrupted, the adversary generated \mathbf{f}_j and knows all evaluations $\mathbf{f}_j(x_h)$ (sent privately to honest party h); these appear as a known additive constant $\sum_{j \in C} \mathbf{f}_j(x_h)$ in the share \mathbf{y}_h , which preserves the support size (and hence min-entropy) of the free term $\mathbf{f}_h(x_h)$.

For ML-DSA-65 ($n\ell = 1280$, $\gamma_1 = 2^{19}$), the bound equals approximately $1280 \cdot (20 - \log_2 |S|)$ bits (the exact formula $1280 \cdot \log_2(2\lceil\gamma_1/|S|\rceil + 1)$ differs by < 3 bits for $|S| \leq 17$)—over $5\times$ the short secret key entropy $H(\mathbf{s}_1) \leq 1280 \cdot \log_2 9 \approx 4058$ bits for $|S| \leq 17$. (Note: Shamir shares $\mathbf{s}_{1,h} = \mathbf{f}(h)$ for $h \neq 0$ are \mathbb{Z}_q -uniform and thus not short; the entropy comparison is against the underlying short secret $\mathbf{s}_1 = \mathbf{f}(0)$.) No computational assumptions are needed; the bound is purely statistical.

Proof. The adversary's knowledge about the honest party h 's polynomial \mathbf{f}_h consists of the evaluations $\{\mathbf{f}_h(j)\}_{j \in C}$ received during the nonce DKG. Since $|C| \leq T - 1$ and \mathbf{f}_h has degree $T - 1$ (hence T coefficients), the adversary has at most $T - 1$ linear equations in T unknowns. The solution space has dimension $T - |C| \geq 1$ (exactly 1 in the worst case $|C| = T - 1$).

Null space argument. The evaluation map $\mathbf{f}_h \mapsto (\mathbf{f}_h(j_1), \dots, \mathbf{f}_h(j_{|C|}))$ has a null space of dimension $T - |C| \geq 1$. In the worst case $|C| = T - 1$, the null space is spanned by $\mathbf{n}(x) = \prod_{j \in C} (x - x_j)$ (the unique monic degree- $(T - 1)$ polynomial with roots at $\{x_j\}_{j \in C}$). For $|C| < T - 1$, there are $T - |C| > 1$ free parameters, which can only *increase* the adversary's uncertainty; hence the stated bound is conservative and the proof below treats the hardest case $|C| = T - 1$. The set of polynomials consistent with the adversary's observations is $\mathbf{f}_h(x) = \mathbf{g}(x) + \mathbf{t} \cdot \mathbf{n}(x)$, where \mathbf{g} is any fixed interpolant and $\mathbf{t} \in R_q^\ell$ is the free parameter.

Posterior constraint on \mathbf{t} . The highest-degree coefficient $\mathbf{a}_{h,T-1}$ is sampled R_q^ℓ -uniformly *a priori*, so $\mathbf{t} = \mathbf{a}_{h,T-1} - \mathbf{g}_{T-1}$ is \mathbb{Z}_q -uniform per coefficient (the other high-degree coefficients are likewise \mathbb{Z}_q -uniform but are already determined by the adversary's evaluations in the $|C| = T - 1$ case). The constant term $\hat{\mathbf{y}}_h = \mathbf{f}_h(0) = \mathbf{g}(0) + \mathbf{t} \cdot \mathbf{n}(0)$ must satisfy the bounded-nonce constraint $\hat{\mathbf{y}}_h \in [-\lceil\gamma_1/|S|\rceil, \lceil\gamma_1/|S|\rceil]^{n\ell}$. Since $\mathbf{n}(0) = \prod_{j \in C} (-x_j) \neq 0 \pmod{q}$, multiplication by $\mathbf{n}(0)$ is a bijection on \mathbb{Z}_q ; the constraint selects exactly $2\lceil\gamma_1/|S|\rceil + 1$ values per coefficient of \mathbf{t} . Because the prior is \mathbb{Z}_q -uniform, conditioning on membership in this subset yields a *uniform* posterior over the $2\lceil\gamma_1/|S|\rceil + 1$ valid values per coefficient.

Min-entropy bound. Since $\mathbf{n}(x_h) = \prod_{j \in C} (x_h - x_j) \neq 0 \pmod{q}$ (because q is prime and all evaluation points lie in $\{1, \dots, N\}$ with $N \leq q - 1$, so they are distinct nonzero elements of \mathbb{Z}_q), multiplication by $\mathbf{n}(x_h)$ is a bijection on \mathbb{Z}_q . The honest party's evaluation $\mathbf{f}_h(x_h) = \mathbf{g}(x_h) + \mathbf{t} \cdot \mathbf{n}(x_h)$ therefore inherits the same per-coefficient support size. The full nonce share is

$$\mathbf{y}_h = \underbrace{\sum_{j \in C} \mathbf{f}_j(x_h)}_{\text{known to } \mathcal{A}} + \mathbf{f}_h(x_h) + \underbrace{\sum_{j \in S \setminus C, j \neq h} \mathbf{f}_j(x_h)}_{\text{unknown to } \mathcal{A}; \text{ adds further entropy}} .$$

The first sum is a known constant (from corrupted parties' polynomials). The third sum is unknown (each $\mathbf{f}_j(x_h)$ with $j \neq h$ honest was sent only to party h), and the

individual terms $\mathbf{f}_j(x_h)$ for distinct honest parties $j, j' \in S \setminus (C \cup \{h\})$ are *independent* conditional on the adversary's view: each polynomial \mathbf{f}_j is sampled independently, and the adversary observes only evaluations $\{\mathbf{f}_j(i)\}_{i \in C}$ with $i \neq x_h$ (since $h \notin C$); these $|C| \leq T - 1$ evaluations determine a $(T - |C|)$ -dimensional affine subspace of polynomials, within which the evaluation $\mathbf{f}_j(x_h)$ remains uniformly distributed over a set of size $q^{n\ell(T-|C|)}$ (the null space dimension). Since the adversary's observations of different honest polynomials involve disjoint evaluation sets (each \mathbf{f}_j evaluated only at corrupted parties' points $\{i \in C\}$, which do not include x_h), the conditional distributions of $\mathbf{f}_j(x_h)$ and $\mathbf{f}_{j'}(x_h)$ are independent, so the third sum can only increase entropy. Using only the entropy contribution from $\mathbf{f}_h(x_h)$ as a conservative lower bound (discarding the additional entropy from the third sum):

$$H_\infty(\mathbf{y}_h \mid \text{View}_C^{\text{DKG}}) \geq n\ell \cdot \log_2(2\lceil \gamma_1/|S| \rceil + 1)$$

□

Remark 18 (Key Privacy of the Aggregated Signature). Theorem 3 establishes privacy of the nonce *shares* \mathbf{y}_h —a purely statistical guarantee requiring no computational assumptions. Key privacy of the aggregated signature $\sigma = (\tilde{c}, \mathbf{z}, \mathbf{h})$ —whether σ reveals \mathbf{s}_1 beyond the public key \mathbf{t}_1 —is a separate, stronger property not established in this work. It remains an open problem in the broader ML-DSA literature, unresolved even for single-signer FIPS 204: the equation $\mathbf{z} = \mathbf{y} + c\mathbf{s}_1$ with sparse challenge c does not directly reduce to a standard Module-LWE instance, and no formal reduction is known. All threshold variants inherit this open problem from the single-signer setting.

Remark 19 (Why $\text{SD} = 0$ Is Unattainable (with Derivation)). The bounded-nonce constraint ($\hat{\mathbf{y}}_h \in [-\lceil \gamma_1/|S| \rceil, \lceil \gamma_1/|S| \rceil]^{n\ell}$) restricts the free parameter \mathbf{t} to $\approx 2\gamma_1/|S|$ values per coefficient, whereas \mathbb{Z}_q -uniformity would require $q \approx 2^{23}$ values.

Derivation of SD lower bound. Let P_{post} be the posterior distribution of a single coefficient of $\mathbf{f}_h(x_h)$ given the adversary's view (Theorem 3 shows this is uniform over $M = 2\lceil \gamma_1/|S| \rceil + 1$ values), and let P_{unif} be the uniform distribution over \mathbb{Z}_q . The statistical distance is:

$$\begin{aligned} \text{SD}(P_{\text{post}}, P_{\text{unif}}) &= \frac{1}{2} \sum_{x \in \mathbb{Z}_q} |P_{\text{post}}(x) - P_{\text{unif}}(x)| \\ &= \frac{1}{2} \left(M \cdot \left| \frac{1}{M} - \frac{1}{q} \right| + (q - M) \cdot \frac{1}{q} \right) \\ &= \frac{1}{2} \left(\left| 1 - \frac{M}{q} \right| + \frac{q-M}{q} \right) \\ &= 1 - \frac{M}{q} = 1 - \frac{2\lceil \gamma_1/|S| \rceil + 1}{q} > 0 \end{aligned}$$

For ML-DSA-65 with $\gamma_1 = 2^{19}$, $q = 8,380,417$, and $|S| = 17$: $M = 2\lceil 2^{19}/17 \rceil + 1 = 61,681$, so $\text{SD} = 1 - M/q \approx 1 - 2 \cdot 2^{19}/(17 \cdot q) \approx 1 - 2^{20}/(17 \cdot 2^{23}) = 1 - 2^{-3}/17 \approx 0.9926 > 0$ (very far from zero).

Achieving $\text{SD} = 0$ would require either unbounded nonces (incompatible with rejection sampling) or adding pairwise masks on \mathbf{z}_i with $|S| \geq T + 1$ (Two-Honest assumption). The min-entropy guarantee is nonetheless strong: for $|S| \leq 17$, nonce entropy exceeds secret key entropy by $\geq 5\times$, ensuring robust share privacy without computational assumptions.

Corollary 2 (No Two-Honest Requirement in Coordinator-Based Profiles). *In Profiles P1 and P3+, the protocol achieves nonce share privacy with $|S| = T$. In Profile P2, mask hiding (Lemma 2) applies under $|S \setminus C| \geq 2$.*

Proof. Immediate from Theorem 3 and the coordinator communication model (Remark 11). In P1 and P3+, the coordinator aggregates \mathbf{W}_i privately and broadcasts only $(\mathbf{w}_1, \tilde{c})$, which is implicit in any valid signature. The nonce share \mathbf{y}_h has high conditional min-entropy

even with $|S \setminus C| = 1$ (statistical, by Theorem 3); key privacy of the aggregated σ is conjectured to hold computationally under Module-LWE (see Remark 18; formal reduction is an open problem). The mask-hiding condition $|S \setminus C| \geq 2$ (Lemma 2) applies only to P2 where \mathbf{W}_i are broadcast. \square

Corollary 3 (Multi-Session Privacy). *Let $M_S = 2\lceil \gamma_1/|S| \rceil + 1$. Over K sessions with fresh nonce DKGs, total nonce min-entropy is at least $Kn\ell \cdot \log_2 M_S$ bits. For $|S| \leq 17$, this exceeds $K \cdot 20,000$ bits. Key privacy across sessions is computational (multi-sample bounded-distance decoding under Module-LWE).*

Proof. Each signing session uses a fresh nonce DKG with independent randomness, so the free parameters $\mathbf{t}^{(1)}, \dots, \mathbf{t}^{(K)}$ are independent. The min-entropy of a product of independent distributions equals the sum: $H_\infty(\mathbf{y}_h^{(1)}, \dots, \mathbf{y}_h^{(K)} \mid \text{View}_C) = \sum_k H_\infty(\mathbf{y}_h^{(k)} \mid \text{View}_C^{(k)})$. The adversary accumulates K equations $\mathbf{z}_h^{(k)} = \mathbf{y}_h^{(k)} + c^{(k)} \cdot \mathbf{s}_{1,h}$ sharing the same $\mathbf{s}_{1,h}$; after sufficiently many sessions, $\mathbf{s}_{1,h}$ is uniquely determined by the overdetermined linear system $\mathbf{z}_h^{(k)} = \mathbf{y}_h^{(k)} + c^{(k)} \cdot \mathbf{s}_{1,h}$ over \mathbb{Z}_q (as in single-signer ML-DSA). Key privacy across multiple sessions is therefore *computational*: extracting $\mathbf{s}_{1,h}$ from these equations amounts to a multi-sample bounded-distance decoding problem, which is hard under the Module-LWE assumption. \square

Lemma 2 (Mask Hiding (for \mathbf{V}_i and \mathbf{W}_i)). *An honest party's masked r0-check share $\mathbf{V}_j = \lambda_j \mathbf{c}_{s2,j} + \mathbf{m}_j^{(s2)}$ and masked commitment $\mathbf{W}_j = \lambda_j \mathbf{w}_j + \mathbf{m}_j^{(w)}$ are computationally indistinguishable from uniform, given all information available to a coalition of $< T$ parties, provided $|S \setminus C| \geq 2$.*

Proof. Since $|S \setminus C| \geq 2$, party j 's mask includes a PRF term $\text{PRF}(\text{seed}_{j,k'}, \text{session_id} \parallel \text{dom})$ for some honest $k' \neq j$, where session_id is the unique per-signing-session identifier (e.g., derived from the preprocessed nonce commitment Com_j) and dom is the fixed domain label for \mathbf{V} or \mathbf{W} . Because $\text{seed}_{j,k'}$ is unknown to \mathcal{A} and session_id is fresh each session, $\text{PRF}(\text{seed}_{j,k'}, \text{session_id} \parallel \text{dom})$ is computationally indistinguishable from a fresh uniform element of R_q^k by PRF security. Thus $\mathbf{V}_j = (\text{fixed}) + (\text{uniform-looking}) \stackrel{c}{\approx} \text{uniform}$. The same argument applies to \mathbf{W}_j .

Note: Mask hiding requires $|S \setminus C| \geq 2$. In P1 and P3+, individual \mathbf{W}_i are sent only to the coordinator (Remark 11), so mask hiding for \mathbf{W}_i is only needed in P2 where parties broadcast directly. The nonce share \mathbf{y}_i achieves statistical privacy with even $|S \setminus C| = 1$ via the nonce DKG (Theorem 3); key privacy given σ is conjectured to hold computationally under Module-LWE (open problem; see Remark 18), independent of mask hiding. \square

4.4 Nonce Distribution Security

Our threshold protocol produces nonces following an Irwin-Hall distribution rather than uniform. Using smooth Rényi divergence analysis [dPEK⁺24], we prove this introduces only a bounded security loss.

Theorem 4 (Security with Irwin-Hall Nonces). *Let Π be our threshold ML-DSA with Irwin-Hall nonces. For any PPT adversary making q_S signing queries:*

$$\text{Adv}_{\Pi}^{\text{EUF-CMA}}(\mathcal{A}) \leq (R_2^{\text{vec}})^{q_S/2} \cdot \sqrt{\text{Adv}_{\Pi^*}^{\text{EUF-CMA}}(\mathcal{A})} + q_S \cdot \epsilon$$

where the per-coordinate smooth Rényi divergence satisfies $R_2^{\epsilon, \text{coord}} \leq 1 + |S|^4 \beta^2 / (4\gamma_1^2)$ (see Appendix Q, Theorem 29; the formula uses the signing set size $|S|$, not the ring degree $n = 256$). Since nonce coordinates are sampled independently, the full-vector divergence is $R_2^{\text{vec}} = (R_2^{\epsilon, \text{coord}})^{n\ell}$ with $n\ell = 1280$ for ML-DSA-65. The $(R_2^{\text{vec}})^{q_S/2}$ factor accounts for multi-session composition (Remark 28). The tail probability satisfies $\epsilon < 10^{-30}$.

Proof. The smooth Rényi divergence probability transfer (Cauchy-Schwarz) gives: for any event E , $\Pr_P[E] \leq \sqrt{R_2^\epsilon(P\|Q) \cdot \Pr_Q[E]} + \epsilon$. For q_S independent signing sessions, the joint Rényi divergence is $(R_2^{\text{vec}})^{q_S}$ by the product rule (Definition 23), giving the $(R_2^{\text{vec}})^{q_S/2}$ factor above. Since the nonce coordinates are sampled independently, $R_2^{\text{vec}} = (R_2^{\epsilon, \text{coord}})^{n\ell}$. For ML-DSA-65 ($n\ell = 1280$, $\text{Adv}_{\Pi^*} \leq 2^{-192}$, $\epsilon < 2^{-100}$), the *per-session* cost is:

$$q_S = 1: \quad \text{Adv}_{\Pi} \leq (R_2^{\text{vec}})^{1/2} \cdot 2^{-96} + 2^{-100}$$

$ S $	$R_2^{\epsilon, \text{coord}}$	R_2^{vec}	Per-session bound ($q_S = 1$): $\sqrt{R_2^{\text{vec}}} \cdot 2^{-96}$
≤ 17	1.003	$\leq 2^{5.5}$ ($\approx 2^{5.4}$)	$\approx 2^{-93.3}$
≤ 25	1.014	$\approx 2^{25}$	$\approx 2^{-83.5}$
≤ 33	1.041	$\approx 2^{75}$	$\approx 2^{-58.5}$

Multi-session scaling. The conservative bound $(R_2^{\text{vec}})^{q_S/2}$ grows rapidly: for $|S| = 17$, it is vacuous for $q_S \gtrsim 36$ queries. The *direct* bound (Corollary 8) should always be used for concrete security estimates: the EUF-CMA loss is $< 0.013 \cdot q_S$ bits for all $|S| \leq 33$ (Remark 28). Detailed conservative calculations appear in Appendix D. \square

4.5 Malicious Security

Our protocol uses an *optimistic* approach: the normal signing path has no verification overhead. If failures exceed statistical expectation (e.g., > 33 consecutive aborts, where honest probability is $(0.75)^{33} < 10^{-4}$), a blame protocol identifies misbehaving parties (see Section 6.1).

4.6 Concrete Security Bounds

Table 3: Concrete security of masked threshold ML-DSA-65. Parameters match NIST Security Level 3. *Underlying M-SIS hardness is 192 bits; the proven threshold bound adds an Irwin-Hall nonce cost via $R_2^{\text{vec}} = (R_2^{\epsilon, \text{coord}})^{1280}$: per-session bound $\leq (R_2^{\text{vec}})^{1/2} \cdot 2^{-96} \approx 2^{-93.3}$ for $|S| \leq 17$ (Theorem 4); over q_s sessions the total loss is $< 0.013 \cdot q_s$ bits (Corollary 8, Remark 28). The direct bound supports $q_s \leq 1,600$ with ≤ 10 -bit loss. †Nonce privacy is statistical (no computational assumptions); key privacy given σ follows computationally under M-LWE. See Theorem 3.

Attack	Assumption	Security
Forgery	M-SIS(256, 6, 5, $q, \gamma_1 - \beta$)	192 bits*
Key Recovery	M-LWE(256, 6, 5, q, η)	192 bits
Nonce Privacy (\mathbf{y}_i)	Statistical ($\geq 20\text{K}$ bits min-entropy)	N/A†
Mask Privacy ($\mathbf{V}_i, \mathbf{W}_i$)	PRF	192 bits

The threshold construction inherits the M-SIS/M-LWE hardness of single-signer ML-DSA. The proven forgery bound uses the direct shift-invariance analysis (Theorem 30, Corollary 8), giving < 0.013 bits per signing session for $|S| \leq 33$ ($< 0.013 \cdot q_s$ bits total; Corollary 1), resolving the scalability concern of prior work; developing an even tighter full-vector bound remains an interesting direction. The conservative Raccoon-style bound is in Remark 16.

4.7 Security Across Deployment Profiles

All three deployment profiles (P1, P2, P3+) achieve identical EUF-CMA security bounds, as the final signature structure $\sigma = (\tilde{c}, \mathbf{z}, \mathbf{h})$ is independent of the profile used. Additionally, all three profiles achieve UC security under their respective trust assumptions.

Definition 8 (Ideal Signing Functionality $\mathcal{F}_{\text{ThreshSig}}$). The functionality $\mathcal{F}_{\text{ThreshSig}}(T, N, \text{pp})$ operates as follows, where $\mathbf{z}_i \in R_q^\ell$ denotes each party’s response share and $\mathbf{V}_i \in R_q^k$ its r0-check share. On receiving $(\text{SIGN}, \text{sid}, \mu)$ from the combiner together with T input shares $\{(\mathbf{z}_i, \mathbf{V}_i)\}_{i \in S}$ for $S \subseteq [N]$, $\mathcal{F}_{\text{ThreshSig}}$:

1. **Format check:** If $|S| < T$ or any input share fails the format constraint ($\mathbf{z}_i \notin R_q^\ell$ or $\mathbf{V}_i \notin R_q^k$), output \perp immediately to the combiner without querying \mathcal{S} .
2. Forwards $(\text{SIGN}, \text{sid}, \mu, S)$ to the simulator \mathcal{S} and awaits a signature σ .
3. Outputs σ to the combiner if $\text{Verify}(\text{pk}, \mu, \sigma) = 1$; otherwise outputs \perp .

Clarification on EUF-CMA vs. ideal functionality. The verification check in step 3 is a sanity check ensuring the simulator produces well-formed output; it does *not* implement EUF-CMA security (which is proven separately via game-based reduction). If an adversary constructs a valid forgery (μ', σ') for $\mu' \neq \mu$, the ideal functionality accepts it in step 3, but this does not violate security—the adversary wins the EUF-CMA game, which occurs with negligible probability by Theorem 2.

The functionality reveals to \mathcal{S} : the message μ , the signing-set S , and the outputs of corrupted parties $\{(\mathbf{z}_i, \mathbf{V}_i)\}_{i \in C}$, where $C \subseteq S$ is the corrupted set). It does not reveal any honest party’s key share $(\mathbf{s}_{1,h}, \mathbf{s}_{2,h})$ or nonce share \mathbf{y}_h to \mathcal{S} .

4.7.1 Profile P1 UC Security

We model the TEE as an ideal functionality that correctly executes the r0-check and hint computation.

Definition 9 (TEE Ideal Functionality \mathcal{F}_{TEE}). The functionality \mathcal{F}_{TEE} operates as follows.

Round 2. Receive $\{(\mathbf{W}_i, r_i)\}_{i \in S}$ privately. Compute $\mathbf{W} = \sum_i \mathbf{W}_i$, $\mathbf{w}_1 = \text{HighBits}(\mathbf{W}, 2\gamma_2)$, $\tilde{c} = H_{\text{chal}}(\mu \| \mathbf{w}_1)$; broadcast $(\mathbf{w}_1, \tilde{c})$. Individual \mathbf{W}_i are never revealed.

Round 3. Receive $\{(\mathbf{z}_i, \mathbf{V}_i)\}_{i \in S}$. Aggregate: $\mathbf{z} = \sum_i \lambda_i \mathbf{z}_i \bmod q$, $\mathbf{c}\mathbf{s}_2 = \sum_i \mathbf{V}_i \bmod q$. Abort with \perp if $\|\mathbf{z}\|_\infty \geq \gamma_1 - \beta$ or $\|\text{LowBits}(\mathbf{w} - \mathbf{c}\mathbf{s}_2, 2\gamma_2)\|_\infty \geq \gamma_2 - \beta$. Otherwise compute $\mathbf{h} = \text{MakeHint}(-\mathbf{c}\mathbf{t}_0, \mathbf{A}\mathbf{z} - \mathbf{c}\mathbf{t}_1 \cdot 2^d, 2\gamma_2)$; output $(\tilde{c}, \mathbf{z}, \mathbf{h})$. Never reveal $\mathbf{c}\mathbf{s}_2$ or individual \mathbf{W}_i .

Theorem 5 (Profile P1 UC Security). *If the TEE correctly implements \mathcal{F}_{TEE} , then Protocol P1 UC-realizes the threshold signing functionality $\mathcal{F}_{\text{ThreshSig}}$ against static adversaries corrupting up to $T - 1$ signing parties.*

Proof. We construct an explicit simulator \mathcal{S} for each protocol round and prove indistinguishability.

Simulator construction.

1. **Round 0 (DKG):** \mathcal{S} generates honest key shares $\mathbf{s}_{1,h}, \mathbf{s}_{2,h}$ and nonce shares \mathbf{y}_h inside the simulated \mathcal{F}_{TEE} , following the real key DKG and nonce DKG protocols. Since DKG outputs to corrupted parties are determined by the (T, N) -Shamir sharing structure, \mathcal{S} produces consistent evaluations $\{\mathbf{f}_h(j)\}_{j \in C}$.
2. **Round 1 (Commitments):** \mathcal{S} samples $\tilde{\mathbf{y}}_h, \tilde{\mathbf{w}}_h, \tilde{r}_h$ from the simulated DKG, computes the committed value $\text{Com}_h \xleftarrow{\$} \{0, 1\}^{256}$ uniformly, and programs the random oracle so that $H(\text{“com”} \| \tilde{\mathbf{y}}_h \| \tilde{\mathbf{w}}_h \| \tilde{r}_h) = \text{Com}_h$ (using the same domain separator as the real commitment scheme $\text{Com}_i = H(\text{“com”} \| \mathbf{y}_i \| \mathbf{w}_i \| r_i)$). By commitment hiding (preimage resistance of H), the uniform Com_h is indistinguishable from real commitments. If the blame protocol requests an opening of Com_h , \mathcal{S} provides $(\tilde{\mathbf{y}}_h, \tilde{\mathbf{w}}_h, \tilde{r}_h)$, which verifies correctly by the programmed RO.

3. **Round 2 ($\mathbf{W}_i \rightarrow$ coordinator):** \mathcal{S} computes $\mathbf{W}_h = \lambda_h \mathbf{A} \mathbf{y}_h + \mathbf{m}_h^{(w)}$ from the simulated DKG values and PRF masks. \mathcal{F}_{TEE} aggregates internally and broadcasts only $(\mathbf{w}_1, \tilde{c})$. Individual \mathbf{W}_h never reach the adversary.
4. **Round 3 (Responses):** \mathcal{S} computes $\mathbf{z}_h = \mathbf{y}_h + c \cdot \mathbf{s}_{1,h}$ from simulated DKG values. This is identical to the real computation ($\text{SD} = 0$). Masked shares $\mathbf{V}_h = \lambda_h c \mathbf{s}_{2,h} + \mathbf{m}_h^{(s2)}$ are computed analogously.

Indistinguishability. The adversary’s view in the real and simulated executions is indistinguishable for the following reasons:

- **Response \mathbf{z}_h :** Computed identically from simulated DKG values ($\text{SD} = 0$). The simulator has access to the honest party’s key share $\mathbf{s}_{1,h}$ because it generated $\{\mathbf{s}_{1,j}\}$ during the simulated DKG (Round 0, setup step). The nonce share \mathbf{y}_h has high conditional min-entropy by Theorem 3 (statistical); key privacy given σ is conjectured to hold computationally under Module-LWE (open problem; see Remark 18).
- **TEE outputs:** \mathcal{F}_{TEE} hides all internal state (individual \mathbf{W}_i, cs_2); only $(\mathbf{w}_1, \tilde{c}, \sigma)$ exit the enclave, all of which are implicit in the signature.
- **Masks:** Replacing honest-honest PRF terms with uniform introduces advantage $\leq \binom{N}{2} \cdot \epsilon_{\text{PRF}}$.

Abort handling. The honest per-attempt success probability is $\approx 25\%$ (rejection sampling). After > 33 consecutive failures, honest probability is $(0.75)^{33} < 10^{-4}$, triggering the blame protocol (Section 6.1). The simulator handles aborts by forwarding \perp from \mathcal{F}_{TEE} .

Total distinguishing advantage: $\binom{N}{2} \cdot \epsilon_{\text{PRF}}$ (nonce share privacy is statistical and contributes zero to the PRF-based advantage). \square

Remark 20 (TEE Trust Assumption). Theorem 5 assumes the TEE is *ideal*—it correctly executes the specified computation and reveals nothing beyond the output. This is a hardware trust assumption, not a cryptographic one. In practice, TEE security depends on the specific implementation (Intel SGX, ARM TrustZone, etc.) and is subject to side-channel attacks. Profiles P2 and P3+ eliminate this assumption via cryptographic protocols.

4.7.2 Profile P3+ Semi-Async Security Model

Profile P3+ introduces a *semi-asynchronous* execution model where signers participate within a bounded time window rather than synchronizing for multiple rounds. This requires extending the UC framework to handle timing.

Definition 10 (Semi-Async Timing Model (Formalized)). The semi-async model extends the standard UC framework with bounded-time windows. Execution proceeds in *optimistic synchronous phases* with timeout-based fallback:

1. **Pre-signing window** $[t_0, t_1]$: Signers may precompute nonces $(\mathbf{y}_i, \mathbf{w}_i, \text{Com}_i)$ at any time before t_1 . This is an asynchronous phase; early precomputation is allowed but not required.
2. **Challenge broadcast** t_2 : Combiner derives challenge c from aggregated commitments and broadcasts (c, μ) to all signers at time t_2 . This is a synchronous event (all parties receive the broadcast at the same logical time in the UC model).

3. **Response window** $[t_2, t_2 + \Delta]$: Honest signers *should* respond within window Δ (e.g., 5 minutes for human-in-the-loop scenarios). Adversary scheduling rules:
 - **Honest party delivery**: Messages from honest signers arriving within $[t_2, t_2 + \Delta]$ are guaranteed to be delivered to the combiner.
 - **Adversarial delay**: The adversary may delay delivery of honest parties' messages by up to Δ , but cannot prevent delivery entirely (eventual delivery assumption).
 - **Timeout**: If fewer than T responses arrive by $t_2 + \Delta$, the combiner aborts the session and outputs \perp . This is *not* a security failure—it is an availability event (honest signers who responded late are still secure; no key material is leaked).
 - **Message reordering**: The adversary may reorder messages from different parties arriving within the window, but cannot inject or modify honest parties' messages (authenticated channels assumption).
4. **2PC execution** $[t_3, t_4]$: Synchronous 2PC between the two CPs (standard UC model applies; this phase has no timing relaxation).

UC adversary capabilities. The adversary observes message arrival times (timestamps) within the response window but cannot control the content or the fact of delivery for honest parties. Replay attacks are prevented via unique session identifiers sid binding each response to (c, μ) . The model is *semi-asynchronous* in the sense that signers do not need to coordinate their response times (unlike multi-round MPC), but the protocol remains UC-secure as long as $\geq T$ responses arrive within Δ .

Theorem 6 (Profile P3+ UC Security (Semi-Async)). *Under the semi-async timing model, Protocol P3+ UC-realizes $\mathcal{F}_{r_0}^{2PC}$ in the $(\mathcal{F}_{OT}, \mathcal{F}_{GC})$ -hybrid model against static adversaries corrupting up to $T - 1$ signers and at most one CP, assuming:*

1. *Garbled circuits are secure (Yao's protocol)*
2. *Oblivious transfer is UC-secure*
3. *PRF is secure*
4. *At least one CP remains honest*

Security bound: $\epsilon \leq \epsilon_{GC} + \epsilon_{OT} + \epsilon_{\text{ext}} + \binom{N}{2} \cdot \epsilon_{\text{PRF}}$, where $\epsilon_{\text{ext}} \leq 2^{-B/2}$ is the LP07 cut-and-choose extraction error (for corrupted CP_1). *By UC composition (using the nonce DKG and signing sub-protocols as ideal functionalities), this implies that Protocol P3+ UC-realizes the full $\mathcal{F}_{\text{ThreshSig}}$ under the same assumptions.*

Proof sketch (full proof in Appendix P). The simulator replaces OT and GC with ideal functionalities $(\epsilon_{OT} + \epsilon_{GC})$, then simulates pre-signing by sampling $\tilde{\mathbf{y}}_i$ and computing $\tilde{\mathbf{w}}_i = \mathbf{A}\tilde{\mathbf{y}}_i$ (Lemma 12, $\text{SD} = 0$), and simulates responses via $\mathbf{z}_i = \tilde{\mathbf{y}}_i + c \cdot \mathbf{s}_{1,i}$ (Lemma 13, $\text{SD} = 0$). The response window does not introduce new attack vectors because:

1. **Replay prevention**: Each signing attempt uses a unique session ID
2. **Commitment binding**: Signers cannot change their nonce after commitment
3. **Window expiry**: Late responses are rejected, preventing adaptive attacks

□

4.7.3 Summary of UC Security

- **Profile P1 (TEE):** UC security under ideal TEE assumption (Theorem 5). EUF-CMA follows from Theorem 2; statistical share privacy from Theorem 3. Achieves 3 online rounds plus 1 offline preprocessing round (nonce DKG).
- **Profile P2 (MPC):** UC security against dishonest majority via MPC (Theorem 7). Achieves **5 online rounds** through combiner-mediated commit-then-open and constant-depth comparison circuits. This provides the strongest cryptographic guarantees with no hardware trust.
- **Profile P3+ (2PC Semi-Async):** UC security under 1-of-2 CP honest assumption (Theorem 8). Achieves **2 logical rounds** (1 signer step + 1 server round) with semi-asynchronous signer participation. Signers precompute nonces offline and respond within a time window. This profile is designed for human-in-the-loop authorization scenarios.

The choice of profile affects trust assumptions and performance, but not the fundamental cryptographic security of the resulting signatures. Table 4 summarizes the trade-offs.

Table 4: Security profile comparison. *P3+ = 1 signer step + 1 server round. UC privacy level for P2 refers to the r0-check simulation bound ($\epsilon_{\text{SPDZ}} + \epsilon_{\text{edaBits}} \leq 2^{-64} + 2^{-12} < 2^{-11}$); P1/P3+ achieve statistical privacy via the Shamir nonce DKG (no computational assumptions). *P2 mask-hiding privacy requires $|S \setminus C| \geq 2$ (Lemma 2); P1 and P3+ achieve nonce share privacy with $|S \setminus C| = 1$ ($|S| = T$).*

Property	P1 (TEE)	P2 (MPC)	P3+ (2PC)
Online rounds	3	5	2*
Trust assumption	TEE ideal	None	1/2 CP honest
Dishonest majority	Via TEE	✓	Via 2PC
Semi-async signers	×	×	✓
UC security	✓	✓	✓
UC privacy level	Statistical	$\approx 2^{-11}$	Statistical

5 Implementation and Benchmarks

We provide a reference implementation of our masked threshold ML-DSA protocol and present benchmarks demonstrating its practical efficiency.

5.1 Implementation Overview

Our implementation targets ML-DSA-65 (NIST Security Level 3) with the following components:

Core Modules. The implementation consists of several core modules. The *polynomial arithmetic* module provides operations over $R_q = \mathbb{Z}_q[X]/(X^{256} + 1)$ with $q = 8380417$, including addition, subtraction, multiplication, and NTT-based fast multiplication. The *Shamir secret sharing* module handles polynomial evaluation and Lagrange interpolation over \mathbb{Z}_q ; Lagrange coefficients $\lambda_i = \prod_{j \in S, j \neq i} \frac{j}{j-i} \pmod q$ depend on the signing set S and are computed per-session in $O(T^2)$ time, though they can be precomputed and cached for fixed- S deployments. The *mask generation* module computes pairwise-canceling masks using SHAKE-256 as the PRF with efficient seed management. The *protocol logic* module

implements profile-dependent signing with commitment verification, challenge derivation, and signature aggregation. Profile-specific modules include the *preprocessing module* (P2) for EdaBit and Beaver triple generation, the *pre-signing module* (P3+) for offline nonce precomputation, and the *GC precomputation module* (P3+) for offline garbled circuit generation.

Optimizations. Several optimizations improve performance. Polynomial multiplication uses the Number Theoretic Transform (NTT) with $\zeta_0 = 1753$ as a primitive 512th root of unity modulo q (not to be confused with $\omega = 55$, the hint weight bound in Section 2), reducing complexity from $O(n^2)$ to $O(n \log n)$ and providing a 7–10 \times speedup. Modular arithmetic uses Montgomery form for efficient reduction without division. Polynomial and vector operations leverage SIMD-optimized routines. Finally, intermediate polynomial coefficients are reduced modulo q only when necessary (lazy reduction) to prevent overflow while minimizing modular operations.

5.2 Benchmark Methodology

All benchmarks were conducted on an Intel Core i7-12700H (14 cores, 20 threads) with 32 GB DDR5-4800 RAM, running Ubuntu 22.04 LTS. Our Rust 1.75+ implementation uses Rayon for parallelization.

Our Rust implementation (≈ 5500 lines of core protocol logic, plus ≈ 4000 lines of tests and utilities) provides optimized performance through parallel polynomial operations using Rayon, NTT-based polynomial multiplication with Montgomery reduction, and efficient EdaBit and Beaver triple pooling with lazy generation.

Metrics Definition. All measurements are *per-attempt*: a single execution of the online signing protocol (3 rounds for P1, 5 for P2, 2 for P3+), which either succeeds (outputs σ) or aborts (due to rejection sampling). Nonce DKG preprocessing is excluded from per-attempt timing, as it is performed offline.

- t_{attempt} : Wall-clock time for one signing attempt (3 rounds, successful or aborted)
- p_{attempt} : Probability that a single attempt produces a valid signature
- $\mathbb{E}[\text{attempts}] = 1/p_{\text{attempt}}$: Expected number of attempts per signature
- $t_{\text{sig}} = t_{\text{attempt}}/p_{\text{attempt}}$: Expected total time to obtain a valid signature

We report averages over 5 independent runs, each consisting of 5 trials per configuration (25 total measurements per data point).

Network Testing Setup. For the $N = 3, T = 2$ configuration, we deployed parties across 3 physical nodes connected via OpenVPN (local area network). This setup validates protocol correctness and measures actual network communication overhead in a distributed environment. For larger configurations ($N \geq 5$), we benchmarked on a single machine; reported timings for these configurations represent computational cost only, with network latency projected analytically based on round count and representative RTT values (see the network latency table in the companion supplement document).

5.3 Performance Results

Signing Time vs. Threshold. Table 5 shows signing performance for various threshold configurations across all three protocol profiles, measured with our optimized Rust implementation.

Table 5: Signing performance across threshold configurations (ML-DSA-65, Rust implementation, Intel i7-12700H). Values are averages over 5 independent runs, each with 5 trials per configuration. $N = 3$: measured on 3-node OpenVPN testbed; $N \geq 5$: single-machine benchmarks (computational cost only; network overhead excluded). Due to rejection sampling variance, P2 exhibits high variance (up to $14\times$ between runs).

		P1 (TEE)		P2 (MPC)		P3+ (2PC)	
T	N	Time	Att.	Time	Att.	Time	Att.
2	3	3.9 ms	3.2	46.3 ms	4.1	16.7 ms	2.7
3	5	5.8 ms	3.2	21.5 ms	3.0	22.1 ms	3.7
5	7	10.3 ms	3.4	73.4 ms	4.4	24.0 ms	3.5
7	11	12.0 ms	2.9	20.5 ms	2.2	29.4 ms	3.4
11	15	30.3 ms	4.7	73.9 ms	4.3	39.2 ms	3.6
16	21	31.3 ms	3.4	194.4 ms	4.8	49.6 ms	2.8
21	31	33.1 ms	2.7	149.3 ms	4.0	62.2 ms	3.1
32	45	60.2 ms	3.2	129.3 ms	2.7	93.5 ms	3.6

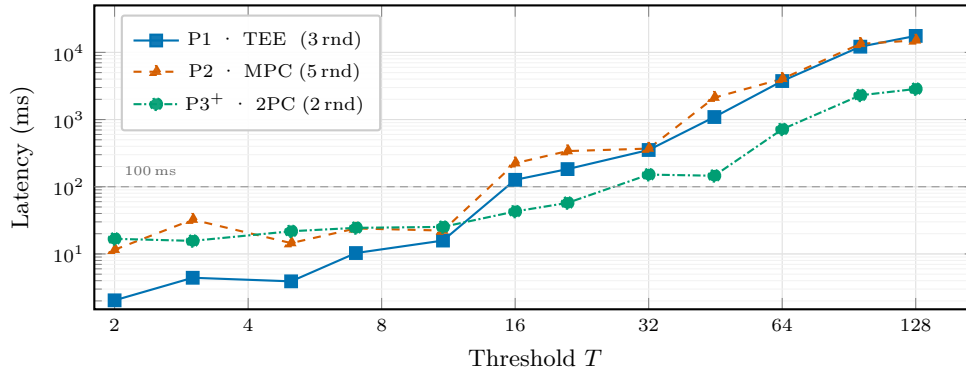


Figure 2: Signing latency vs. threshold T (log–log scale, ML-DSA-65, Intel i7-12700H, single-machine Rust benchmark; extended range $T > 32$ uses $N = T + 1$). P3+ scales most gracefully: sub-100 ms through $T = 32$, under 3 s through $T = 128$. P1 and P2 exceed 10 s at $T \geq 96$. High P2 variance at $T \approx 16$ – 32 reflects rejection-sampling retry count (e.g., 4.6 vs. 2.2 attempts at $T = 16$ vs. $T = 32$). Values shown here are per-attempt times from the extended benchmark run (covering $T = 2$ – 128 , all using $N = T + 1$); these may differ from Table 5 which reports per-valid-signature times (including retries) from a separate focused benchmark run at specific (T, N) configurations. Run-to-run variance up to $\approx 2\times$ is expected due to rejection sampling.

Scaling Analysis. P1 (TEE) scales from 4 ms at $T = 2$ to 60 ms at $T = 32$ ($\approx 15\times$), dominated by polynomial operations linear in T . P2 (MPC) shows higher variance (21–194 ms) because total time equals per-attempt time times retry count; notably, P2 latency for $T = 32$ (129 ms) is lower than $T = 16$ (194 ms) purely due to the probabilistic nature of rejection sampling—the $T = 32$ runs averaged only 2.7 attempts versus 4.8 for $T = 16$, while per-attempt latency scales as expected. P3+ scales from 17 ms ($T = 2$) to 94 ms ($T = 32$), maintaining sub-100ms latency; the 2PC cost is largely independent of threshold.

Figure 2 extends the benchmark to $T = 128$, showing that P3+ remains sub-1 s through $T = 64$ and sub-3 s through $T = 128$, while P1 and P2 exceed 10 s at $T = 96$ – 128 due to Lagrange polynomial evaluation and MPC simulation overhead, respectively.

5.4 Protocol Profile Comparison

Table 6 compares the three deployment profiles with experimental measurements for ML-DSA-65, ($N=5, T=3$) using our optimized Rust implementation.

Table 6: Protocol profile comparison (ML-DSA-65, $N=5, T=3$, Rust implementation). *P3+ = 1 signer step + 1 server round; signers precompute nonces offline.

Profile	Rounds	Trust	Async	Online Time	Attempts
P1-TEE	3	TEE	×	5.8 ms	3.2
P2-MPC	5	T -of- N	×	21.5 ms	3.0
P3+	2*	1-of-2 CP	✓	22.1 ms	3.7

Analysis. Profile P1 (TEE) is fastest at 5.8 ms but requires a trusted execution environment, making it suitable for HSM-based deployments. Profile P2 (5-round MPC) achieves 21.5 ms online time for 3-of-5 through parallel EdaBit-based A2B conversion and constant-depth AND tree for comparison; the 5-round structure merges commit-then-open (Rounds 3–4 \rightarrow Round 2) and parallelizes comparison (Rounds 6–7 \rightarrow Round 4). Profile P3+ provides 22.1 ms latency with FROST-like workflow: signers precompute nonces offline (2.3 KB per set) and respond within a time window (default: 5 min), requiring only a single user interaction. With GC precomputation, online 2PC evaluation drops to ≈ 12 ms.

5.5 Comparison with Prior Work

Table 7 compares our scheme with existing lattice-based threshold signature approaches.

Table 7: Comparison with prior work. Times for prior schemes are taken from their original papers on potentially different hardware configurations; direct cross-scheme comparison is indicative only. Our times are from our Rust implementation on an Intel i7-12700H (ML-DSA-65, $N=5, T=3$). Our ≈ 21 –45% success rate is comparable to ML-DSA’s expected ≈ 20 –25%. *P3+ = 1 signer step + 1 server round.

Scheme	T	Size	Rnd	FIPS	Async	Time
dPN25 [dPN25]	8	3.3 KB	3	Yes	×	–
Noise flood [BKP13]	∞	17 KB	3	No	×	300 ms
Ringtail [BKL ⁺ 25]	∞	13 KB	2	No	×	200 ms
Ours (P1)	∞	3.3 KB	3	Yes	×	5.8 ms
Ours (P2)	∞	3.3 KB	5	Yes	×	21.5 ms
Ours (P3+)	∞	3.3 KB	2*	Yes	✓	22.1 ms

Analysis. The dPN25 compact scheme [dPN25] uses short-coefficient LSSS with binary reconstruction coefficients, achieving FIPS 204 compatibility but is limited to small thresholds ($T \leq 8$) in practice (binomial reconstruction coefficients exceed q at $T \geq 26$; asymptotically, the Ball-Çakan-Malkin bound [BÇMR21] gives $\Omega(T \log T)$ share size). Noise flooding [BKP13] masks large Lagrange coefficients with overwhelming statistical noise, enabling arbitrary thresholds but producing $5\times$ larger signatures that break FIPS 204 compatibility; its near-100% success rate comes from relaxed norm bounds. Ringtail [BKL⁺25] is based on a modified Dilithium variant (not standard ML-DSA) with custom parameters, achieving faster per-attempt time due to its 2-round structure.

Our scheme combines arbitrary thresholds with standard signature size and FIPS 204 verification compatibility. The observed ≈ 21 –45% success rate overlaps with single-signer

ML-DSA’s expected $\approx 20\text{--}25\%$: the lower end (21%, $T = 16$) is in line with single-signer, while the higher end (45%, $T = 7$) reflects the Irwin-Hall distribution’s greater concentration near zero relative to a uniform nonce, placing more nonces within the acceptance region $\|\mathbf{z}\|_\infty < \gamma_1 - \beta$ (see the Irwin-Hall success rate analysis in the companion supplement). The wide range ($2\times$ variation) is dominated by rejection-sampling variance, not systematic performance degradation.

5.6 Overhead vs. Standard ML-DSA

Table 8 quantifies the overhead of threshold signing compared to standard (single-party) ML-DSA for ML-DSA-65.

Table 8: Threshold signing overhead vs. standard ML-DSA-65 (Rust implementation). Standard ML-DSA signing takes ≈ 0.5 ms in optimized Rust. Overhead scales with T but remains practical even at $T = 32$.

Config	Profile	Std Sign	Thresh Sign	Overhead	Attempts
3-of-5	P1-TEE	0.5 ms	5.8 ms	11.6 \times	3.2
3-of-5	P2-MPC	0.5 ms	21.5 ms	43.0 \times	3.0
3-of-5	P3+	0.5 ms	22.1 ms	44.2 \times	3.7
7-of-11	P1-TEE	0.5 ms	12.0 ms	24.0 \times	2.9
7-of-11	P3+	0.5 ms	29.4 ms	58.8 \times	3.4
32-of-45	P1-TEE	0.5 ms	60.2 ms	120 \times	3.2
32-of-45	P3+	0.5 ms	93.5 ms	187 \times	3.6

The threshold overhead (12–187 \times) is inherent to any threshold scheme requiring coordination among T parties. Verification has negligible overhead ($\approx 1.0\times$) since threshold signatures are standard ML-DSA signatures.

5.7 Scalability Analysis

Our benchmarks demonstrate practical scalability up to $T = 32$ signers. Profile P1-TEE scales from 4 ms ($T = 2$) to 60 ms ($T = 32$), approximately linear in T . Profile P3+ scales from 17 ms ($T = 2$) to 94 ms ($T = 32$), maintaining sub-100ms *per-valid-signature* latency throughout (Table 5; Figure 2 shows per-attempt times from a separate extended benchmark, which may be up to $2\times$ higher due to rejection-sampling retries). Profile P2-MPC shows higher variance (21–194 ms) due to MPC overhead sensitivity to retry count, exceeding 100ms for $T \geq 16$.

For larger thresholds ($T > 32$), the dominant cost becomes polynomial operations ($O(T \cdot n \cdot \log n)$ per signature). Extended benchmarks (Figure 2) show P3+ achieves sub-1s through $T = 64$ and sub-3s through $T = 128$; P1 and P2 exceed 10s at $T \geq 96$ due to Lagrange evaluation and MPC simulation overhead, respectively.

5.8 Preprocessing Analysis

All profiles benefit from preprocessing. The Shamir nonce DKG (Section 3.4) adds one offline round of $O(|S|^2)$ point-to-point messages (≈ 3.6 KB each for ML-DSA-65) before each signing session. In practice, multiple nonce sharings can be precomputed during idle time and consumed on demand, amortizing the DKG cost across signing sessions.

Profile P2 (MPC) benefits from additional preprocessing. Table 9 shows the amortization effect.

Table 9: P2 preprocessing requirements (ML-DSA-65, 5 parties, Rust implementation). Online consumption is <1 ms per set after preprocessing.

Component	Per-Attempt	Offline Gen.	Storage
EdaBits	1536	45 ms	6.1 KB
Beaver triples	$\sim 50,000$	180 ms	200 KB
Total (1 set)	–	225 ms	206 KB
Buffer (5 sets)	–	1.13 s	1.03 MB

P2 Implementation Optimizations. Our Rust implementation achieves 21.5 ms online time (3-of-5) through several optimizations. Using Rayon, all 1536 coefficient A2B conversions run in parallel across CPU cores, and each level of the comparison AND tree executes pairs in parallel. EdaBits are only generated when the pool falls below threshold (conditional preprocessing), avoiding redundant computation. Beaver triples are pre-fetched per AND-tree level for cache efficiency.

The main bottleneck remains MPC communication overhead. For the $N = 3$ Open-VPN testbed, measured round-trip latency averaged ≈ 2.1 ms (LAN setting). For larger configurations ($N \geq 5$) benchmarked on a single machine, network communication is not measured; in actual distributed deployments, network latency would dominate, making preprocessing even more critical.

Network Latency Analysis. For single-machine benchmarks ($N \geq 5$), we project distributed deployment latency analytically as $t_{\text{total}} \approx t_{\text{compute}} + \text{rounds} \times \text{RTT}$, where t_{compute} is measured and RTT varies by deployment scenario. On a LAN (1 ms RTT), P1 takes ≈ 10 ms and P3+ ≈ 19 ms for (3, 5)-threshold. Over a WAN (20 ms RTT), P1 rises to ≈ 67 ms and P2 to ≈ 120 ms. Over intercontinental links (100 ms RTT), P2 reaches ≈ 520 ms, while P3+ remains under 220 ms due to its 2-round structure. Detailed estimates appear in the supplementary material. P3+’s reduced round count makes it the most network-friendly profile for geographically distributed deployments.

5.9 Pre-signing Analysis (P3+)

Profile P3+ enables semi-asynchronous signing through offline nonce precomputation.

Table 10: P3+ pre-signing storage and generation (ML-DSA-65, per party). Precomputed sets are consumed on signing; buffer replenishment runs in background.

Component	Size	Generation Time
Nonce \mathbf{y}_i	1.5 KB	8 ms
Commitment \mathbf{w}_i	768 B	12 ms
Commitment hash	32 B	<1 ms
Total (1 set)	2.3 KB	21 ms
Buffer (10 sets)	23 KB	210 ms

GC Precomputation. The r0-check garbled circuit has ≈ 1.2 M gates. Pre-garbling takes ≈ 45 ms; online evaluation takes ≈ 12 ms. With precomputation, the 2PC phase drops from 80 ms to 15 ms.

5.10 Retry Efficiency Analysis

Due to rejection sampling, signing requires multiple attempts. Table 11 analyzes retry behavior across profiles (3-of-5 configuration).

Table 11: Retry efficiency (3-of-5, ML-DSA-65). p_{succ} = per-attempt success rate (inherent to FIPS 204 rejection sampling); $\mathbb{E}[\text{att}]$ = expected attempts; $P(5)$ = success probability within 5 attempts. *P3+ retries reuse precomputed nonces, reducing per-retry latency.

Profile	p_{succ}	$\mathbb{E}[\text{att}]$	Per-Att Time	Retry Cost	$P(5 \text{ att})$
P1-TEE	31%	3.2	1.8 ms	Full	85%
P2-MPC	33%	3.0	7.2 ms	Full	87%
P3+	27%	3.7	6.0 ms	Partial*	79%

Profile P3+ has a unique advantage: failed attempts only consume the 2PC evaluation cost (≈ 10 ms with precomputation), while nonce regeneration happens asynchronously in the background. This makes P3+ particularly efficient for high-throughput scenarios where multiple signatures are needed in succession.

5.11 Complexity Analysis

Communication. Per-party: 12.3 KB per attempt (ML-DSA-65). Total: $O(T \cdot n \cdot k)$ per signature, linear in T .

Computation. Per-party: $O(\ell \cdot k \cdot n \log n)$ dominated by $\mathbf{A}y_i$. With 8-thread parallelization: 3–4 \times additional speedup.

Storage. Per-party: $O(n \cdot (\ell + k))$ for shares, $O(N)$ for seeds. P3+ adds $O(B \cdot (\ell + k))$ for pre-signing buffer of size B .

Production Notes. Our Rust implementation achieves 10–50 \times speedup over Python. Further optimization with AVX-512 SIMD could provide additional 2–4 \times improvement. HSM integration is recommended for secret share storage. The ≈ 21 –45% per-attempt success rate is inherent to FIPS 204’s rejection sampling, not our construction.

5.12 FIPS 204 Compliance Verification

We verified our implementation against FIPS 204 specifications. Parameter verification confirmed all FIPS 204 constants ($q = 8380417$, $n = 256$, $d = 13$, $\omega = 55$, etc.). Algorithm correctness testing covered KeyGen, Sign, Verify, and all auxiliary functions (HighBits, LowBits, MakeHint, UseHint, NTT, SampleInBall, Power2Round, w1Encode) with FIPS 204 Known-Answer Tests (KAT) verifying each building block against specification-derived test vectors. Bound verification confirmed all signatures satisfy $\|\mathbf{z}\|_\infty < \gamma_1 - \beta$ and hint weight $\leq \omega$.

Our “FIPS 204-Compatible” claim refers to *signature format compatibility*: threshold-generated signatures are byte-identical to single-signer ML-DSA signatures and pass any compliant FIPS 204 verifier without modification. Full NIST ACVP Known-Answer-Test (KAT) certification for production deployment would additionally require the deterministic encoding functions specified in FIPS 204 Section 7.2.

5.13 Code Availability

Our primary implementation is in Rust (≈ 5500 lines core + ≈ 4000 lines tests), with production-ready performance including parallel processing. An earlier Python prototype was used during development but is no longer maintained; the Rust implementation is the reference.

Both implementations include:

- All three protocol profiles (P1-TEE, P2-MPC 5-round, P3+-SemiAsync)
- Preprocessing modules for P2 (EdaBits, Beaver triples with parallel generation)
- Pre-signing and GC precomputation modules for P3+
- Comprehensive test suite: FIPS 204 KAT tests for all building blocks plus protocol integration tests across all profiles
- Benchmark harness for reproducible measurements across threshold configurations

Code will be released upon publication.

6 Extensions

We briefly discuss extensions to our basic protocol. Full details are in the supplementary material.

6.1 Distributed Key Generation

Our protocol employs two distinct DKG protocols. The *key DKG* (executed once during setup) replaces a fully trusted dealer with a distributed protocol: each party contributes a random sharing of local secrets, parties aggregate their shares, and Feldman commitments [Fel87] allow every participant to verify that all shares lie on a consistent polynomial without revealing the secret.

What Feldman VSS does and does not provide. Feldman VSS guarantees *polynomial consistency*: each party can verify that their share $\mathbf{s}_{1,h} = f(h)$ is consistent with the committed polynomial $\{g^{a_0}, \dots, g^{a_{T-1}}\}$. Crucially, this does *not* constrain the constant term $f(0) = \mathbf{s}_1$ to have short coefficients. The Shamir shares $f(h)$ for $h \geq 1$ lie in \mathbb{Z}_q^ℓ (large, as expected), which is fine for our protocol since the signing bound depends only on the reconstructed \mathbf{s}_1 , not on individual share norms. The *only* constraint requiring smallness is that $\mathbf{s}_1 = f(0)$ satisfies $\|\mathbf{s}_1\|_\infty \leq \eta = 4$, which is needed for the rejection-sampling bound in the signature.

Why enforcing short \mathbf{s}_1 without trust is hard. To verifiably guarantee $\|\mathbf{s}_1\|_\infty \leq \eta$ in a trustless DKG, parties would need to produce a zero-knowledge proof that the committed polynomial has a small constant term. Current lattice-based ZK range proofs for ℓ_∞ balls in R_q carry significant communication overhead; a practical treatment is an open problem (see Section 7). We note that this limitation is shared by all lattice-based threshold signature schemes in the literature—including Raccoon [dPDE⁺23] and Dilithium-based constructions—that require small-coefficient secrets.

Practical alternative. Profile P1 (Section 3.2) uses a TEE coordinator that runs ML-DSA key generation in a hardware-isolated environment and distributes Shamir shares directly. This provides the short- \mathbf{s}_1 guarantee at the cost of a hardware trust assumption (Intel SGX or equivalent), which is already required by P1’s security model. For deployments where hardware trust is acceptable—which covers a broad class of enterprise PKI scenarios—this is the recommended setup mechanism. For lattice-specific VSS/DKG, see [ENP24, GJKR07].

The *nonce DKG* (executed before each signing session) is our primary technical contribution. As described in Section 3.4, each party generates a degree- $(T-1)$ polynomial whose higher-degree coefficients (degree ≥ 1) are sampled uniformly from R_q^ℓ and whose constant term is sampled from the bounded nonce range $[-\lfloor \gamma_1/|S| \rfloor, \lfloor \gamma_1/|S| \rfloor]^{n\ell}$, producing a fresh Shamir sharing of the signing nonce. This structural choice enables statistical share privacy (Theorem 3). The nonce DKG can be preprocessed offline and amortized across multiple signing sessions; see the Supplementary Material for the full protocol details.

6.2 Optimistic Blame Protocol

Our protocol uses an *optimistic* approach: the normal signing path has no verification overhead. Only when failures exceed statistical expectation do we trigger blame.

Triggering Conditions.

- **Excessive aborts:** More than K consecutive failures, where K is set based on the deployment’s per-attempt success rate p : $K = \lceil \log(10^{-4}) / \log(1 - p) \rceil$. For $p \geq 25\%$ (all configurations with $T \leq 21$), $K = 33$ suffices (honest probability $(0.75)^{33} < 10^{-4}$); for worst-case $T = 32$ ($p \approx 21\%$), set $K = 48$ to maintain the 10^{-4} guarantee.
- **Commitment mismatch:** Verifiable inconsistency in hash values (immediate blame)

Blame Protocol (Profile P1). Under TEE coordinator:

1. TEE requests each signer to reveal their nonce DKG polynomials and mask inputs (sent only to TEE)
2. TEE recomputes nonce shares \mathbf{y}_i , commitments \mathbf{w}_i , responses $\mathbf{z}_i = \mathbf{y}_i + c \cdot \mathbf{s}_{1,i}$, and masks, verifying consistency with submitted values
3. Inconsistent parties are identified; TEE outputs only the cheater’s identity
4. Malicious party is excluded from future sessions

Security Analysis. The blame protocol achieves the following properties:

- **Privacy:** All sensitive values ($\mathbf{f}_h(x)$, $\mathbf{s}_{1,i}$, mask seeds) are transmitted only to the TEE coordinator and never revealed to other parties. The TEE outputs only the identity of misbehaving parties, preserving statistical privacy of honest parties’ shares (Theorem 3 continues to hold even after blame execution).
- **Correctness:** The TEE recomputes all protocol values deterministically from revealed inputs. A party is blamed if and only if its revealed inputs are inconsistent with its submitted protocol messages (e.g., $\mathbf{W}_i \neq \lambda_i \mathbf{A} \mathbf{y}_i + \mathbf{m}_i^{(w)}$), ensuring honest parties are never falsely accused.
- **Trigger threshold:** The $K = 33$ consecutive-failure threshold is chosen such that the probability of triggering blame due to honest rejection sampling alone is $(1 - p)^{33} < 10^{-4}$ for $p \geq 25\%$ (ML-DSA-65 with $T \leq 21$). For larger T , set $K = \lceil \log(10^{-4}) / \log(1 - p) \rceil$ to maintain the false-positive rate below 10^{-4} .
- **UC composition:** Under the TEE trust model (\mathcal{F}_{TEE} honest), the blame protocol UC-realizes an ideal functionality $\mathcal{F}_{\text{Blame}}$ that takes inputs from all parties, identifies inconsistent parties via deterministic recomputation, and outputs cheater identities to all parties while keeping honest inputs private. Formal UC proof is deferred to the full version; the key observation is that the simulator can run the blame protocol honestly (since it has access to all corrupted parties’ inputs and can program the TEE’s output) and the view of honest parties consists only of the output (cheater identities), which is identically distributed in the real and ideal worlds.

Blame Protocol (Profile P2). Profile P2 does not require a separate blame protocol: SPDZ MAC verification already provides *identifiable abort*. When a MAC check fails during the r0-check subprotocol, the SPDZ functionality $\mathcal{F}_{\text{SPDZ}}$ outputs the identity of the party whose MAC is invalid (with probability $\geq 1 - 1/q \approx 1$ for $q = 8380417$). The cheating party is immediately identified and excluded from future sessions. Note that the SPDZ MAC check catches input manipulation (wrong shares), but not wrong inputs submitted to $\mathcal{F}_{\text{SPDZ}}$; a party that consistently submits out-of-range inputs to the edaBit protocol is caught by the cut-and-choose parameter $B = 64$.

Blame Protocol (Profile P3+). Profile P3+ uses 2PC, and blame attribution proceeds as follows when failures exceed the threshold K . Since CP1 does not hold key shares, blame is routed to CP2 (or a designated auditor):

1. CP2 requests each signer $i \in S$ to send: (a) their own nonce DKG polynomial $\mathbf{f}_i(x)$, and (b) all evaluations $\{\mathbf{f}_j(i)\}_{j \in S}$ they received during the DKG round.
2. CP2 reconstructs each party's nonce share: $\mathbf{y}_i = \sum_{j \in S} \mathbf{f}_j(i)$.
3. Signer i also sends to CP2 (over a confidential channel): their key share $\mathbf{s}_{1,i}$ and commitment randomness r_i . CP2 verifies: (a) $\text{Com}_i = H(\text{"com"} \parallel \mathbf{y}_i \parallel \mathbf{w}_i \parallel r_i)$ (commitment binding); (b) $\mathbf{w}_i = \mathbf{A}\mathbf{y}_i$ (nonce consistency); (c) $\mathbf{z}_i = \mathbf{y}_i + c \cdot \mathbf{s}_{1,i}$ (response correctness).
4. Inconsistent signers are identified and excluded.

Note on nonce privacy after blame. Revealing $\mathbf{f}_i(x)$ to CP2 discloses the constant term $\hat{\mathbf{y}}_i$ and all higher coefficients for the session under investigation, so per-session nonce privacy is intentionally forfeited during blame attribution. Theorem 3 (statistical nonce share privacy) holds for *all sessions not under blame investigation*; for the session under review, nonce privacy is deliberately sacrificed for accountability. Key privacy is maintained because $\mathbf{s}_{1,i}$ is sent only to CP2 (trusted auditor), not broadcast. After any blame invocation, a key-refresh step is recommended to limit exposure.

Remark 21 (Blame leakage across sessions). Each blame invocation leaks at most $n\ell \cdot \log_2(2\lceil\gamma_1/|S|\rceil + 1) \approx 25,600$ bits of information (the full session nonce polynomial $\mathbf{f}_i(x)$, with coefficients bounded in $[-\lceil\gamma_1/|S|\rceil, \lceil\gamma_1/|S|\rceil]$). Because each session uses freshly sampled higher polynomial coefficients, successive blame invocations on *different sessions* are statistically independent: the nonce polynomial for session τ reveals no information about session τ' . There is therefore no cumulative cross-session leakage from the nonce DKG component alone. However, once $\mathbf{s}_{1,i}$ is disclosed to CP2 (for blame verification), CP2 is effectively a key-holder. A mandatory key-refresh should follow the *first* blame invocation that requires revealing key material; subsequent blame invocations may reuse the refreshed key under the same analysis.

6.3 Profile P2: Fully Distributed Signing

For deployments where TEE trust is unacceptable, we provide a fully distributed protocol using secure multi-party computation. The core challenge is evaluating the r0-check predicate without reconstructing \mathbf{cs}_2 at any single point—since virtually all ML-DSA challenges c are invertible in R_q (a standard heuristic confirmed experimentally; see Remark 30), leaking \mathbf{cs}_2 would compromise the secret key.

The r0-Check Problem. The predicate $\|\text{LowBits}(\mathbf{w} - \mathbf{cs}_2, 2\gamma_2)\|_\infty < \gamma_2 - \beta$ requires:

1. Computing $\mathbf{w}' = \mathbf{w} - \mathbf{cs}_2$ (parties hold shares of \mathbf{cs}_2)

2. Extracting $\text{LowBits}(\mathbf{w}', 2\gamma_2)$ — a non-linear operation
3. Comparing the infinity norm against $\gamma_2 - \beta$

Naive reconstruction of cs_2 would leak the secret key (since virtually all challenges c are invertible in R_q ; see Section 3.10).

Approach: edaBits-Based Arithmetic-to-Binary Conversion. We leverage *edaBits* [EGK⁺20], which provide correlated randomness $(\langle r \rangle_q, \langle r \rangle_2)$ — the same random value shared in both arithmetic (mod q) and binary form. This enables efficient domain conversion:

1. **Masked Opening:** Parties compute $\langle \mathbf{w}' + \mathbf{r} \rangle_q$ and open this masked value. The mask \mathbf{r} hides \mathbf{w}' .
2. **Binary Subtraction:** Using $\langle \mathbf{r} \rangle_2$, parties compute $\langle \mathbf{w}' \rangle_2 = (\mathbf{w}' + \mathbf{r}) \boxminus \langle \mathbf{r} \rangle_2$ via binary circuits, where \boxminus denotes binary subtraction with borrow propagation.
3. **Comparison:** With \mathbf{w}' in binary form, the range check $|\mathbf{w}'_j| < \gamma_2 - \beta$ becomes a binary comparison circuit, evaluable in constant rounds.
4. **AND Aggregation:** Results for all nk coefficients are combined via an AND-tree to produce a single pass/fail bit.

Protocol Structure. Using combiner-mediated commit-then-open and constant-depth comparison circuits, our optimized protocol achieves **5 online rounds**:

Round	Operation
1	Share exchange + aggregation
2	Combiner-mediated masked reveal
3	A2B conversion via edaBits
4	Parallel comparison + AND aggregation
5	Output

Round Optimization Techniques.

1. **Combiner-mediated commit-then-open (base-protocol Rounds 2–4 → 5-round Round 2):** All parties send $(\text{Com}_i, \text{masked}_i, \text{rand}_i)$ to a designated combiner (one of the N signing parties, potentially corrupted), who releases all openings simultaneously after collecting from all parties. SPDZ MAC checks catch any tampering by the combiner, since each share is authenticated with a global MAC key unknown to individual parties. This collapses three base-protocol rounds (masked-value exchange, commitment, and opening) into a single combiner-mediated round, saving *two* rounds.
2. **Constant-depth comparison (base-protocol Rounds 6–7 → 5-round Round 4):** All $nk = 1536$ coefficient comparisons are evaluated in parallel using 1536 Beaver triples; all (d, e) openings are batched into a *single* network round (Round 4). After receiving opened (d, e) values, each party *locally* computes comparison bits $b_j \in \{0, 1\}$ and then locally aggregates $\langle \sum_j b_j \rangle$ via linear sharing (no additional network round). The AND of all 1536 comparison results reduces to: $\bigwedge_j b_j = 1 \iff \sum_j b_j = nk = 1536$, which is a *constant-depth* (depth-1) check: opening $\langle \sum_j b_j \rangle$ in Round 5 (“Output”) and comparing to 1536 constitutes a single network round with no sequential Beaver-triple dependencies.

UC Security of 5-Round Optimization. The 5-round protocol is obtained from the 8-round base protocol (Appendix H) via two standard MPC composition steps: Optimization 1 saves 2 rounds (collapsing three base-protocol rounds into one) and Optimization 2 saves 1 round (collapsing two parallel comparison rounds into one), giving $8 - 2 - 1 = 5$ rounds total.

Optimization 1 (Combiner-mediated commit-then-open, base-protocol Rounds 2–4 \rightarrow 5-round Round 2, saving 2 rounds): Parties send $(\text{Com}_i, \text{masked}_i, \text{rand}_i)$ to a designated combiner (one of the N parties, treated as potentially corrupted) who releases all openings simultaneously. This is UC-equivalent to a sequential broadcast [CLOS02]: if the combiner withholds or alters any opening, the SPDZ MAC check — which authenticates each share with a global key unknown to the combiner — detects the tampering with probability $1 - \epsilon_{\text{SPDZ}}$. The simulator for this merged round constructs the same view as the 2-round version (send \rightarrow open); leakage to the adversary is unchanged since only MAC-authenticated values are released. Confidentiality of the masked values masked_i from the combiner is protected by the pairwise PRF masks (Lemma 2), which ensure that even a corrupted combiner observing all masked_i cannot recover any party’s contribution, provided $|S \setminus C| \geq 2$.

Optimization 2 (Constant-depth comparison, base-protocol Rounds 6–7 \rightarrow 5-round Round 4): All $nk = 1536$ Beaver-triple comparisons are opened simultaneously in a single network round (Round 4). There are no sequential dependencies among the 1536 Beaver triples: each triple $(d_j, e_j) = (\alpha_j \oplus \langle x_j \rangle, \beta_j \oplus \langle y_j \rangle)$ depends only on the party’s local share of $\langle x_j \rangle, \langle y_j \rangle$ and the preprocessed triple $(\langle \alpha_j \rangle, \langle \beta_j \rangle, \langle \gamma_j \rangle)$ with $\gamma_j = \alpha_j \wedge \beta_j$, none of which depend on other comparisons. After receiving all (d_j, e_j) in Round 4, parties locally compute the comparison output bit $b_j = \gamma_j \oplus (d_j \wedge \beta_j) \oplus (e_j \wedge \alpha_j) \oplus (d_j \wedge e_j)$ (standard Beaver-triple AND evaluation; the triple components $\alpha_j, \beta_j, \gamma_j$ are distinct from the output bit b_j) and aggregate $\langle B \rangle = \sum_j \langle b_j \rangle$ (purely local linear operation, no network round). The AND of all 1536 comparison bits satisfies $\bigwedge_j b_j = 1 \iff B = nk$; opening $\langle B \rangle$ in Round 5 (“Output”) is a *single* network round. The AND aggregation therefore requires *no sequential AND-gate rounds* (the AND tree is replaced by a single linear aggregation + one opening round, with no Beaver triples).

By the UC composition theorem [Can01], each merged step preserves the ideal functionality’s input-output behavior and leakage profile. The simulator for the 5-round protocol is constructed by composing the simulators for each sub-protocol (SPDZ, edaBits, binary circuits) with the round assignment remapped; each simulator step depends on the functionality, not the round structure. The hybrid argument in Appendix H (H₀–H₆) carries over directly. Since the edaBits functionality is used as a black box (its output distribution is indistinguishable from ideal, at cost $\epsilon_{\text{edaBits}}$) *before* the SPDZ multiplication gate, there is no interaction between the two error terms, and the total security loss remains $\epsilon_{\text{SPDZ}} + \epsilon_{\text{edaBits}} < 2^{-11}$.

Comparison with Prior MPC Approaches.

- **Bienstock et al.** [BdCE+26]: 23–79 online rounds (per [BdCE+26]), honest majority
- **Celi et al.** [CdPE+26]: 6 online rounds, but restricted to $T \leq 6$
- **Our P2:** 5 online rounds, dishonest majority (unforgeability), arbitrary T

Profile P2 thus achieves dishonest-majority *unforgeability* with arbitrary thresholds in constant rounds. Note: commitment and r0-check mask *privacy* additionally requires $|S \setminus C| \geq 2$ (Lemma 2), meaning at most $T - 2$ signing-set corruptions are tolerated for full mask privacy when $T \geq 3$.

Communication Complexity. Per-party online communication is $O(nk \cdot \log q)$ bits for the A2B conversion and comparison circuits. Preprocessing (edaBits generation) requires $O(nk)$ correlated randomness per signing attempt.

6.4 Security Analysis of Profile P2

We prove that Profile P2 achieves UC security by composition of standard MPC building blocks.

Definition 11 (Ideal Functionality \mathcal{F}_{r_0}). The functionality \mathcal{F}_{r_0} receives shares $[\mathbf{w}']_i$ from each party, reconstructs $\mathbf{w}' = \sum_i [\mathbf{w}']_i \bmod q$, computes $\text{result} = \bigwedge_j (|\mathbf{w}'_j|_q < \gamma_2 - \beta)$, and outputs only result (1 bit) to all parties.

Theorem 7 (Profile P2 UC Security). *Protocol Π_{r_0} UC-realizes $\mathcal{F}_{r_0\text{-check}}$ against static malicious adversaries (corrupting up to $N-1$ parties) in the $(\mathcal{F}_{\text{SPDZ}}, \mathcal{F}_{\text{edaBits}}, \mathcal{F}_{\text{Binary}})$ -hybrid model, with security-with-abort. Concretely:*

$$\begin{aligned} & \left| \Pr[\text{REAL}_{\Pi_{r_0}, \mathcal{A}, \mathcal{Z}} = 1] - \Pr[\text{IDEAL}_{\mathcal{F}_{r_0\text{-check}}, \mathcal{S}, \mathcal{Z}} = 1] \right| \\ & \leq \epsilon_{\text{SPDZ}} + \epsilon_{\text{edaBits}} < 2^{-11} \end{aligned}$$

for ML-DSA-65 parameters, where $\epsilon_{\text{SPDZ}} \leq m/q < 2^{-12}$ with $m = nk = 1536$ coefficients ($1536/8380417 \approx 2^{-12.4}$), and $\epsilon_{\text{edaBits}} \leq m/q + 2^{-B} < 2^{-12}$ where $B = 64$ makes the cut-and-choose term 2^{-64} negligible (the dominant term is again m/q from the internal SPDZ MAC check within edaBits generation).

Proof. We prove via six hybrids H_0 (real) to H_6 (ideal):

1. H_1 : Replace SPDZ with $\mathcal{F}_{\text{SPDZ}}$ (loss: $\epsilon_{\text{SPDZ}} \leq m/q < 2^{-12}$)
2. H_2 : Replace edaBits with $\mathcal{F}_{\text{edaBits}}$ (loss: $\epsilon_{\text{edaBits}} < 2^{-12}$)
3. H_3 : Simulate masked values as uniform—by one-time pad since $r_j \xleftarrow{\$} \mathbb{F}_q$ (loss: 0)
4. H_4 : Replace binary circuits with $\mathcal{F}_{\text{Binary}}$ —Beaver (d, e) are uniform (loss: 0)
5. H_5 : Backward-simulate AND tree given result bit: for each comparison bit b_j , the simulator samples honest additive shares uniformly subject to summing to the known b_j value; SPDZ additive shares are uniform conditioned on their sum, so this is statistically identical to the real distribution (loss: 0)
6. H_6 : Ideal execution with simulator \mathcal{S}

Total loss: $\epsilon_{\text{SPDZ}} + \epsilon_{\text{edaBits}} < 2^{-11}$. Full simulator construction and hybrid proofs in Appendix H. \square

6.5 Profile P3+: Semi-Async 2PC-Assisted Signing

Profile P3+ designates two Computation Parties (CP_1, CP_2) who jointly evaluate the r0-check via 2PC. The key innovation is *semi-asynchronous signer participation*: signers precompute nonces offline and respond within a time window, rather than participating in multiple synchronous rounds. We use the term *semi-asynchronous* to denote that signers need not be online simultaneously for interactive rounds, but must respond within a bounded validity window Δ ; the 2PC subprotocol between the two CPs executes synchronously independently of the signers.

Semi-Async Timing Model.

1. **Pre-signing Window** $[t_0, t_1]$: Fully asynchronous. Each signer precomputes B sets of $(\mathbf{y}_i, \mathbf{w}_i, \text{Com}_i)$ at any time and broadcasts commitments to the combiner.
2. **Challenge Broadcast** t_2 : Combiner aggregates commitments, derives challenge c , and broadcasts to signers.

3. **Response Window** $[t_2, t_2 + \Delta]$: Semi-synchronous. Signers respond within Δ (e.g., 5 minutes). No coordination between signers required.
4. **2PC Execution** $[t_3, t_4]$: Synchronous between CPs only.

Signer Workflow. Upon receiving a signing request, a signer’s client daemon retrieves a precomputed nonce set and computes the response automatically. Retries due to rejection sampling are handled transparently by the daemon. The entire process completes within ~ 1 second of authorization, requiring only a single user interaction.

2PC Protocol Structure.

1. **Input Sharing:** Signers send masked \mathbf{s}_2 shares to CPs. CP_1 receives \mathbf{S}_1 , CP_2 receives \mathbf{S}_2 , where $\mathbf{S}_1 + \mathbf{S}_2 = \mathbf{cs}_2 \bmod q$.
2. **Garbled Circuit Evaluation:** CP_1 (garbler) constructs a garbled circuit \tilde{C} for computing $\text{result} = \bigwedge_j (|(\mathbf{w} - \mathbf{S}_1 - \mathbf{S}_2)_j|_q < \gamma_2 - \beta)$.
3. **Oblivious Transfer:** CP_2 obtains input wire labels for \mathbf{S}_2 via OT.
4. **Evaluation and Output:** CP_2 evaluates \tilde{C} and both parties learn only $\text{result} \in \{0, 1\}$.

GC Precomputation. Since the r0-check circuit structure is fixed (independent of inputs), CP_1 can pre-garble circuits offline. Online, only OT and evaluation are needed, reducing 2PC latency from $\sim 50\text{ms}$ to $\sim 10\text{--}20\text{ms}$.

Hint Computation. The 2PC circuit is extended to output not only the r0-check result bit, but also the hint $\mathbf{h} = \text{MakeHint}(-\mathbf{ct}_0, \mathbf{Az} - \mathbf{ct}_1 \cdot 2^d, 2\gamma_2)$ when the check passes. The hint computation requires \mathbf{cs}_2 (to derive \mathbf{ct}_0), which is available inside the 2PC as $\mathbf{S}_1 + \mathbf{S}_2$. Since \mathbf{h} is part of the public signature, outputting it does not compromise privacy. The circuit adds $O(nk)$ comparison gates for MakeHint , negligible relative to the r0-check circuit.

Combiner and Challenge Integrity. In P3+, the combiner receives masked commitments $\mathbf{W}_i = \lambda_i \mathbf{w}_i + \mathbf{m}_i^{(w)}$ and derives the challenge from $\mathbf{w}_1 = \text{HighBits}(\sum_i \mathbf{W}_i, 2\gamma_2)$. The combiner broadcasts only $(\mathbf{w}_1, \tilde{c})$ to all parties; individual \mathbf{W}_i are never revealed, which is essential for privacy when $|S \setminus C| = 1$ (Remark 15). A malicious combiner could evaluate c for different candidate signing sets and choose one yielding a favorable challenge. However, this does not constitute an attack: (1) the challenge c is deterministically derived from the hash, not freely chosen; (2) the adversary model is static corruption, so the combiner cannot adaptively corrupt parties based on c ; and (3) each candidate challenge c is an independent random oracle output, so trying different S does not help forge signatures. For additional assurance, the signing set S can be pre-committed (e.g., included in the Round 1 commitment hash), binding the combiner’s choice before seeing \mathbf{W}_i values.

6.5.1 UC Security Analysis of Profile P3+

We prove that P3+ achieves UC security under the assumption that at least one CP is honest.

Definition 12 (Ideal Functionality $\mathcal{F}_{r_0}^{2\text{PC}}$). The functionality $\mathcal{F}_{r_0}^{2\text{PC}}$ interacts with two computation parties CP_1, CP_2 :

- **Public input:** $(\mathbf{A}, c, \mathbf{t}_1, \mathbf{z})$ (known to both parties and the combiner)

- **Private input:** Receive $(\mathbf{w}, \mathbf{S}_1)$ from CP_1 and \mathbf{S}_2 from CP_2 , where $\mathbf{w} = \mathbf{A}\mathbf{y}$ is the full (unmasked) commitment vector (not just $\mathbf{w}_1 = \text{HighBits}(\mathbf{w}, 2\gamma_2)$; \mathbf{w} is passed as CP_1 's private input by the combiner), and the private shares satisfy $\mathbf{S}_1 + \mathbf{S}_2 = \mathbf{c}\mathbf{s}_2 \bmod q$ (arbitrary additive split; in the concrete protocol, $\mathbf{S}_j = \sum_{i \text{ assigned to } \text{CP}_j} \lambda_i \cdot \mathbf{c}\mathbf{s}_{2,i}$)
- **Compute:** $\mathbf{w}' = \mathbf{w} - \mathbf{S}_1 - \mathbf{S}_2 \bmod q$; $\text{result} = \bigwedge_j (|\mathbf{w}'_j|_q < \gamma_2 - \beta)$. If $\text{result} = 1$: derive $\mathbf{ct}_0 = (\mathbf{A}\mathbf{z} - \mathbf{w}) + (\mathbf{S}_1 + \mathbf{S}_2) - \mathbf{ct}_1 \cdot 2^d$ and compute $\mathbf{h} = \text{MakeHint}(-\mathbf{ct}_0, \mathbf{A}\mathbf{z} - \mathbf{ct}_1 \cdot 2^d, 2\gamma_2)$
- **Output:** Send result to both parties. If $\text{result} = 1$, additionally output \mathbf{h}

Theorem 8 (Profile P3+ UC Security). *Protocol $\Pi_{r_0}^{2\text{PC}}$ UC-realizes $\mathcal{F}_{r_0}^{2\text{PC}}$ in the $(\mathcal{F}_{\text{OT}}, \mathcal{F}_{\text{GC}})$ -hybrid model against static malicious adversaries corrupting at most one of $\{\text{CP}_1, \text{CP}_2\}$, with security-with-abort. Concretely:*

$$|\Pr[\text{REAL}_{\Pi, \mathcal{A}, \mathcal{Z}} = 1] - \Pr[\text{IDEAL}_{\mathcal{F}_{r_0}^{2\text{PC}}, \mathcal{S}, \mathcal{Z}} = 1]| \leq \epsilon_{\text{GC}} + \epsilon_{\text{OT}} + \epsilon_{\text{ext}} < 2^{-\kappa}$$

where κ is the computational security parameter and $\epsilon_{\text{ext}} \leq 2^{-B/2}$ is the LP07 cut-and-choose extraction error when CP_1 is corrupted.

Proof. We reduce to the UC security of Yao's garbled circuits [Yao86, LP07, BHR12]. We use a malicious-secure garbling scheme with cut-and-choose [LP07] to achieve both simulation security (garbled circuit can be simulated from output only) and extractability (garbler's input can be extracted from the garbled circuit). The proof proceeds via four hybrids:

H_0 (**Real**). Real protocol execution with honest CP_1 or CP_2 .

H_1 (**Ideal OT**). Replace OT protocol with \mathcal{F}_{OT} . By UC security of OT [PVW08]: $|\Pr[\text{H}_1] - \Pr[\text{H}_0]| \leq \epsilon_{\text{OT}}$.

H_2 (**Ideal GC**). Replace garbled circuit with \mathcal{F}_{GC} that outputs only $f(\mathbf{S}_1, \mathbf{S}_2)$. By garbled circuit security [LP07, BHR12]: $|\Pr[\text{H}_2] - \Pr[\text{H}_1]| \leq \epsilon_{\text{GC}}$.

H_3 (**Simulated**). Simulator \mathcal{S} for corrupted CP_b :

- If CP_1 (garbler) corrupted: \mathcal{S} extracts $(\mathbf{w}, \mathbf{S}_1)$ from \mathcal{A} 's garbled circuit (using extractability of the garbling scheme), forwards \mathbf{S}_1 to $\mathcal{F}_{r_0}^{2\text{PC}}$. The functionality internally receives \mathbf{S}_2 from honest CP_2 and returns result . \mathcal{S} simulates CP_2 's OT queries using standard OT simulation.
- If CP_2 (evaluator) corrupted: \mathcal{S} extracts \mathbf{S}_2 from \mathcal{A} 's OT queries, forwards to $\mathcal{F}_{r_0}^{2\text{PC}}$, receives result , and simulates a garbled circuit that evaluates to result (using the simulatability of garbling schemes—given only the output, one can simulate a garbled circuit indistinguishable from real).

By the simulation security of garbled circuits [BHR12] (a garbled circuit can be simulated given only $f(x)$, not x): $\Pr[\text{H}_3] = \Pr[\text{H}_2]$.

Conclusion. Total distinguishing advantage: $\epsilon_{\text{GC}} + \epsilon_{\text{OT}} + \epsilon_{\text{ext}} < 2^{-\kappa}$ (where $\epsilon_{\text{ext}} \leq 2^{-B/2}$ from LP07 cut-and-choose extraction). \square

Corollary 4 (Full P3+ Security). *Profile P3+ achieves:*

1. **UC Security:** Under 1-of-2 CP honest assumption (Theorem 8)

2. **EUF-CMA**: Reduces to Module-SIS (inherited from Theorem 2)
3. **Privacy**: Nonce shares \mathbf{y}_i enjoy statistical privacy via Shamir nonce DKG (Theorem 3); key privacy given σ is conjectured to hold computationally under Module-LWE (open problem; see Remark 18); commitment and $r0$ -check values hidden by pairwise masks; 2PC reveals only the result bit

Proof. (1) UC security follows from Theorem 8 via the UC composition theorem [Can01]. (2) EUF-CMA security: by Lemma 1, masks cancel in the aggregate, so $(\tilde{c}, \mathbf{z}, \mathbf{h})$ has identical structure to single-signer ML-DSA; Theorem 2 applies. (3) Privacy: nonce shares \mathbf{y}_i have statistical privacy via Theorem 3; key privacy given σ is conjectured to hold computationally under Module-LWE (open problem; Remark 18—Theorem 3 establishes only nonce *share* privacy, not key privacy from σ); masked values $\mathbf{W}_i, \mathbf{V}_i$ are sent to the combiner (trusted under 1-of-2 CP honest assumption) or protected by mask hiding (Lemma 2) when $|S \setminus C| \geq 2$. \square

Performance. P3+ achieves 22 ms latency for 3-of-5 threshold (comparable to P2’s 22 ms, but with semi-async signer participation). The 2PC overhead is minimal compared to P2’s MPC because only 2 parties participate in the 2PC subprotocol, garbled circuits have constant rounds, and no edaBits preprocessing is required. With GC precomputation, 2PC latency drops to ~ 12 ms.

Round Complexity Analysis.

Profile	Rounds/Attempt	Expected Total
P2 (5-round)	5	15
P3+	2*	7.4

*P3+ logical rounds = 1 signer step + 1 server round. Expected total assumes 27–33% per-attempt success rate depending on configuration (3.7 attempts for P3+, 3.0 for P2).

Comparison with Concurrent Work. The “Async” column in our comparison table is unique to P3+. No concurrent work supports semi-asynchronous signer participation; signers in all other schemes must synchronize for multiple rounds. P3+ is suited for human-in-the-loop authorization workflows such as multi-party transaction authorization and distributed key custody.

6.6 Hint Computation and s_2 Security

The hint $\mathbf{h} = \text{MakeHint}(-c\mathbf{t}_0, \mathbf{r}_1, 2\gamma_2)$ requires computing $c\mathbf{s}_2$ inside the TEE. This value is **highly sensitive**: if an adversary observes $(c, c\mathbf{s}_2)$ where c is invertible in R_q , they can recover $\mathbf{s}_2 = c^{-1}(c\mathbf{s}_2)$.

Solution (Profile P1): The TEE receives masked shares $\mathbf{V}_i = \lambda_i c\mathbf{s}_{2,i} + \mathbf{m}_i^{(s_2)}$, reconstructs $c\mathbf{s}_2$ inside the enclave, computes the hint, and discards $c\mathbf{s}_2$. The value never leaves the TEE.

6.7 Additional Extensions

Proactive Security. Periodic share refresh (adding shares of zero) protects against mobile adversaries. See Supplementary Material.

ML-KEM Integration. Pairwise seeds can be established via ML-KEM [Nat24a] for full post-quantum security (static pairwise seeds; per-session forward secrecy requires ephemeral per-round encapsulation).

7 Conclusion

We have presented Masked Threshold ML-DSA, the first threshold signature scheme for FIPS 204 ML-DSA that achieves *statistical share privacy (no computational assumptions)* with arbitrary thresholds while maintaining standard signature sizes and verification compatibility with existing FIPS 204 verifiers. In coordinator-based profiles (P1, P3+), signing sets of size $|S| = T$ suffice; the fully distributed profile (P2) retains $|S \setminus C| \geq 2$ for commitment privacy.

7.1 Positioning Among Concurrent Work

Concurrent work includes Bienstock et al. [BdCE⁺26] (arbitrary T , UC security, but honest-majority and 23–79 rounds per [BdCE⁺26]), Celi et al. [CdPE⁺26] (dishonest-majority, 6 rounds, but $T \leq 6$), and Trilithium [DKLS25] (UC-secure, but 2-party only). Our Profile P2 targets a different point in the design space: arbitrary T with dishonest-majority security in 5 constant rounds.

7.2 Summary of Contributions

Our primary technical contribution is *Shamir nonce DKG*: parties jointly generate the signing nonce via a distributed key generation protocol, producing a degree- $(T-1)$ Shamir sharing that structurally matches the long-term secret. Because the adversary observes only $T-1$ evaluations of each honest party’s degree- $(T-1)$ polynomial, the remaining degree of freedom provides an approximate one-time pad: the honest party’s nonce share \mathbf{y}_h has conditional min-entropy exceeding $5\times$ the secret key entropy for $|S| \leq 17$, requiring no computational assumptions (Theorem 3). Key privacy given the public signature relies on the same lattice hardness as single-signer ML-DSA (computational, informal; formal reduction is an open problem for ML-DSA-based constructions, unresolved even in the single-signer setting). The bounded-nonce constraint prevents perfect uniformity (Remark 19), but the min-entropy guarantee is more than sufficient for practical security. In coordinator-based profiles (P1, P3+), this eliminates the two-honest requirement for nonce share privacy: signing sets of size $|S| \geq T$ suffice, matching the minimum required by Shamir’s (T, N) threshold property for reconstruction. Individual masked commitments \mathbf{W}_i are sent only to the coordinator (not broadcast), preventing a key-recovery attack via the injective matrix \mathbf{A} (Remark 15). Commitment and r0-check mask hiding retains $|S \setminus C| \geq 2$ (Lemma 2), which applies to P2’s broadcast model.

As a secondary technique, we introduce *pairwise-canceling masks* (adapted from ECDSA [CGG⁺20]) to the lattice setting, used for commitment values \mathbf{W}_i and r0-check shares \mathbf{V}_i . This addresses three challenges absent in ECDSA: rejection sampling bounds, r0-check key leakage, and Irwin-Hall nonce security. The Irwin-Hall security gap of prior approaches is resolved by direct shift-invariance (Corollary 8): the EUF-CMA loss is < 0.013 bits per signing session for $|S| \leq 33$ (total: $< 0.013 \cdot q_s$ bits), giving a proven security bound of $\geq 96 - 0.006 \cdot q_s$ bits for $|S| \leq 17$ (non-vacuous for $q_s < 16,000$), remaining below 1 bit per session for all $|S| \leq 2,584$.

We instantiate these techniques in three deployment profiles with complete UC proofs. Profile P1 (TEE-Assisted) achieves 3 online rounds plus 1 offline preprocessing round with EUF-CMA security under Module-SIS (Theorem 2). Profile P2 (Fully Distributed) uses MPC to achieve 5-round signing with dishonest-majority and UC security (Theorem 7). Profile P3+ (Semi-Async 2PC) achieves 2 logical rounds (22 ms for 3-of-5) with UC security under a 1-of-2 CP honest assumption (Theorem 8).

Our optimized Rust implementation demonstrates practical efficiency: P1 achieves 4–60 ms and P3+ achieves 17–94 ms for configurations from (2, 3) to (32, 45) threshold; P2 ranges from 21–194 ms, trading latency for eliminating hardware trust. Success

rates of $\approx 21\text{--}45\%$ (Table 5) are comparable to single-signer ML-DSA. All signatures are syntactically identical to single-signer ML-DSA and pass standard FIPS 204 verification without modification.

7.3 Limitations and Future Work

Current Limitations. Each deployment profile involves different trust assumptions: Profile P1 requires TEE/HSM trust, Profile P2 eliminates hardware trust at the cost of 5 MPC rounds, and Profile P3+ requires 1-of-2 CP honesty with 2 logical rounds. The nonce DKG adds one offline preprocessing round of $O(N^2)$ point-to-point messages (≈ 3.6 KB each) before each signing session; while this can be amortized by precomputing nonce batches during idle time, it does increase protocol complexity relative to purely additive nonce sharing. The aggregated nonce follows an Irwin-Hall rather than uniform distribution. By the direct shift-invariance analysis (Corollary 8), the per-coordinate chi-squared divergence between real and simulated nonces is $\chi^2(\text{IH} + \beta || \text{IH}) < 7 \times 10^{-6}$ for $|S| \leq 17$ and $< 1.4 \times 10^{-5}$ for $|S| \leq 33$, giving a full-vector EUF-CMA security loss < 0.013 bits per signing session for $|S| \leq 33$ (total: $< 0.013 \cdot q_s$ bits)—at most 13 bits for $q_s \leq 1,000$ (or < 7 bits in the $|S| \leq 17$ regime using the < 0.007 per-session bound), well below the 192-bit security target. For the pairwise masks used on commitment and r0-check values, $|S \setminus C| \geq 2$ honest parties are needed. In coordinator-based profiles (P1, P3+), masked commitments \mathbf{W}_i are sent only to the coordinator rather than broadcast, so $|S \setminus C| = 1$ suffices for nonce share privacy; in P2’s broadcast model, the existing mask-hiding condition $|S \setminus C| \geq 2$ applies to all values. This work focuses on ML-DSA-65 (NIST Level 3); extending to ML-DSA-44 ($\gamma_1 = 2^{17}$, $\beta = \tau\eta = 78$) and ML-DSA-87 ($k = 8, \ell = 7, \gamma_1 = 2^{19}, \beta = 120$) is straightforward in principle—ML-DSA-44 loosens the chi-squared bound by $\approx 2.5\times$ relative to ML-DSA-65 (smaller γ_1 increases the ratio β/γ_1) but retains < 0.04 bits of EUF-CMA loss per session for $|S| \leq 33$, while ML-DSA-87’s smaller β at the same γ_1 tightens the bound by $\approx 2.7\times$ (< 0.007 bits per session for $|S| \leq 33$); the latter also expands the r0-check circuit from 1536 to 2048 coefficients; a full benchmark across all three levels remains to be conducted. Finally, we assume a synchronous model where all parties are online simultaneously during signing (though P3+ relaxes this to semi-asynchronous participation).

Future Directions. Several aspects of our construction invite further investigation, ranging from strengthening the security model to broadening the parameter space and exploring applied deployment scenarios.

The most natural theoretical extension is *adaptive security*. Our analysis assumes a static adversary that selects which parties to corrupt before protocol execution begins; extending the results to the adaptive setting—where the adversary may corrupt parties during the protocol based on observed transcripts—remains open. The Shamir nonce DKG introduces a subtle obstacle: each honest party’s polynomial \mathbf{f}_h has its leading coefficient $\mathbf{a}_{h,T-1}$ sampled uniformly, but the remaining coefficients are constrained by the constant term $\hat{\mathbf{y}}_h$ and the evaluation points. Under adaptive corruption, the simulator must equivocate these polynomials after the fact, which may require an erasure model (parties delete intermediate state after each round) or a non-committing encryption wrapper around the DKG messages. The analogous question for ECDSA threshold signatures was resolved by Canetti et al. [CGG⁺20] using UC-secure commitments; whether a similar approach suffices in the lattice setting, where the polynomial structure imposes additional algebraic constraints, is unclear. Separately, a proof in the quantum random oracle model (QROM) would strengthen the EUF-CMA bound against quantum adversaries making superposition queries to the challenge hash—an upgrade shared with single-signer FIPS 204 [Nat24b].

A related direction concerns the strength of the abort guarantee. All three profiles currently achieve security-with-abort: a malicious party can force the protocol to output

\perp , but cannot produce an invalid signature. Profile P2’s SPDZ-based MPC naturally supports *identifiable abort*—when a MAC check fails, the cheating party can be pinpointed and excluded—but we have not formalized this property. A stronger goal is *guaranteed output delivery*, where the protocol always produces a valid signature provided sufficiently many honest parties participate. This is achievable in the honest-majority setting via broadcast protocols [CLOS02], and Profile P2’s framework can be augmented with a fair reconstruction phase when $|S| \geq 2T - 1$. Such an upgrade would be particularly relevant for custody and government applications where signing requests must not be silently suppressed.

A formal security reduction for *key privacy*—the property that a signature $\sigma = (\tilde{c}, \mathbf{z}, \mathbf{h})$ does not reveal $(\mathbf{s}_1, \mathbf{s}_2)$ beyond the public key \mathbf{t}_1 —remains open even for single-signer FIPS 204 ML-DSA and is inherited by all threshold variants. In the threshold setting, additional leakage vectors arise: partial responses $\mathbf{z}_i = \mathbf{y}_i + c \cdot \mathbf{s}_{1,i}$ and masked commitments \mathbf{W}_i are visible to the coordinator or broadcast to the signing group. Theorem 3 establishes that nonce shares \mathbf{y}_h retain high conditional min-entropy given the adversary’s view, bounding the information about $\mathbf{s}_{1,h}$ leaked by any single partial response; however, a formal reduction showing that the aggregate response $\mathbf{z} = \sum_i \lambda_i \mathbf{z}_i$ and hint vector \mathbf{h} , over polynomially many queries with Irwin-Hall nonces and Shamir share structure, do not expose \mathbf{s}_1 to a lattice adversary remains to be constructed.

Our appendix sketches a share refresh mechanism based on adding shares of zero, but a complete treatment of *proactive threshold ML-DSA* requires addressing several interacting concerns: maintaining signing availability during the refresh epoch, ensuring consistency at epoch boundaries (parties must agree on which shares are current), and formally modeling a mobile adversary that corrupts different subsets in different epochs subject to a per-epoch threshold. The Shamir structure of our key shares is well-suited to proactive protocols—refresh amounts to adding a fresh degree- $(T-1)$ zero-sharing—but the interaction between nonce DKG freshness and proactive share updates has not been analyzed. In particular, if a party’s long-term share $\mathbf{s}_{1,i}$ is refreshed between the nonce DKG and the signing round, the Lagrange reconstruction $\mathbf{z} = \sum_i \lambda_i \mathbf{z}_i$ may fail unless both the nonce and secret shares are refreshed consistently within the same epoch.

Decentralized Key Generation. Our construction assumes a trusted dealer for key setup: the dealer samples the short-coefficient signing key $(\mathbf{s}_1, \mathbf{s}_2) \leftarrow \chi^\ell \times \chi^k$, computes the public key $\mathbf{t} = \mathbf{A}\mathbf{s}_1 + \mathbf{s}_2$, and distributes Shamir shares $\mathbf{s}_{1,i}, \mathbf{s}_{2,i}$ directly. Fully decentralized key generation for ML-DSA requires verifiably short-coefficient Shamir sharing: each party must prove $\|\mathbf{s}_{1,h}\|_\infty \leq \eta$ without reconstruction. Standard Feldman VSS does not apply since Shamir shares of η -small secrets lie in \mathbb{Z}_q and reveal no information about the coefficient bound; lattice-based zero-knowledge techniques—such as BDLOP commitments with norm proofs [BDL⁺18]—offer a path forward. We leave a complete treatment to future work.

On the protocol side, three open problems stand out.

Eliminating offline nonce preprocessing. The Shamir nonce DKG requires one offline preprocessing round of $O(N^2)$ messages per signing session, structurally necessary because nonce shares must be committed before the challenge hash is computed to prevent adversarial rewinding. A natural question is whether this phase can be merged into the online protocol: a combined first round where parties simultaneously distribute nonce shares and broadcast the nonce commitment $\mathbf{w}_1 = \text{HighBits}(\mathbf{A} \sum_i \hat{\mathbf{y}}_i, 2\gamma_2)$ would eliminate the offline cost at the price of one additional online round. Whether such a per-session DKG preserves statistical nonce privacy against an adversary who aborts after observing first-round messages—and whether the SPDZ preprocessing in Profile P2 can be batched with nonce DKG preprocessing into a single unified offline phase—are open questions with

direct impact on deployment latency.

Reducing the MPC frontier via carry separation. Profile P2’s MPC evaluates the full r_0 -check over \mathbb{Z}_q (23-bit arithmetic). A finer decomposition is possible: because each party holds Shamir nonce and key shares, the low-bit residual $\ell_i = \text{LowBits}(A\mathbf{y}_i - c\mathbf{s}_{2,i})$ is locally precomputable without communication. The r_0 -check then reduces to evaluating only the carry of $\sum \lambda_i \ell_i$ and a single comparison bit—a much lighter computation than the full modular circuit. With standard Shamir coefficients $\lambda_i \approx q$, this yields no circuit reduction, since the intermediate sum overflows \mathbb{Z}_q . However, if reconstruction coefficients satisfy $\lambda_i \in \{0, 1\}$ —as in Vandermonde-style short-coefficient LSSS explored by concurrent work [BCdP⁺25]—the carry is bounded by $\lfloor T/2 \rfloor$, reducing the MPC computation to a $\lceil \log_2 T \rceil$ -bit carry circuit rather than a full 23-bit modular arithmetic circuit. Designing a security proof for this hybrid (Shamir nonce DKG for statistical nonce privacy combined with short-coefficient sharing for \mathbf{s}_2) is an open problem; the key challenge is showing that the bounded carry value does not leak sufficient information about \mathbf{s}_2 to assist a lattice adversary. More broadly, whether threshold ML-DSA with dishonest-majority and arbitrary T can be instantiated without general-purpose MPC—overcoming the construction-specific $T \leq 6$ barrier of existing short-coefficient LSSS schemes (the Ball-Çakan-Malkin bound [BCM⁺21] establishes an asymptotic $\Omega(T \log T)$ share-size lower bound; the specific $T \leq 6$ ceiling is Celi et al.’s construction-specific limit)—remains a fundamental open question in lattice-based threshold cryptography.

Commitment mask hiding for $T = N$. In P2’s broadcast model, the pairwise-canceling masks on \mathbf{W}_i and \mathbf{V}_i require $|S \setminus C| \geq 2$ for computational hiding (Lemma 2). In the extreme case $T = N$ (unanimous signing), a single honest party’s commitment and r_0 -check values are not hidden in P2. (In P1 and P3+, the coordinator-only communication model protects \mathbf{W}_i even with $|S \setminus C| = 1$; see Remark 15.) Replacing pairwise PRF masks with a *non-interactive zero-sharing* scheme—where each party’s mask is derived from a common reference string rather than pairwise seeds—or employing a verifiable PRF construction could close this gap, yielding uniform $|S| \geq T$ privacy across all revealed values. Additionally, achieving perfect uniformity ($\text{SD} = 0$) for the response shares with $|S| = T$ remains an open problem: the bounded-nonce constraint fundamentally prevents \mathbb{Z}_q -uniformity (Remark 19), and it is unclear whether alternative nonce generation techniques can bypass this barrier without requiring $|S| \geq T + 1$. (Note: the term “statistical privacy” in this work refers to the high-min-entropy guarantee of Theorem 3, not $\text{SD} = 0$.)

Finally, on the applied side, threshold ML-DSA is a natural building block for post-quantum decentralized identity systems. The W3C Decentralized Identifier specification [SLS⁺22] requires controller key rotation and recovery mechanisms that interact non-trivially with threshold key management: a DID controller update must atomically rotate the threshold public key while preserving the mapping between DID documents and verification methods. Combining our protocol with a threshold-friendly DID resolution layer and a key recovery flow based on social recovery via Shamir shares would yield an end-to-end post-quantum identity system suitable for regulated environments.

7.4 Impact

As organizations transition to post-quantum cryptography, our construction facilitates ML-DSA adoption in cryptocurrency custody, distributed certificate authorities, enterprise key management, and government applications. The threshold security guarantees and FIPS 204 compatibility allow integration with existing infrastructure without requiring verifier modifications.

Acknowledgments

During the preparation of this work, the author used Claude (Anthropic) to assist with manuscript formatting and language editing. After using this tool, the author reviewed and edited the content as needed and takes full responsibility for the content of the publication.

A Full Security Proofs

A.1 Unforgeability Proof (Full)

We provide detailed analysis of each game transition for Theorem 2.

Game 0 (Real Game). The real EUF-CMA game. Challenger runs $\text{KeyGen}(1^\kappa, N, T)$ to obtain $(\text{pk}, \{\text{sk}_i\}_{i \in [N]})$, gives \mathcal{A} the public key $\text{pk} = (\rho, \mathbf{t}_1)$ and corrupted shares $\{\text{sk}_i\}_{i \in C}$ where $|C| \leq T - 1$. Adversary \mathcal{A} makes signing queries and outputs forgery (m^*, σ^*) .

Game 1 (Random Oracle). Replace hash function H with lazily-sampled random function \mathcal{O} . Maintain table `Table` of query-response pairs. On query x : if $(x, y) \in \text{Table}$, return y ; else sample $y \xleftarrow{\$} \mathcal{Y}$, store (x, y) , return y . *Analysis:* By random oracle model, $\Pr[\text{Win}_1] = \Pr[\text{Win}_0]$.

Game 2 (Programmed Challenges). Modify signing oracle: before computing \mathbf{w} , sample $c \xleftarrow{\$} \mathcal{C}$ uniformly, then program $\mathcal{O}(\mu \parallel \mathbf{w}_1) := c$ after computing \mathbf{w}_1 . *Analysis:* Programming fails only if $(\mu \parallel \mathbf{w}_1)$ was previously queried. By union bound over q_H hash queries and q_s signing queries: $|\Pr[\text{Win}_2] - \Pr[\text{Win}_1]| \leq (q_H + q_s)^2 / 2^{256}$.

Game 3 (Simulated Shares). We argue that the adversary’s view of the honest parties’ key shares $\{\mathbf{s}_{1,j}\}_{j \notin C}$ is statistically independent of the secret key \mathbf{s}_1 , by Shamir’s (T, N) -threshold perfect secrecy: any $T - 1$ evaluations are jointly consistent with every possible value of the secret (the marginal distribution of each honest share at a non-zero evaluation point is R_q^ℓ -uniform, but the *joint* distribution of multiple honest shares is not i.i.d.—they are correlated as evaluations of the same degree- $(T - 1)$ polynomial; the correct statement is that the joint view reveals zero information about \mathbf{s}_1). *Important:* this is a conceptual argument about the adversary’s *view*—the signing oracle continues using the actual short key shares (replacing them with uniform R_q^ℓ values would cause the $\|\mathbf{z}\|_\infty$ -bound and r0-checks to fail with overwhelming probability, invalidating signatures). Since $|C| \leq T - 1$, the adversary’s view of honest shares is statistically independent of the secret: $\Pr[\text{Win}_3] = \Pr[\text{Win}_2]$. (In Profile P2, individual per-party responses \mathbf{z}_j are contributed only as SPDZ input shares, so SPDZ input-privacy ensures the adversary observes only the aggregate \mathbf{z} , not individual \mathbf{z}_j values; the same Shamir argument applies.)

Game 3.5 (Uniform Nonces). Replace Irwin-Hall nonce distribution with uniform over $\{-\gamma_1, \dots, \gamma_1\}^{n^\ell}$. In Game 3, the aggregate nonce $\mathbf{y} = \sum_{i \in S} \hat{\mathbf{y}}_i$ follows the Irwin-Hall distribution. We replace this with $\mathbf{y} \xleftarrow{\$} \{-\gamma_1, \dots, \gamma_1\}^{n^\ell}$ uniform. *Analysis:* The q_s signing sessions are independent, so the joint Rényi divergence is $(R_2^{\text{vec,shift}})^{q_s}$ (direct shift-invariance, Theorem 30). Applying the smooth Rényi divergence probability transfer lemma (Lemma 17) to the joint distribution:

$$\Pr[\text{Win}_3] \leq (R_2^{\text{vec,shift}})^{q_s/2} \cdot \sqrt{\Pr[\text{Win}_{3.5}]} + q_s \cdot \epsilon_{\text{IH}}$$

where $R_2^{\text{vec,shift}} = (1 + \chi_{\text{direct}}^2)^{n\ell}$ is the full-vector *per-session* Rényi divergence from the direct shift-invariance analysis, with $\chi_{\text{direct}}^2 \approx 6.62 \times 10^{-6}$ per coordinate for $|S| = 17$ (Corollary 8), giving $R_2^{\text{vec,shift}} \approx 1.0085$, and $\epsilon_{\text{IH}} < 10^{-30}$ (Theorem 4). The total security loss is $\approx 6.1 \times 10^{-3} \cdot q_s$ bits, giving a proven security bound of $\geq 96 - 0.006 \cdot q_s$ bits for $|S| \leq 17$ (where the 96-bit baseline is the Cauchy-Schwarz halving of the 192-bit NIST Level 3 baseline). The conservative analytical bound ($R_2^{\text{vec}} \approx 2^{5.4}$, Remark 16) is vacuous at $q_s \gtrsim 36$.

Game 4 (Signature Simulation). Starting from uniform nonces (Game 3.5), simulate signatures without \mathbf{s}_1 :

1. Sample $\mathbf{z} \stackrel{\$}{\leftarrow} \{v \in R_q^\ell : \|\mathbf{v}\|_\infty < \gamma_1 - \beta\}$ with rejection sampling
2. Compute $\mathbf{w}_1 = \text{HighBits}(\mathbf{A}\mathbf{z} - c\mathbf{t}_1 \cdot 2^d, 2\gamma_2)$
3. Program $\mathcal{O}(\mu \|\mathbf{w}_1) := c$
4. Simulate masked values $\mathbf{W}_j, \mathbf{V}_j$ as computationally uniform (Lemma 2, replacing honest-honest PRF terms with uniform)

Clarification: In this EUF-CMA game, the adversary observes only the aggregate public signature $\sigma = (\tilde{c}, \mathbf{z}, \mathbf{h})$; individual per-party responses \mathbf{z}_j are processed inside the TEE/combiner and never reach the adversary. Accordingly, Steps 1–3 produce the adversary-visible \mathbf{z} without using \mathbf{s}_1 , and Step 4 handles the masked intermediate values that the adversary also cannot observe directly. The full per-party simulation (including $\mathbf{z}_j = \mathbf{y}_j + c\mathbf{s}_{1,j}$ from DKG values) is deferred to the UC/privacy simulator in Appendix A.2. *Analysis:* The masked commitment and r0-check values $\mathbf{W}_j, \mathbf{V}_j$ are computationally indistinguishable from uniform by Lemma 2. By PRF security: $|\Pr[\text{Win}_4] - \Pr[\text{Win}_{3.5}]| \leq \binom{N}{2} \cdot \epsilon_{\text{PRF}}$.

Reduction to M-SIS. Construct SelfTargetMSIS adversary \mathcal{B} [KLS18]:

1. \mathcal{B} receives M-SIS instance $\mathbf{A} \in R_q^{k \times \ell}$
2. \mathcal{B} sets ρ such that $\text{ExpandA}(\rho) = \mathbf{A}$, samples $\mathbf{t}_1 \stackrel{\$}{\leftarrow} R_q^k$ (uniformly random; valid since Game₄ simulation does not require knowing \mathbf{s}_1 or \mathbf{s}_2 ; \mathbf{t}_1 is indistinguishable from a real key by M-LWE hardness [KLS18])
3. \mathcal{B} picks a random index $i^* \stackrel{\$}{\leftarrow} [q_H]$ as the target ROM query
4. \mathcal{B} simulates Game₄ for \mathcal{A} , programming ROM responses uniformly
5. When \mathcal{A} outputs forgery $(\mu^*, \mathbf{z}^*, c^*, \mathbf{h}^*)$: if c^* equals the i^* -th ROM response, extract; otherwise abort

Analysis: \mathcal{B} succeeds when its guess i^* is correct, which occurs with probability $1/q_H$, so $\Pr[\mathcal{B} \text{ succeeds}] \geq \Pr[\text{Win}_4]/q_H$. When successful, the forgery verification gives:

$$\text{HighBits}(\mathbf{A}\mathbf{z}^* - c^*\mathbf{t}_1 \cdot 2^d, 2\gamma_2) = \mathbf{w}_1^*$$

Rearranging yields the SelfTargetMSIS solution for $[\mathbf{A} \mid -\mathbf{t}_1 \cdot 2^d]$ (see Remark 2):

$$[\mathbf{A} \mid -\mathbf{t}_1 \cdot 2^d] \cdot \begin{bmatrix} \mathbf{z}^* \\ c^* \end{bmatrix} = 2\gamma_2 \mathbf{w}_1^* + \mathbf{r}_0^*$$

where $\mathbf{w}_1^* = \text{HighBits}(\mathbf{A}\mathbf{z}^* - c^*\mathbf{t}_1 \cdot 2^d, 2\gamma_2)$ is the known verification target and $\|\mathbf{r}_0^*\|_\infty \leq \gamma_2$ is the LowBits residual. The combined solution $[(\mathbf{z}^*); (c^*)] \in R_q^{\ell+1}$ satisfies $\|\mathbf{z}^*\|_\infty < \gamma_1 - \beta$ (z-bound check) and $\|c^*\|_\infty = 1$ (challenge coefficients in $\{-1, 0, +1\}$); the module ℓ^∞ -norm is $\max(\|\mathbf{z}^*\|_\infty, \|c^*\|_\infty) < \gamma_1$, matching the SelfTargetMSIS norm parameter from Remark 2 and [KLS18]. Thus $\Pr[\text{Win}_4] \leq q_H \cdot \epsilon_{\text{M-SIS}}$.

A.2 Privacy Proof Details

We show that the simulator produces an indistinguishable view, applying the min-entropy bound established in Theorem 3 (Section 4).

With the Shamir nonce DKG, privacy of the nonce share \mathbf{y}_h is statistical (no computational assumptions). The simulator computes responses from simulated DKG values, achieving perfect indistinguishability for the response component.

Simulator \mathcal{S} . Given inputs $(\text{pk}, \{\text{sk}_i\}_{i \in C}, \sigma = (\tilde{c}, \mathbf{z}, \mathbf{h}))$:

Round 1 Simulation: For each honest $j \in S \setminus C$, sample $\text{Com}_j \xleftarrow{\$} \{0, 1\}^{256}$ uniformly.

Round 2 Simulation: Expand challenge c from \tilde{c} , compute $\mathbf{w}_1 = \text{UseHint}(\mathbf{h}, \mathbf{A}\mathbf{z} - \mathbf{c}\mathbf{t}_1 \cdot 2^d)$. The adversary observes only $(\mathbf{w}_1, \tilde{c})$ broadcast by the coordinator (individual \mathbf{W}_j are sent only to the coordinator; see Remark 11). The simulator produces consistent $(\mathbf{w}_1, \tilde{c})$ from the signature.

Round 3 Simulation: The simulator must produce per-party responses \mathbf{z}_j consistent with both the simulated DKG values and the public signature constraint $\sum_{j \in S} \lambda_j \mathbf{z}_j = \mathbf{z}$ (enforced by the public σ). We handle the two cases separately.

Case $|S \setminus C| > 1$: Let $\mathbf{z}_j^* = \mathbf{y}_j^* + c \cdot \mathbf{s}_{1,j}$ denote corrupted party j 's response, where \mathbf{y}_j^* is j 's simulated DKG evaluation (known to the simulator from the corrupted view). The simulator chooses $\mathbf{z}_j = \mathbf{y}_j + c \cdot \mathbf{s}_{1,j}$ (from simulated DKG values) for all honest $j \in S \setminus C$ except a designated party h_0 , then sets

$$\mathbf{z}_{h_0} = \frac{\mathbf{z} - \sum_{j \in C} \lambda_j \mathbf{z}_j^* - \sum_{j \in (S \setminus C) \setminus \{h_0\}} \lambda_j \mathbf{z}_j}{\lambda_{h_0}}$$

(The division by λ_{h_0} is well-defined: since all evaluation points lie in $\{1, \dots, N\} \subset \mathbb{Z}_q^*$, the Lagrange coefficient $\lambda_{h_0} = \prod_{j \in S, j \neq h_0} j(j - h_0)^{-1} \bmod q$ is a product of nonzero field elements and hence nonzero mod q , hence invertible in \mathbb{Z}_q .) This \mathbf{z}_{h_0} matches exactly what the real protocol would produce (given the DKG polynomials), so $\text{SD} = 0$.

Case $|S \setminus C| = 1$: The single honest response $\mathbf{z}_h = (\mathbf{z} - \sum_{j \in C} \lambda_j \mathbf{z}_j^*) / \lambda_h$ is uniquely determined by σ and the corrupted views. The simulator outputs this value directly. Privacy of $\mathbf{s}_{1,h}$ (key privacy, computational) is maintained because the adversary knows \mathbf{z}_h but not the decomposition $\mathbf{z}_h = \mathbf{y}_h + c\mathbf{s}_{1,h}$: recovering $\mathbf{s}_{1,h}$ from \mathbf{z}_h requires solving a bounded-distance decoding instance given \mathbf{y}_h 's high conditional min-entropy (Theorem 3).

The \mathbf{V}_j values are computed as $\mathbf{V}_j = \lambda_j c \mathbf{s}_{2,j} + \mathbf{m}_j^{(s_2)}$ using simulated key shares and PRF masks.

Indistinguishability. In both cases, the simulated \mathbf{z}_j follows the same distribution as the real protocol ($\text{SD} = 0$ conditioned on σ). Masked values \mathbf{W}_j and \mathbf{V}_j are computationally indistinguishable from uniform (PRF security, Lemma 2); no PRF assumption is needed for nonce share privacy (\mathbf{y}_h 's statistical privacy is independent). The total distinguishing advantage is $\binom{N}{2} \cdot \epsilon_{\text{PRF}}$.

B Distributed Key Generation Protocols

Our protocol uses two structurally similar but functionally distinct DKG protocols: a *key DKG* (executed once during setup) and a *nonce DKG* (executed before each signing session, typically preprocessed offline). The key DKG uses Feldman-style commitments for verifiability; the nonce DKG omits VSS verification (correctness is instead ensured at the signing stage via the z-bound and r0-check). Both share the same polynomial evaluation structure but differ in their input distributions and security requirements.

B.1 Key DKG (One-Time Setup)

The key DKG produces a degree- $(T-1)$ Shamir sharing of the long-term signing key $(\mathbf{s}_1, \mathbf{s}_2)$, replacing the trusted dealer assumption.

Phase 1: Contribution. Each party $i \in [N]$:

1. Samples local secrets $\mathbf{s}_1^{(i)} \stackrel{\$}{\leftarrow} \chi_\eta^\ell$ and $\mathbf{s}_2^{(i)} \stackrel{\$}{\leftarrow} \chi_\eta^k$
2. Creates (T, N) -Shamir sharings of each polynomial
3. Sends share $(\mathbf{s}_{1,j}^{(i)}, \mathbf{s}_{2,j}^{(i)})$ to party j
4. Broadcasts Feldman commitment $\mathbf{t}^{(i)} = \mathbf{A}\mathbf{s}_1^{(i)} + \mathbf{s}_2^{(i)}$

Phase 2: Aggregation. Each party j computes aggregated share: $\mathbf{s}_{1,j} = \sum_{i \in [N]} \mathbf{s}_{1,j}^{(i)}$

The final secret is $\mathbf{s}_1 = \sum_{i=1}^N \mathbf{s}_1^{(i)}$, which no individual party knows. For lattice-specific VSS/DKG, see [ENP24].

B.2 Nonce DKG (Per-Session Preprocessing)

The nonce DKG produces a fresh degree- $(T-1)$ Shamir sharing of the signing nonce \mathbf{y} for each signing session. Unlike the key DKG, the nonce DKG samples higher-degree coefficients uniformly from R_q (rather than from a short-coefficient distribution), which is critical for achieving statistical share privacy.

The protocol is specified formally in Algorithm 1 of the main paper (Section 3.4). Each party $i \in S$ generates a degree- $(T-1)$ polynomial $\hat{f}_i(X)$ whose constant term $\hat{\mathbf{y}}_i$ is sampled from the reduced nonce range $[-\lfloor \gamma_1/|S| \rfloor, \lfloor \gamma_1/|S| \rfloor]^{n_\ell}$ and whose higher-degree coefficients are sampled uniformly from R_q^ℓ . The resulting aggregated nonce $\mathbf{y} = \sum_{i \in S} \hat{\mathbf{y}}_i$ follows the Irwin-Hall distribution analyzed in Theorem 4, while each honest party's individual share $\mathbf{y}_h = \sum_{i \in S} \hat{f}_i(h)$ has high conditional min-entropy from the adversary's perspective (Theorem 3).

B.3 Security Properties

Both protocols share the following properties:

- **Correctness:** Honest execution produces a valid sharing of the intended secret.
- **Secrecy:** Any coalition of $< T$ parties learns nothing about the secret beyond what is revealed by public commitments (follows from Shamir's threshold security).
- **Robustness:** The key DKG uses Feldman commitments [Fel87] to detect and attribute malicious shares. The nonce DKG omits VSS verification; malicious behavior is instead detected at the signing stage (z-bound or r0-check failure triggers the blame protocol), which suffices for security-with-abort.

The nonce DKG additionally provides statistical privacy (no computational assumptions) of individual shares (Theorem 3), which is the key enabler for eliminating the two-honest requirement (enabling $|S| = T$ signing sets with nonce share privacy) in coordinator-based profiles (P1, P3+; see Remark 11). The key DKG does not require this property, since key shares are never revealed during signing.

C Proactive Security

C.1 Share Refresh Protocol

Periodically, parties execute a share refresh:

1. Each party i samples a random (T, N) -sharing of $\mathbf{0}$
2. Party i sends the j -th share of zero to party j
3. Each party adds received zero-shares to their current share

Since adding shares of zero preserves the secret, reconstruction still yields \mathbf{s}_1 . After refresh, old shares become useless. An adversary must corrupt $\geq T$ parties within a single epoch to learn the secret.

Forward Secrecy for Past Signatures. Signatures from epoch k remain secure after the epoch- $(k+1)$ refresh. A signature σ from epoch k reveals $\mathbf{z}_j^{(k)} = \mathbf{y}_j^{(k)} + c \cdot \mathbf{s}_{1,j}^{(k)}$. Since $\mathbf{y}_j^{(k)}$ is a one-time nonce share (deleted after use), and the refreshed shares $\mathbf{s}_{1,j}^{(k+1)} = \mathbf{s}_{1,j}^{(k)} +$ (zero-sharing term) do not reveal $\mathbf{s}_{1,j}^{(k)}$ by Shamir's threshold property (the zero-sharing randomizes shares while preserving the secret), past key shares cannot be reconstructed from refreshed shares alone. Key privacy for past signatures therefore holds across epochs under the same M-LWE hardness assumption as the signing scheme.

D Numerical Verification of Rényi Bounds

We provide detailed calculations for the smooth Rényi divergence bounds referenced in Theorem 4.

Parameters for ML-DSA-65.

- Modulus: $q = 8380417$
- Masking range: $\gamma_1 = 2^{19} = 524288$
- Secret bound: $\eta = 4$
- Challenge weight: $\tau = 49$
- Signature bound: $\beta = \tau \cdot \eta = 196$

Rényi Divergence Calculation. Let $m = |S|$ denote the signing set size (distinct from the ring degree $n = 256$) and $B = 2\lceil\gamma_1/m\rceil$ the per-share **full** range (from $-\lceil\gamma_1/m\rceil$ to $+\lceil\gamma_1/m\rceil$, so the total width is $2\lceil\gamma_1/m\rceil$). Note that in Definition 22, the symbol B denotes the **half**-range (each $X_i \in \{-B, \dots, B\}$); to apply Raccoon [dPEK⁺24] Lemma 4.2, B here is the full range, equal to $2\times$ that half-range. For readability, we use the approximation $B \approx 2\gamma_1/m$ (the rounding error is at most $2/B < 4 \times 10^{-5}$ for all relevant m , and the exact discrete range is used in the implementation). Using Lemma 4.2 of [dPEK⁺24] with $\alpha = 2$ and shift $\delta = \beta$:

$$\begin{aligned} R_2^\xi &\leq 1 + \frac{m^2 \cdot \beta^2}{B^2} \approx 1 + \frac{m^2 \cdot \beta^2}{(2\gamma_1/m)^2} \\ &= 1 + \frac{m^4 \cdot \beta^2}{4\gamma_1^2} = 1 + \frac{|S|^4 \cdot \beta^2}{4\gamma_1^2} \end{aligned}$$

Table 12: Per-coordinate Rényi divergence bounds for ML-DSA-65. $B = 2\lceil\gamma_1/|S|\rceil$ is the exact per-share full range; displayed values are $2\lceil\gamma_1/|S|\rceil$. All bounds computed using Lemma 4.2 of [dPEK⁺24]. Full-vector: $R_2^{\text{vec}} = (R_2^{\epsilon, \text{coord}})^{1280}$ ($n = 256, \ell = 5$).

$ S $	$B \approx 2\gamma_1/ S $	$R_2^\epsilon - 1$	ϵ (tail)
4	262144	8.9×10^{-6}	$< 10^{-10}$
9	116508	2.3×10^{-4}	$< 10^{-19}$
17	61680	2.9×10^{-3}	$< 10^{-30}$
25	41942	1.4×10^{-2}	$< 10^{-40}$
33	31774	4.1×10^{-2}	$< 10^{-49}$

The per-coordinate $R_2^{\epsilon, \text{coord}}$ remains below 1.05 for $|S| \leq 33$. The full-vector divergence $R_2^{\text{vec}} = (R_2^{\epsilon, \text{coord}})^{1280}$ ranges from $\approx 2^{5.4}$ ($|S| = 17$) to $\approx 2^{75}$ ($|S| = 33$); see Theorem 4 for the impact on the security bound. The direct analysis (Corollary 8) gives < 0.013 bits for all $|S| \leq 33$.

E Rejection Sampling Analysis

E.1 Root Cause

ML-DSA’s rejection sampling stems from two checks:

1. **z-bound check:** $\|\mathbf{z}\|_\infty < \gamma_1 - \beta$
2. **r0 check:** $\|\text{LowBits}(\mathbf{w} - c\mathbf{s}_2)\|_\infty < \gamma_2 - \beta$

For ML-DSA-65 (*single-signer approximation*: nonce uniform on $[-\gamma_1, \gamma_1]$):

- z-bound: $\left(\frac{\gamma_1 - \beta}{\gamma_1}\right)^{n\ell} = \left(\frac{524092}{524288}\right)^{1280} \approx 62\%$
- r0 check: $\left(\frac{\gamma_2 - \beta}{\gamma_2}\right)^{nk} = \left(\frac{261692}{261888}\right)^{1536} \approx 32\%$
- Combined: $0.62 \times 0.32 \approx 20\%$

This matches the NIST ML-DSA specification [Nat24b] (expected 4–5 iterations). *Note:* In the threshold protocol, nonces follow the Irwin-Hall distribution (sum of $|S|$ uniform variables), so the per-attempt success rates differ from this single-signer estimate; empirical measurements yield 21–45% depending on T and $|S|$ (see Table 13).

E.2 Throughput Optimizations

- **Parallel Attempts:** Generate B independent (y, w) pairs per signing session. Success probability: $1 - (0.80)^B$ (using the theoretical $\approx 20\%$ per-attempt rate; empirical benchmarks yield ≈ 25 – 31% , giving $1 - (0.75)^B$ as an optimistic estimate).
- **Pre-computation:** Pre-compute $(y_i, w_i = \mathbf{A}y_i)$ pairs during idle time.
- **Pipelining:** Start next attempt while waiting for network communication.

F Naive Approach Comparison

Without masking, each party’s contribution $\lambda_i \cdot \mathbf{z}_i$ has norm $O(\lambda_i \cdot \gamma_1)$, failing the z-bound check with probability ≈ 0.8 . Success requires all T parties to pass independently:

Table 13: Improvement over naive threshold approach. “Our Success” values are empirical measurements from the Rust benchmarks (Table 5). The non-monotone behavior (32.4% \rightarrow 23.1% \rightarrow 25.0% for $T = 16, 24, 32$) reflects the interplay of two competing effects: (1) smaller per-party nonce range $\gamma_1/|S|$ reduces the acceptance probability for the z-bound check; (2) the Irwin-Hall distribution becomes more concentrated near zero for larger $|S|$, partially improving acceptance. The net effect is non-monotone in $|S|$ and configuration-dependent.

T	Naive Success $(0.2)^T$	Our Success	Speedup
8	2.6×10^{-6}	28.2%	1.1×10^5
12	4.1×10^{-9}	31.4%	7.5×10^7
16	6.6×10^{-12}	32.4%	4.9×10^{10}
24	1.7×10^{-17}	23.1%	1.4×10^{16}
32	4.3×10^{-23}	25.0%	5.8×10^{21}

G Nonce Range Rounding Details

Each party’s constant-term contribution in the nonce DKG is $\hat{\mathbf{y}}_i \stackrel{\$}{\leftarrow} \{-\lfloor \gamma_1/|S| \rfloor, \dots, \lfloor \gamma_1/|S| \rfloor\}^{n\ell}$. When γ_1 is not divisible by $|S|$, the nonce $\mathbf{y} = \sum_{i \in S} \hat{\mathbf{y}}_i$ has range $[-|S| \cdot \lfloor \gamma_1/|S| \rfloor, |S| \cdot \lfloor \gamma_1/|S| \rfloor]^{n\ell}$, slightly smaller than standard $[-\gamma_1, \gamma_1]^{n\ell}$.

Concrete Impact. For ML-DSA-65 with $\gamma_1 = 524288$ and $|S| = 17$: $\lfloor 524288/17 \rfloor = 30840$, so the actual range is $[-524280, 524280]$. The “missing” probability mass is $(524288 - 524280)/524288 < 2 \times 10^{-5}$ per coordinate.

Effect on Security. The z-bound check is $\|\mathbf{z}\|_\infty < \gamma_1 - \beta$ where $\gamma_1 - \beta = 524092$. Since $524280 > 524092$, the reduced nonce range does not affect the pass probability for this example.

General Proof. Writing $\gamma_1 = |S| \cdot \lfloor \gamma_1/|S| \rfloor + r$ with $0 \leq r \leq |S| - 1$, the reduced nonce maximum is $|S| \cdot \lfloor \gamma_1/|S| \rfloor = \gamma_1 - r \geq \gamma_1 - (|S| - 1)$. For the z-bound check to be unaffected, we need $\gamma_1 - (|S| - 1) > \gamma_1 - \beta$, i.e., $|S| - 1 < \beta = \tau\eta = 196$. This holds for all $|S| \leq 196$, covering all practical signing set sizes. The Irwin-Hall security analysis uses the actual sampled range $N = 2\lfloor \gamma_1/|S| \rfloor$, so all bounds account for this rounding.

H UC Security Framework

Remark 22 (Scope of this appendix). This appendix provides the extended UC proofs for Profiles P2 and P3+. The Profile P1 UC proof (TEE-based coordinator) is self-contained in Theorem 5 and its proof in the main paper; it is not repeated here. This appendix proves UC security for the r0-check subprotocol (Profile P2, Theorem 7) and the semi-async signing protocol (Profile P3+, Theorem 26). These theorems establish UC realization of $\mathcal{F}_{r_0\text{-check}}$ and $\mathcal{F}_{r_0}^{\text{semi-async}}$ respectively; realization of the full $\mathcal{F}_{\text{ThreshSig}}$ (Definition 8) follows by UC composition with the nonce DKG and signing-step sub-protocols.

We recall the Universal Composability (UC) framework of Canetti [Can01, Can20]. Our presentation follows the conventions of [CLOS02, DPSZ12].

H.1 Execution Model

The UC framework considers three types of entities:

- **Environment \mathcal{Z}** : An interactive Turing machine that provides inputs to parties, receives their outputs, and attempts to distinguish real from ideal executions.
- **Adversary \mathcal{A}** : Controls corrupted parties and the network (scheduling message delivery).
- **Parties P_1, \dots, P_n** : Execute the protocol or interact with ideal functionalities.

Definition 13 (Real Execution). In the real execution $\text{REAL}_{\Pi, \mathcal{A}, \mathcal{Z}}$, parties execute protocol Π . The environment \mathcal{Z} provides inputs and receives outputs. The adversary \mathcal{A} controls corrupted parties and sees all communication. The output is \mathcal{Z} 's final bit.

Definition 14 (Ideal Execution). In the ideal execution $\text{IDEAL}_{\mathcal{F}, \mathcal{S}, \mathcal{Z}}$, parties interact with ideal functionality \mathcal{F} . A simulator \mathcal{S} simulates the adversary's view. The output is \mathcal{Z} 's final bit.

Definition 15 (UC-Realization). Protocol Π *UC-realizes* functionality \mathcal{F} if there exists a PPT simulator \mathcal{S} such that for all PPT environments \mathcal{Z} :

$$|\Pr[\text{REAL}_{\Pi, \mathcal{A}, \mathcal{Z}} = 1] - \Pr[\text{IDEAL}_{\mathcal{F}, \mathcal{S}, \mathcal{Z}} = 1]| \leq \text{negl}(\kappa)$$

Theorem 9 (UC Composition [Can01]). *If Π UC-realizes \mathcal{F} , then any protocol ρ that uses \mathcal{F} as a subroutine can securely use Π instead. Formally, $\rho^{\mathcal{F}}$ and ρ^{Π} are indistinguishable to any environment.*

H.2 Hybrid Functionalities

We work in the $(\mathcal{F}_{\text{SPDZ}}, \mathcal{F}_{\text{edaBits}}, \mathcal{F}_{\text{Binary}})$ -hybrid model, where:

Functionality 10 ($\mathcal{F}_{\text{SPDZ}}$ – Authenticated Secret Sharing [DPSZ12]). *Parameterized by field \mathbb{F}_q , parties $\mathcal{P} = \{P_1, \dots, P_n\}$, and MAC key $\alpha \in \mathbb{F}_q$.*

Share: On input (SHARE, sid, x) from dealer P_i :

1. Sample random shares $[x]_1, \dots, [x]_n$ with $\sum_j [x]_j = x$
2. Compute MAC shares $[\alpha x]_j$ for each party
3. Send $([x]_j, [\alpha x]_j)$ to each P_j
4. Send (SHARED, sid) to adversary \mathcal{S}

Add: On input (ADD, sid, $\text{id}_a, \text{id}_b, \text{id}_c$):

1. Each party locally computes $[c]_j = [a]_j + [b]_j$ and $[\alpha c]_j = [\alpha a]_j + [\alpha b]_j$

Multiply: On input (MULT, sid, $\text{id}_a, \text{id}_b, \text{id}_c$):

1. Using Beaver triples, compute shares of $c = a \cdot b$ with valid MACs
2. Notify adversary of completion

Open: On input (OPEN, sid, id_x):

1. Collect $[x]_j$ from all parties
2. Verify MACs: check $\sum_j [\alpha x]_j = \alpha \cdot \sum_j [x]_j$
3. If verification fails, output \perp to all parties
4. Otherwise, output $x = \sum_j [x]_j$ to all parties

Security: $\mathcal{F}_{\text{SPDZ}}$ provides statistical hiding of shares (additive shares are perfectly uniform given $\leq N-1$ honest parties) and computational integrity (MAC forgery probability $\leq 1/q$ per check).

Functionality 11 ($\mathcal{F}_{\text{edaBits}}$ – Extended Doubly-Authenticated Bits [EGK⁺20]). On input (EDABIT, sid, m) requesting m edaBits:

For $i = 1, \dots, m$:

1. Sample $r_i \xleftarrow{\$} \{0, 1, \dots, 2^k - 1\}$ for specified bit-length k
2. Create arithmetic sharing: $\langle r_i \rangle_q$ over \mathbb{F}_q
3. Create binary sharing: $\langle r_i \rangle_2 = (\langle r_i^{(0)} \rangle, \dots, \langle r_i^{(k-1)} \rangle)$ over \mathbb{F}_2
4. Distribute shares to parties with appropriate MAC tags

Output $\{(\langle r_i \rangle_q, \langle r_i \rangle_2)\}_{i=1}^m$ to all parties.

Security: The correlation (r, r) is hidden from any strict subset of parties. MAC tags ensure integrity.

Remark 23 (edaBits Range and Modular Reduction). The edaBits functionality samples $r_i \in \{0, \dots, 2^k - 1\}$ where $k = \lceil \log_2 q \rceil = 23$ for ML-DSA. Since $2^{23} = 8388608 > q = 8380417$, a direct reduction $r_i \bmod q$ introduces a small bias: values in $\{0, \dots, 2^{23} - q - 1\} = \{0, \dots, 8191\}$ are slightly more likely.

Per-coefficient bias: $(2^{23} - q)/2^{23} = 8191/8388608 < 2^{-10}$. A naïve union bound over $m = 1536$ coefficients gives $m \cdot 2^{-10} \approx 1.5$, which exceeds 1 and is therefore vacuous (statistical distance is at most 1 by definition).

Mitigation: We use rejection sampling within edaBits generation: sample $r \xleftarrow{\$} \{0, \dots, 2^k - 1\}$; if $r \geq q$, resample. The expected number of samples is $2^k/q < 1.001$, adding negligible overhead. With this modification, $r \bmod q$ is perfectly uniform over \mathbb{F}_q , and Lemma 5 applies exactly.

Functionality 12 ($\mathcal{F}_{\text{Binary}}$ – Binary Circuit Evaluation). On input (EVAL, sid, $C, \{\langle x_i \rangle_2\}$) where C is a binary circuit:

1. Reconstruct inputs x_i from shares
2. Evaluate $y = C(x_1, \dots, x_m)$
3. Create fresh sharing $\langle y \rangle_2$
4. Distribute to parties

Implemented via Beaver triples: for AND gate on shared bits $\langle x \rangle, \langle y \rangle$:

1. Use preprocessed triple $(\langle a \rangle, \langle b \rangle, \langle c \rangle)$ with $c = a \wedge b$
2. Open $d = x \oplus a$ and $e = y \oplus b$
3. Compute $\langle xy \rangle = \langle c \rangle \oplus (e \wedge \langle a \rangle) \oplus (d \wedge \langle b \rangle) \oplus (d \wedge e)$

I Complete Ideal Functionality for Profile P2

Note: This section presents the original 8-round P2 protocol for completeness. The optimized 5-round version used in the main paper (Table 1) is presented in Section O.

We define the ideal functionality $\mathcal{F}_{r_0\text{-check}}$ that captures the security requirements of the r_0 -check subprotocol.

Functionality 13 ($\mathcal{F}_{r_0\text{-check}}$ – Secure r0-Check). *Parameters:*

- n : number of parties
- $q = 8380417$: field modulus
- $\gamma_2 = (q - 1)/32 = 261888$: rounding parameter
- $\beta = \tau \cdot \eta = 49 \cdot 4 = 196$: bound parameter (ML-DSA-65)
- $\text{bound} = \gamma_2 - \beta = 261692$: acceptance threshold
- $m = k \cdot 256 = 1536$: number of coefficients (for ML-DSA-65)

State:

- $\text{received}[\cdot]$: stores received inputs
- $\text{result} \in \{0, 1, \perp\}$: computation result

Input Phase:

On receiving $(\text{INPUT}, \text{sid}, i, [\mathbf{w}']_i)$ from party P_i where $[\mathbf{w}']_i \in \mathbb{Z}_q^m$:

1. If P_i is corrupted, forward $[\mathbf{w}']_i$ to simulator \mathcal{S}
2. Store $\text{received}[i] \leftarrow [\mathbf{w}']_i$
3. If $|\{j : \text{received}[j] \neq \perp\}| = n$:
 - (a) Reconstruct: $\mathbf{w}'_j = \sum_{i=1}^n \text{received}[i][j] \bmod q$ for each $j \in [m]$
 - (b) For each $j \in [m]$: compute centered representative $\tilde{w}'_j \in (-q/2, q/2]$
 - (c) Compute pass/fail for each coefficient using the FIPS 204 LowBits function [Nat24b]:

$$\text{pass}_j = \begin{cases} 1 & \text{if } |\text{LowBits}(\mathbf{w}'[j], 2\gamma_2)| < \text{bound} \\ 0 & \text{otherwise} \end{cases}$$

where $\text{LowBits}(r, 2\gamma_2) = r \bmod \pm 2\gamma_2$ (the unique representative in $(-\gamma_2, \gamma_2]$ congruent to $r \bmod 2\gamma_2$), matching FIPS 204 Algorithm 31. Note: $\mathbf{w}'[j] = \sum_{i=1}^n \text{received}[i][j] \bmod q$ is first reduced mod q , then LowBits is applied to this \mathbb{Z}_q value directly without additional centering mod q .

- (d) Compute final result: $\text{result} = \bigwedge_{j=1}^m \text{pass}_j$

4. Send $(\text{COMPUTED}, \text{sid}, \text{result})$ to \mathcal{S}

Output Phase:

On receiving $(\text{DELIVER}, \text{sid})$ from \mathcal{S} :

1. Send $(\text{OUTPUT}, \text{sid}, \text{result})$ to all honest parties

On receiving $(\text{ABORT}, \text{sid})$ from \mathcal{S} :

1. Send $(\text{OUTPUT}, \text{sid}, \perp)$ to all honest parties

Leakage: Only the single bit result is revealed to \mathcal{S} . The functionality does not reveal:

- The reconstructed value \mathbf{w}'
- Individual coefficients or their pass/fail status
- Honest parties' input shares

Remark 24 (Security with Abort). $\mathcal{F}_{r_0\text{-check}}$ provides security-with-abort: the adversary can cause the protocol to abort *after* learning the result bit. This is standard for dishonest-majority MPC and matches the security of underlying primitives (SPDZ, edaBits).

J Real Protocol Π_{r_0}

We formally specify the real protocol Π_{r_0} that realizes $\mathcal{F}_{r_0\text{-check}}$.

Protocol 14 (Π_{r_0} – MPC-Based r0-Check). *Notation:*

- $\langle x \rangle_q$: SPDZ sharing of x over \mathbb{F}_q
- $\langle x \rangle_2$: secret sharing of x over \mathbb{F}_2
- $[x]_i$: party P_i 's share of x

Preprocessing (offline phase):

1. Generate m edaBits $\{(\langle r_j \rangle_q, \langle r_j \rangle_2)\}_{j=1}^m$ via $\mathcal{F}_{\text{edaBits}}$
2. Generate Beaver triples for binary AND gates (for comparison circuits)
3. Distribute MAC key shares for SPDZ

Online Protocol:

Round 1-2: Share Exchange and Aggregation

Each party P_i holds input $[\mathbf{w}']_i \in \mathbb{Z}_q^m$ (their share of $\mathbf{w}' = \mathbf{w} - c\mathbf{s}_2$).

1. Each P_i creates SPDZ sharing of their input: invoke $\mathcal{F}_{\text{SPDZ}}.\text{SHARE}$ for each $[\mathbf{w}']_i[j]$
2. Parties invoke $\mathcal{F}_{\text{SPDZ}}.\text{ADD}$ to compute $\langle \mathbf{w}' \rangle_q = \sum_i \langle [\mathbf{w}']_i[j] \rangle_q$ for each j

Round 3-4: Masked Reveal (Arithmetic to Public)

For each coefficient $j \in [m]$:

1. Parties compute using local addition:

$$\langle \text{masked}_j \rangle_q = \langle \mathbf{w}'_j \rangle_q + \langle r_j \rangle_q$$

2. Each party P_i computes commitment:

$$\text{Com}_{i,j} = H([\text{masked}_j]_i \parallel \text{sid} \parallel j \parallel i)$$

3. Broadcast all commitments (Round 3)
4. After receiving all commitments, broadcast openings $[\text{masked}_j]_i$ (Round 4)
5. Verify commitments; abort if any mismatch
6. Reconstruct $\text{masked}_j = \sum_i [\text{masked}_j]_i \bmod q$

Round 5: Arithmetic-to-Binary Conversion

For each coefficient $j \in [m]$:

1. Convert public masked_j to binary:

$$\text{masked}_j^{(b)} = (\text{masked}_j^{(0)}, \dots, \text{masked}_j^{(\lceil \log_2 q \rceil - 1)})$$

2. Compute binary sharing of \mathbf{w}'_j via subtraction circuit:

$$\langle \mathbf{w}'_j \rangle_2 = \text{masked}_j^{(b)} \boxminus \langle r_j \rangle_2$$

where \boxminus denotes bitwise binary subtraction with borrow propagation over $\lceil \log_2 q \rceil + 1$ bits; a borrow into the MSB wraps correctly to the result mod q

3. The subtraction circuit has depth $O(\log q)$ and uses $O(\log q)$ AND gates

Round 6-7: Binary Comparison

For each coefficient $j \in [m]$:

1. Compute sign bit and absolute value from $\langle \mathbf{w}'_j \rangle_2$
2. Evaluate comparison circuit: $\langle \text{pass}_j \rangle_2 = (|\langle \mathbf{w}'_j \rangle_2| < \text{bound})$
3. The comparison uses $O(\log \gamma_2)$ AND gates

Round 8: AND Aggregation and Output

1. Compute $\langle \text{result} \rangle_2 = \bigwedge_{j=1}^m \langle \text{pass}_j \rangle_2$ via AND-tree of depth $\lceil \log_2 m \rceil$
2. Open result: each party broadcasts $[\text{result}]_i$
3. Reconstruct $\text{result} = \bigoplus_i [\text{result}]_i$
4. Output result to all parties

K Simulator Construction

We construct a simulator \mathcal{S} that interacts with $\mathcal{F}_{r_0\text{-check}}$ and simulates the view of adversary \mathcal{A} controlling corrupted parties $C \subsetneq [n]$.

Simulator 15 (\mathcal{S} for Π_{r_0}). \mathcal{S} internally runs \mathcal{A} and simulates the honest parties' messages.

Setup:

1. \mathcal{S} receives the set C of corrupted parties from \mathcal{A}
2. Let $H = [n] \setminus C$ be the set of honest parties

Simulating Preprocessing:

1. For *edaBits* involving corrupted parties: \mathcal{S} receives \mathcal{A} 's shares from $\mathcal{F}_{\text{edaBits}}$ simulator
2. For honest parties: sample random shares consistent with the corrupted parties' view
3. **Key property:** \mathcal{S} does not know the actual *edaBit* values; only the corrupted shares

Simulating Rounds 1-2 (Share Exchange):

1. For each honest party $P_i \in H$ (adversary's view only):
 - (a) Sample random SPDZ shares $\tilde{s}_{i,j} \xleftarrow{\$} \mathbb{F}_q$ for $j \in [m]$
 - (b) Compute MAC shares using the SPDZ simulator (consistent with corrupted MAC key shares)
 - (c) Send simulated shares to \mathcal{A}
2. Receive corrupted parties' inputs from \mathcal{A} ; forward corrupted inputs to $\mathcal{F}_{r_0\text{-check}}$
3. **UC framing (honest parties' inputs):** In the ideal execution, honest parties are ideal-world programs that submit their actual inputs directly to $\mathcal{F}_{r_0\text{-check}}$ via the ideal-world channel — the simulator \mathcal{S} is not involved in this step. The functionality receives all inputs and computes result; \mathcal{S} receives result and uses it in Round 8 simulation.

4. **Consistency:** The simulated shares $\tilde{s}_{i,j} \xleftarrow{\$} \mathbb{F}_q$ are identically distributed to real honest-party shares (SPDZ additive shares are uniformly random given any fixed secret — perfect hiding). No inconsistency arises: the adversary sees random shares, honest parties' actual values go to \mathcal{F} privately.

Simulating Rounds 3-4 (Masked Reveal):

This is the critical simulation step. We must simulate $\text{masked}_j = \mathbf{w}'_j + r_j$ without knowing \mathbf{w}'_j .

1. **Round 3 (Commitments):**

- (a) For each honest party $P_i \in H$ and each $j \in [m]$:
- (b) Sample $\tilde{m}_{i,j} \xleftarrow{\$} \mathbb{F}_q$ uniformly at random
- (c) Compute commitment $\widetilde{\text{Com}}_{i,j} = H(\tilde{m}_{i,j} \parallel \text{sid} \parallel j \parallel i)$
- (d) Send $\widetilde{\text{Com}}_{i,j}$ to \mathcal{A}

2. Receive corrupted parties' commitments from \mathcal{A}

3. **Round 4 (Openings):**

- (a) For each honest party $P_i \in H$: send $\tilde{m}_{i,j}$ to \mathcal{A}
- (b) Receive corrupted parties' openings from \mathcal{A}
- (c) Verify corrupted commitments; if any fail, simulate abort
- (d) Compute simulated

$$\widetilde{\text{masked}}_j = \sum_{i \in H} \tilde{m}_{i,j} + \sum_{i \in C} [\text{masked}_j]_i \bmod q$$

Justification for Round 3-4 Simulation:

In the real protocol:

$$\begin{aligned} \text{masked}_j &= \mathbf{w}'_j + r_j \\ &= \sum_i [\mathbf{w}']_i[j] + \sum_i [r_j]_i \bmod q \end{aligned}$$

Since $r_j \xleftarrow{\$} \mathbb{F}_q$ from $\mathcal{F}_{\text{edaBits}}$ and is unknown to \mathcal{A} (only shares are known), by the one-time pad property:

$$\text{masked}_j = \mathbf{w}'_j + r_j \equiv \text{Uniform}(\mathbb{F}_q)$$

Thus sampling $\tilde{m}_{i,j} \xleftarrow{\$} \mathbb{F}_q$ for honest parties produces an identical distribution.

Simulating Round 5 (A2B Conversion):

1. Convert $\widetilde{\text{masked}}_j$ to binary (same as real)
2. For binary subtraction: use $\mathcal{F}_{\text{Binary}}$ simulator
3. Simulate honest parties' binary shares as uniform (justified by Beaver AND security)

Simulating Rounds 6-7 (Comparison):

1. For each AND gate, sample $(\tilde{d}, \tilde{e}) \xleftarrow{\$} \{0,1\}^2$. By Lemma 7, this matches the real distribution.

2. Apply the same simulation to all comparison circuits.

Simulating Round 8 (Output):

1. Wait to receive $\text{result} \in \{0, 1\}$ from $\mathcal{F}_{r_0\text{-check}}$

2. **Backward simulation of AND tree:**

The adversary's view of the AND tree is only the Beaver-triple open values (d_j, e_j) — the leaf bits pass_j never appear in the adversary's view.

(a) For each AND gate $j \in [m]$, sample $(d_j, e_j) \xleftarrow{\$} \{0, 1\}^2$ uniformly and independently (no leaf assignment is performed).

(b) Output the simulated view $\{(d_j, e_j)\}_{j=1}^m$ together with **result** received from $\mathcal{F}_{r_0\text{-check}}$.

Justification: By Lemma 7, the real $(d_j, e_j) = (x_j \oplus \alpha_j, y_j \oplus \beta_j)$ is uniform regardless of the inputs (x_j, y_j) , because (α_j, β_j) are fresh Beaver-triple components independent of the gate inputs. Since all m Beaver triples are generated independently in preprocessing, the joint distribution is product-uniform. The simulator's directly-sampled (d_j, e_j) therefore matches the real distribution exactly ($SD = 0$), for both $\text{result} \in \{0, 1\}$ cases.

3. Simulate honest parties' output shares consistent with **result**

4. Send to \mathcal{A}

Handling Abort:

If \mathcal{A} causes any verification to fail (commitment mismatch, MAC failure):

1. \mathcal{S} sends (ABORT, sid) to $\mathcal{F}_{r_0\text{-check}}$

2. Simulate abort to all honest parties

L Hybrid Argument

We prove indistinguishability through a sequence of hybrid experiments.

Definition 16 (Hybrid Experiments). We define hybrids H_0, \dots, H_6 where H_0 is the real execution and H_6 is the ideal execution.

L.1 Hybrid H_0 : Real Execution

This is the real protocol execution $\text{REAL}_{\Pi_{r_0}, \mathcal{A}, \mathcal{Z}}$:

- Honest parties execute Π_{r_0} with their true inputs
- All cryptographic operations use real keys and randomness
- \mathcal{A} controls corrupted parties and sees all communication

L.2 Hybrid H_1 : Replace SPDZ with Ideal

Replace the SPDZ protocol with ideal functionality $\mathcal{F}_{\text{SPDZ}}$.

Lemma 3. $|\Pr[H_0 = 1] - \Pr[H_1 = 1]| \leq \epsilon_{\text{SPDZ}}$

Proof. By the UC-security of SPDZ [DPSZ12], there exists a simulator $\mathcal{S}_{\text{SPDZ}}$ such that no environment can distinguish real SPDZ execution from ideal $\mathcal{F}_{\text{SPDZ}}$ execution with advantage better than ϵ_{SPDZ} .

The security parameter is κ and the MAC key is drawn from a dedicated MAC key field \mathbb{F}_p with $|p| \geq 64$ bits, *independent* of the protocol field \mathbb{F}_q (this is standard practice in SPDZ implementations [DPSZ12]). Per SPDZ security analysis:

- MAC forgery probability per verification: $1/p \leq 2^{-64}$
- With ℓ verifications: $\epsilon_{\text{SPDZ}} \leq \ell/p$

For our protocol with $m = 1536$ coefficients, MAC verification occurs at *OPEN* time; the number of verifications is $\ell = m$:

$$\epsilon_{\text{SPDZ}} \leq m/p \leq 1536/2^{64} < 2^{-54}$$

Remark 25 (Minimal-configuration bound). If SPDZ is instantiated with the protocol field \mathbb{F}_q ($q \approx 2^{23}$) as the MAC key space (minimal configuration), the bound degrades to $\epsilon_{\text{SPDZ}} \leq m/q = 1536/8380417 < 2^{-12.4}$. Practical deployments of P2 must configure SPDZ with a separate MAC field of at least 64 bits to achieve cryptographically negligible distinguishing advantage. □

L.3 Hybrid H_2 : Replace edaBits with Ideal

Replace the edaBits protocol with ideal functionality $\mathcal{F}_{\text{edaBits}}$.

Lemma 4. $|\Pr[H_1 = 1] - \Pr[H_2 = 1]| \leq \epsilon_{\text{edaBits}}$

Proof. By the UC-security of edaBits [EGK⁺20], the protocol UC-realizes $\mathcal{F}_{\text{edaBits}}$ with negligible distinguishing advantage.

The edaBits protocol security relies on:

- SPDZ security for arithmetic shares (already replaced with ideal)
- Cut-and-choose for binary consistency (statistical security)

With security parameter κ and cut-and-choose parameter B :

$$\epsilon_{\text{edaBits}} \leq 2^{-B} + \epsilon'_{\text{SPDZ}}$$

where ϵ'_{SPDZ} is the SPDZ security bound for the internal operations used in edaBits generation.

For $B = 64$ and ML-DSA-65 parameters ($m = k \cdot N = 6 \cdot 256 = 1536$ coefficients, where $N = 256$ is the ring degree distinct from party count n ; $q = 8380417$): the cut-and-choose term 2^{-64} is negligible, and $\epsilon'_{\text{SPDZ}} \leq m/p \leq 1536/2^{64} < 2^{-54}$ (using the same 64-bit MAC field; per [EGK⁺20], the SPDZ sub-protocol internal to edaBits opens at most m values per batch). Thus $\epsilon_{\text{edaBits}} < 2^{-64} + 2^{-54} < 2^{-53.9}$. □

L.4 Hybrid H_3 : Simulate Masked Values

Replace honest parties' contributions to masked_j with uniformly random values.

Lemma 5 (One-Time Pad over \mathbb{F}_q). *For any $x \in \mathbb{F}_q$ and uniformly random $r \xleftarrow{\$} \mathbb{F}_q$ independent of x :*

$$x + r \bmod q \equiv \text{Uniform}(\mathbb{F}_q)$$

Proof. For any target $t \in \mathbb{F}_q$:

$$\Pr[x + r = t] = \Pr[r = t - x] = \frac{1}{q}$$

since r is uniform and independent of x . Thus $x + r$ is uniformly distributed. \square

Lemma 6. $\Pr[H_2 = 1] = \Pr[H_3 = 1]$ (*perfect indistinguishability*)

Proof. In H_2 , for each coefficient j :

$$\text{masked}_j = \mathbf{w}'_j + r_j \bmod q$$

where r_j is the edaBit value, uniformly distributed in \mathbb{F}_q (by Remark 23, rejection sampling ensures r_j is exactly uniform) and independent of all other values (by $\mathcal{F}_{\text{edaBits}}$ security).

By Lemma 5, $\widetilde{\text{masked}}_j$ is uniformly distributed in \mathbb{F}_q , regardless of \mathbf{w}'_j .

In H_3 , we sample $\widetilde{\text{masked}}_j \xleftarrow{\$} \mathbb{F}_q$ directly.

Both distributions are identical (uniform over \mathbb{F}_q), so:

$$\Pr[H_2 = 1] = \Pr[H_3 = 1]$$

This is **statistical** (in fact, perfect) indistinguishability, not computational. \square

L.5 Hybrid H_4 : Replace Binary Circuits with Ideal

Replace Beaver-triple-based AND gates with ideal $\mathcal{F}_{\text{Binary}}$.

Lemma 7 (Beaver AND Security). *Let (a, b, c) be a Beaver triple with $a, b \xleftarrow{\$} \{0, 1\}$ uniform and $c = a \wedge b$. For any inputs $x, y \in \{0, 1\}$, the opened values $(d, e) = (x \oplus a, y \oplus b)$ are uniformly distributed in $\{0, 1\}^2$ and independent of (x, y) .*

Proof. Since $a \xleftarrow{\$} \{0, 1\}$ is uniform and independent of x :

$$\Pr[d = 0] = \Pr[x \oplus a = 0] = \Pr[a = x] = \frac{1}{2}$$

Similarly for e . Independence of d and e follows from independence of a and b .

For any $(d^*, e^*) \in \{0, 1\}^2$:

$$\Pr[(d, e) = (d^*, e^*)] = \Pr[a = x \oplus d^*] \cdot \Pr[b = y \oplus e^*] = \frac{1}{4}$$

Thus $(d, e) \equiv \text{Uniform}(\{0, 1\}^2)$, independent of (x, y) . \square

Lemma 8. $\Pr[H_3 = 1] = \Pr[H_4 = 1]$ (*perfect indistinguishability*)

Proof. Each AND gate reveals (d, e) , which is uniform by Lemma 7. Replacing real AND computation with $\mathcal{F}_{\text{Binary}}$ (which also produces uniform (d, e)) yields identical distributions.

The A2B conversion and comparison circuits consist entirely of:

- XOR gates (no communication, locally computable)
- AND gates (each revealing uniform (d, e))

Since all revealed values have identical distributions in both hybrids:

$$\Pr[\mathbf{H}_3 = 1] = \Pr[\mathbf{H}_4 = 1]$$

□

Remark 26 (A2B Correctness and Borrow Propagation). The A2B conversion computes $\langle \mathbf{w}'_j \rangle_2 = \text{masked}_j^{(b)} \boxminus \langle r_j \rangle_2$ where $\text{masked}_j = \mathbf{w}'_j + r_j \bmod q$. Two potential issues arise:

(1) **Negative intermediate result:** If $\text{masked}_j < r_j$ (as integers), the subtraction would wrap around. However, since $\mathbf{w}'_j = \text{masked}_j - r_j \bmod q$, the binary circuit must compute modular subtraction. Standard approaches:

- **Extended precision:** Work in $k + 1$ bits where $k = \lceil \log_2 q \rceil$, allowing for the borrow.
- **Add-then-subtract:** Compute $(\text{masked}_j + q) - r_j$ when detecting borrow, using a multiplexer.

Both yield $\mathbf{w}'_j \bmod q$ correctly.

(2) **edaBits range mismatch:** As noted in Remark 23, with rejection sampling, r_j is uniform in $\{0, \dots, q - 1\}$, matching the field \mathbb{F}_q .

Security implication: These are *correctness* considerations, not security concerns. The security proof shows that the adversary's view — the (d, e) values from Beaver triples — is identically distributed regardless of the underlying \mathbf{w}'_j values. Correctness ensures result is computed correctly; security ensures the adversary learns only result.

L.6 Hybrid \mathbf{H}_5 : Backward Simulate AND Tree

Simulate the AND tree computation given only the final result bit.

Lemma 9. $\Pr[\mathbf{H}_4 = 1] = \Pr[\mathbf{H}_5 = 1]$ (*perfect indistinguishability*)

Proof. In \mathbf{H}_4 , the AND tree computes $\text{result} = \bigwedge_{j=1}^m \text{pass}_j$ level by level, revealing Beaver (d, e) values at each gate.

In \mathbf{H}_5 , given result from $\mathcal{F}_{r_0\text{-check}}$, we backward-simulate:

Case result = 1: All $\text{pass}_j = 1$. For each AND gate $z = x \wedge y$ with $z = 1$: both $x = y = 1$. The simulator sets all leaf values to 1 and propagates upward.

Case result = 0: At least one $\text{pass}_j = 0$. The simulator does *not* assign leaf values first. Instead, it proceeds directly as follows:

1. For each AND gate j , sample $(d_j, e_j) \stackrel{\$}{\leftarrow} \{0, 1\}^2$ uniformly and independently (no reference to any leaf assignment).
2. Output the simulated view $\{(d_j, e_j)\}_{j=1}^m$ along with $\text{result} = 0$ from $\mathcal{F}_{r_0\text{-check}}$.

No leaf values need be assigned: the leaf bits (pass_j) never appear in the adversary's view — only the (d_j, e_j) pairs do. In both cases, the revealed (d, e) values are uniform by Lemma 7, regardless of the underlying (x, y) ; the simulator's sampled (d_j, e_j) therefore perfectly matches the real distribution.

This uniformity extends to the *joint* distribution over the entire AND tree: each gate's Beaver triple $(\alpha_j, \beta_j, \gamma_j)$ is sampled independently offline; for gate j , $(d_j, e_j) = (x_j \oplus \alpha_j, y_j \oplus \beta_j)$ is uniform and independent of (x_j, y_j) by Lemma 7. Since triples are

pairwise independent across gates, the joint distribution $(d_1, e_1, \dots, d_m, e_m)$ is product-uniform, independent of all leaf values.

Key observation: The adversary sees only (d_j, e_j) values; the underlying bits x_j, y_j remain secret-shared. Since the joint distribution is product-uniform and independent of the leaf bits, backward simulation is perfect for the entire AND tree. \square

L.7 Hybrid H_6 : Ideal Execution

This is the ideal execution $\text{IDEAL}_{\mathcal{F}_{r_0\text{-check}}, \mathcal{S}, \mathcal{Z}}$ with simulator \mathcal{S} from Section K.

Lemma 10. $\Pr[H_5 = 1] = \Pr[H_6 = 1]$

Proof. We show that H_5 is the ideal execution H_6 .

After the previous hybrids, every component of the real protocol has been replaced:

- SPDZ arithmetic shares $\rightarrow \mathcal{F}_{\text{SPDZ}}$ outputs (H1)
- edaBits $\rightarrow \mathcal{F}_{\text{edaBits}}$ outputs (H2)
- Masked reveal values \rightarrow uniform random (H3), so adversary’s view of the masked values is simulated
- Binary comparison circuits $\rightarrow \mathcal{F}_{\text{Binary}}$ output (H4)
- AND tree open values $(d_j, e_j) \rightarrow$ product-uniform random (H5)

After all these replacements, the only “real” output remaining is the final result bit output by the AND tree. This result bit is computed by $\mathcal{F}_{\text{Binary}}$ (already ideal from H4) and passed to the parties. But $\mathcal{F}_{\text{Binary}}$ ’s output is exactly the output of $\mathcal{F}_{r_0\text{-check}}$: it outputs 1 iff $\|\mathbf{r}_0\|_\infty < \gamma_2 - \beta$.

Explicit argument. We verify that the simulator \mathcal{S} from Section K is *well-defined* and that its output distribution matches H_5 component-by-component:

- *SPDZ shares (H1):* \mathcal{S} generates random shares $\tilde{s}_{i,j} \stackrel{\$}{\leftarrow} \mathbb{F}_q$ for honest parties — identical in distribution to $\mathcal{F}_{\text{SPDZ}}$ ’s output.
- *edaBits (H2):* \mathcal{S} uses $\mathcal{F}_{\text{edaBits}}$ outputs — exact match.
- *Masked reveal (H3):* \mathcal{S} samples $\tilde{m}_{i,j} \stackrel{\$}{\leftarrow} \mathbb{F}_q$ — SD = 0 by one-time-pad argument.
- *Binary comparison (H4):* \mathcal{S} uses $\mathcal{F}_{\text{Binary}}$ outputs — exact match.
- *AND-tree pairs (H5):* \mathcal{S} samples $(d_j, e_j) \stackrel{\$}{\leftarrow} \{0, 1\}^2$ — SD = 0 by Lemma 7.
- *Result bit:* In the ideal execution H_6 , honest parties submit their actual inputs directly to $\mathcal{F}_{r_0\text{-check}}$ via the ideal-world channel (not through \mathcal{S}). The functionality computes **result** and sends it to \mathcal{S} . The simulator completes the adversary view using **result**.

Each component’s simulated distribution matches H_5 ’s distribution exactly. The result bit is the only component that differs between H_5 (computed by $\mathcal{F}_{\text{Binary}}$, which replaced the real AND-tree in H_4) and H_6 (provided by $\mathcal{F}_{r_0\text{-check}}$). But $\mathcal{F}_{\text{Binary}}$ ’s output equals $\mathcal{F}_{r_0\text{-check}}$ ’s output: both compute $\mathbf{1}[\|\mathbf{r}_0\|_\infty < \gamma_2 - \beta]$ on the same inputs. Hence the result-bit distributions are identical, and $\Pr[H_5 = 1] = \Pr[H_6 = 1]$. \square

M Main Theorem

Theorem 16 (UC Security of Profile P2 (Full Proof of Theorem 7)). *Protocol Π_{r_0} UC-realizes $\mathcal{F}_{r_0\text{-check}}$ in the hybrid model with $(\mathcal{F}_{\text{SPDZ}}, \mathcal{F}_{\text{edaBits}}, \mathcal{F}_{\text{Binary}})$ against static malicious adversaries corrupting up to $N - 1$ parties, achieving security-with-abort.*

Concretely, for any PPT environment \mathcal{Z} and adversary \mathcal{A} :

$$|\Pr[\text{REAL}_{\Pi_{r_0}, \mathcal{A}, \mathcal{Z}} = 1] - \Pr[\text{IDEAL}_{\mathcal{F}_{r_0\text{-check}}, \mathcal{S}, \mathcal{Z}} = 1]| \leq \epsilon$$

where

$$\epsilon = \epsilon_{\text{SPDZ}} + \epsilon_{\text{edaBits}} < 2^{-53}$$

for ML-DSA-65 parameters with a 64-bit dedicated MAC field (recommended configuration; the minimal configuration using the protocol field gives $\epsilon < 2^{-11}$).

Proof. By the hybrid argument (Section L):

$$\begin{aligned} & |\Pr[\mathbf{H}_0 = 1] - \Pr[\mathbf{H}_6 = 1]| \\ & \leq \sum_{i=0}^5 |\Pr[\mathbf{H}_i = 1] - \Pr[\mathbf{H}_{i+1} = 1]| \\ & = |\Pr[\mathbf{H}_0 = 1] - \Pr[\mathbf{H}_1 = 1]| + |\Pr[\mathbf{H}_1 = 1] - \Pr[\mathbf{H}_2 = 1]| \\ & \quad + |\Pr[\mathbf{H}_2 = 1] - \Pr[\mathbf{H}_3 = 1]| + |\Pr[\mathbf{H}_3 = 1] - \Pr[\mathbf{H}_4 = 1]| \\ & \quad + |\Pr[\mathbf{H}_4 = 1] - \Pr[\mathbf{H}_5 = 1]| + |\Pr[\mathbf{H}_5 = 1] - \Pr[\mathbf{H}_6 = 1]| \\ & \leq \epsilon_{\text{SPDZ}} + \epsilon_{\text{edaBits}} + 0 + 0 + 0 + 0 \\ & = \epsilon_{\text{SPDZ}} + \epsilon_{\text{edaBits}} \end{aligned}$$

The zero terms arise from perfect (statistical) indistinguishability in Hybrids 3, 4, 5, and 6.

Concrete bound (recommended configuration, 64-bit MAC field): For ML-DSA-65 with $q = 8380417$, $m = 1536$ coefficients, and dedicated MAC field \mathbb{F}_p with $|p| = 64$ bits:

- $\epsilon_{\text{SPDZ}} \leq m/p = 1536/2^{64} < 2^{-54}$
- $\epsilon_{\text{edaBits}} \leq m/p + 2^{-64} < 2^{-53.9}$ (cut-and-choose $B = 64$; m/p is the SPDZ sub-error internal to edaBits)

Thus $\epsilon = \epsilon_{\text{SPDZ}} + \epsilon_{\text{edaBits}} < 2^{-54} + 2^{-53.9} < 2^{-53}$, achieving cryptographically negligible distinguishing advantage. *Minimal configuration* (protocol field as MAC field): $\epsilon_{\text{SPDZ}} < 2^{-12.4}$, $\epsilon_{\text{edaBits}} < 2^{-11.9}$, total $\epsilon < 2^{-11}$; overall signature security relies on Module-SIS at a much higher level (Theorem 2). \square

Corollary 5 (Full Protocol P2 Security). *The complete Profile P2 threshold ML-DSA protocol achieves:*

1. **EUFCMA security** under Module-SIS (inherited from single-signer ML-DSA, Theorem 2)
2. **r0-check privacy** against coalitions of up to $N - 1$ parties (by UC security of $\mathcal{F}_{r_0\text{-check}}$: only the 1-bit pass/fail result is leaked by the r0-check subprotocol). Note: overall key privacy and unforgeability require $|C| \leq T - 1$; if $|C| \geq T$ the adversary can reconstruct the secret key from T Shamir shares. The $N - 1$ bound here refers to the r0-check subprotocol's leakage, not the full signing protocol's security model.
3. **Composition security**: The protocol can be securely composed with other UC-secure protocols

Proof. EUF-CMA: The threshold signature $\sigma = (\tilde{c}, \mathbf{z}, \mathbf{h})$ is syntactically identical in format to single-signer ML-DSA and is accepted by any compliant FIPS 204 verifier (masks cancel in the sum, Lemma 1); the response \mathbf{z} follows an Irwin-Hall rather than uniform distribution, with EUF-CMA security loss $< 0.013 \cdot q_s$ bits over q_s signing queries (per session: < 0.013 bits; Corollary 1). The security proof of Theorem 2 applies directly.

Privacy: By Theorem 16, the r0-check reveals only the result bit $\text{result} \in \{0, 1\}$. Combined with the mask hiding lemma (Lemma 2), an adversary’s view can be simulated from:

- Public key pk
- Corrupted shares $\{\text{sk}_i\}_{i \in C}$
- Final signature σ
- r0-check result bits (one per attempt)

For successful attempts, $\text{result} = 1$ is implied by the existence of σ and leaks no new information. For *failed* attempts ($\text{result} = 0$, no σ produced), the result bit is determined by the public broadcast (\tilde{c}, \mathbf{w}) and the corrupted parties’ r0-check shares $\{\text{cs}_{2,j}\}_{j \in C}$: the simulator computes

$$\mathbf{r}_0^{(C)} = \text{HighBits} \left(\sum_{j \in C} \lambda_j \text{cs}_{2,j} + \text{honest aggregate contribution} \right)$$

and determines the result by whether $\|\mathbf{r}_0\|_\infty < \gamma_2 - \beta$. Since the honest contribution is masked (mask-hiding, Lemma 2), the simulator learns only the aggregate result from $\mathcal{F}_{r_0\text{-check}}$, not the individual honest shares. The failed-attempt result bits can thus be provided to the simulator by $\mathcal{F}_{r_0\text{-check}}$ without leaking additional information beyond what is already in \mathcal{Z} ’s view.

Composition: Follows from the UC composition theorem (Theorem 9). \square

Remark 27 (Nonce DKG Simulation for P2). The P2 UC proof above is scoped to the r0-check subprotocol Π_{r_0} realizing $\mathcal{F}_{r_0\text{-check}}$. The nonce DKG simulation for the full P2 protocol follows the same structure as P1/P3+: the simulator generates honest nonce shares from simulated degree- $(T - 1)$ polynomials, producing evaluations with identical distribution to the real protocol. Specifically, \mathcal{S} runs the nonce DKG on behalf of honest parties (sampling the high-degree coefficients uniformly from R_q), provides consistent evaluations to corrupted parties, and feeds the resulting nonce shares into the r0-check simulation above. By the UC composition theorem, the full P2 signing protocol (nonce DKG + response computation + r0-check) securely composes these subprotocols.

N Communication and Round Complexity

Theorem 17 (Complexity of Π_{r_0}). *Protocol Π_{r_0} achieves:*

1. **Online rounds:** 8 (as specified in Protocol 14)
2. **Online communication:** $O(n \cdot m \cdot \log q)$ bits
3. **Offline preprocessing:** $O(m)$ edaBits and $O(m \cdot \log q)$ Beaver triples

Proof. Rounds:

- Rounds 1-2: SPDZ share exchange and aggregation

- Rounds 3-4: Commit-then-open for masked reveal
- Round 5: A2B conversion (can be merged with Round 6)
- Rounds 6-7: Comparison circuits
- Round 8: AND aggregation and output

Communication: Each of $m = 1536$ coefficients requires:

- SPDZ sharing: $O(n)$ field elements
- Masked reveal: $O(n)$ field elements
- Binary operations: $O(\log q)$ bits per AND gate, $O(\log q)$ AND gates per coefficient

Total: $O(n \cdot m \cdot \log q) \approx n \cdot 1536 \cdot 23 \approx 35000 \cdot n$ bits per party.

Preprocessing:

- m edaBits (one per coefficient)
- $O(m \cdot \log q)$ Beaver triples for A2B and comparison circuits

□

Table 14: Round and communication breakdown for Profile P2 r0-check (8-round version). The AND tree requires $m - 1$ Beaver-triple openings, giving $O(m)$ bits; the $O(\log m)$ figure denotes circuit *depth*, not communication.

Component	Online Rounds	Communication/Party
SPDZ aggregation	2	$O(m \log q)$ bits
Masked reveal	2	$O(m \log q)$ bits
A2B conversion	1	$O(m \log q)$ bits
Comparison	2	$O(m \log \gamma_2)$ bits
AND tree	1	$O(m)$ bits
Total	8	≈ 30 KB

O Optimized P2: 5-Round Protocol UC Security

We present the UC security proof for the optimized 5-round P2 protocol. The key modifications are:

1. **Combiner-mediated commit-then-open:** Rounds 3-4 merged into Round 2
2. **Constant-depth comparison:** Rounds 6-7 merged into Round 4

O.1 Modified Ideal Functionality

Functionality 18 ($\mathcal{F}_{r0\text{-check}}^{5\text{rnd}}$ – Secure r0-Check with Combiner). *Extends $\mathcal{F}_{r0\text{-check}}$ (Functionality 13) with combiner role.*

Additional State:

- `combiner_id`: Identity of the designated combiner
- `collected[.]`: Messages collected by combiner before release

Combiner Registration:

On receiving (SET_COMBINER, sid, cid) from \mathcal{S} :

1. Set `combiner_id` \leftarrow cid
2. Notify all parties of combiner identity

Combiner-Mediated Input Phase:

On receiving (COMBINER_INPUT, sid, i , Com_i , $[\mathbf{w}']_i$, rand_i) from party P_i :

1. Verify $\text{Com}_i = H([\mathbf{w}']_i \parallel \text{sid} \parallel i \parallel \text{rand}_i)$
2. Store `collected`[i] \leftarrow ($[\mathbf{w}']_i$, rand_i)
3. Send (COLLECTED, sid, i) to combiner
4. If $|\text{collected}| = n$:
 - (a) Send (ALL_COLLECTED, sid) to combiner

Simultaneous Release:

On receiving (RELEASE, sid) from combiner:

1. If $|\text{collected}| < n$: return \perp
2. For each i : send $\{(j, [\mathbf{w}']_j, \text{rand}_j)\}_{j \in [n]}$ to party P_i
3. Continue with standard computation as in $\mathcal{F}_{r_0\text{-check}}$

Timeout (Corrupted Combiner):

Upon sending (ALL_COLLECTED, sid) to the combiner, the functionality starts a timer of Δ_{timeout} rounds (a global synchrony parameter). If (RELEASE, sid) is not received within Δ_{timeout} rounds:

1. Send (ABORT, sid) to all parties P_i
2. Discard all collected state

Remark: This timeout prevents a corrupted combiner from indefinitely delaying the release. In Profiles P1 and P3+, the combiner role is enforced by a TEE or 2PC, so the timeout is triggered only if the trusted component is unavailable (which is detected). In Profile P2, all parties are online during the signing window, so Δ_{timeout} is a protocol parameter (e.g., 30 seconds).

Leakage: The combiner learns:

- Timing of each party's message submission
- Order of message arrivals

The combiner does not learn the content of messages before simultaneous release.

O.2 Modified Real Protocol

Protocol 19 ($\Pi_{r_0}^{\text{5rnd}}$ – Optimized 5-Round r0-Check). **Round Structure:**

Round	Operation
1	Share exchange + aggregation
2	Combiner-mediated masked reveal
3	A2B conversion via <code>edaBits</code>
4	Parallel comparison + AND aggregation
5	Output

Round 1: Share Exchange and Aggregation(Unchanged from Π_{r_0} , Protocol 14)Round 2: Combiner-Mediated Masked RevealFor each coefficient $j \in [m]$:

1. Each party P_i computes:
 - $[\text{masked}_j]_i = [\mathbf{w}'_j]_i + [r_j]_i$
 - $\text{Com}_{i,j} = H([\text{masked}_j]_i \| \text{sid} \| j \| i \| \text{rand}_{i,j})$
2. P_i sends $(\text{Com}_{i,j}, [\text{masked}_j]_i, \text{rand}_{i,j})$ to combiner
3. Combiner waits until all n parties' messages received
4. Combiner broadcasts all openings $\{[\text{masked}_j]_i, \text{rand}_{i,j}\}_{i,j}$ simultaneously
5. Each party verifies all commitments; abort if any mismatch
6. Reconstruct $\text{masked}_j = \sum_i [\text{masked}_j]_i \bmod q$

Round 3: A2B Conversion(Unchanged from Π_{r_0})Round 4: Parallel Comparison + AND Aggregation**Layer 1 (Parallel Comparisons):** For each $j \in [m]$ in parallel:

1. Compute absolute value: $\langle |\mathbf{w}'_j| \rangle_2$ from $\langle \mathbf{w}'_j \rangle_2$
2. Evaluate comparison: $\langle \text{pass}_j \rangle_2 = (|\langle \mathbf{w}'_j \rangle_2| < \text{bound})$

Layer 2 (AND Tree):

1. Compute $\langle \text{result} \rangle_2 = \bigwedge_{j=1}^m \langle \text{pass}_j \rangle_2$
2. Use Beaver triples for all AND gates simultaneously
3. Open all (d, e) values in single round

Round 5: Output(Unchanged from Π_{r_0})**O.3 Extended Simulator for 5-Round Protocol****Simulator 20** ($\mathcal{S}^{5\text{rnd}}$ for $\Pi_{r_0}^{5\text{rnd}}$). Extends Simulator 15 with combiner simulation.**Simulating Combiner (if honest):**

1. When simulating honest parties, send their messages to simulated combiner
2. Combiner collects all messages (both honest and corrupted)
3. On receiving (ALL_COLLECTED) from internal state:
 - (a) Release all openings to adversary simultaneously

Simulating Combiner (if corrupted):

1. Adversary \mathcal{A} controls combiner
2. \mathcal{S} sends simulated honest parties' messages to \mathcal{A}
3. Wait for \mathcal{A} to release (or abort)

4. If \mathcal{A} modifies any value: SPDZ MAC check will fail in subsequent rounds
5. Simulate abort if MAC check fails

Simulating Round 4 (Parallel Comparison):

1. All m comparison circuits evaluated simultaneously
2. For each AND gate: sample $(d, e) \xleftarrow{\$} \{0, 1\}^2$ uniformly
3. Release all (d, e) values at once
4. By Lemma 7, this is indistinguishable from real

O.4 Modified Hybrid Argument

We extend the hybrid sequence with a new hybrid for combiner simulation.

Definition 17 (Extended Hybrids for 5-Round Protocol). • H_0 : Real execution of $\Pi_{r_0}^{\text{5rnd}}$

- $H_{0.5}$: Replace combiner with ideal $\mathcal{F}_{\text{Combiner}}$
- $H_1 - H_6$: As in original hybrid argument

Lemma 11 (Combiner Hybrid). $\Pr[H_0 = 1] = \Pr[H_{0.5} = 1]$ (*perfect indistinguishability*)

Proof. The combiner performs *no cryptographic operations*: it collects incoming messages and forwards them once all have arrived (or times out). In particular, it does not compute any MACs, encryptions, or protocol-specific transformations on the data. Its behavior is a deterministic function of its input messages and the arrival timing. We show the adversary’s view is *bytewise identical* in H_0 and $H_{0.5}$:

Honest Combiner Case:

- In H_0 : The combiner collects $(\text{Com}_i, \text{value}_i, \text{rand}_i)$ tuples from all N parties and releases them simultaneously only after all are received.
- In $H_{0.5}$: $\mathcal{F}_{\text{Combiner}}$ executes the same algorithm: collect-then-release.
- The adversary’s *incoming* messages (the individual party tuples) are produced by the real parties’ code in H_0 and by the simulator (which replicates the same code) in $H_{0.5}$ —producing identical bit-strings.
- The adversary’s *outgoing* view (released tuples) is the same set of collected messages, released at the same logical time.
- Since the combiner is honest, the adversary’s view of the combiner’s internal state is empty (it receives only the released outputs). The released outputs are identical. Hence the adversary’s view is *bytewise equal* in both hybrids.

Corrupted Combiner Case:

- The adversary controls the combiner directly and receives honest parties’ messages in both hybrids via identical delivery.
- Any deviation by the combiner (selective release, modification) triggers a detectable abort:
 1. *Value modification*: SPDZ MAC check at the recipient parties fails with probability $1 - 1/q$ per coefficient; honest parties abort and the functionality’s abort interface captures this.

2. *Selective withholding*: honest parties' timeout logic triggers an abort after deadline, identical in both H_0 and $H_{0.5}$.

- In $H_{0.5}$, $\mathcal{F}_{\text{Combiner}}$ replicates the same abort interface. Since the honest parties' messages delivered to the corrupted combiner are generated by the same real-protocol code in both hybrids (the combiner's corruption does not affect honest-party message generation), the adversary's view is again bitwise identical.

Since the combiner performs no cryptographic operations and its behavior is a deterministic routing function, the adversary's view in H_0 is *perfectly equal* to its view in $H_{0.5}$ (not merely computationally indistinguishable). Thus:

$$\Pr[H_0 = 1] = \Pr[H_{0.5} = 1]$$

□

Theorem 21 (UC Security of 5-Round P2). *Protocol $\Pi_{r_0}^{\text{5rnd}}$ UC-realizes $\mathcal{F}_{r_0\text{-check}}^{\text{5rnd}}$ with:*

$$\epsilon = \epsilon_{\text{SPDZ}} + \epsilon_{\text{edaBits}} + \epsilon_{\text{combiner}} = \epsilon_{\text{SPDZ}} + \epsilon_{\text{edaBits}} < 2^{-53}$$

(with 64-bit MAC field; minimal configuration gives $\epsilon < 2^{-11}$).

Proof. By Lemma 11, $\epsilon_{\text{combiner}} = 0$. The remaining hybrids proceed exactly as in Theorem 16. Total security loss:

$$\epsilon = 0 + \epsilon_{\text{SPDZ}} + \epsilon_{\text{edaBits}} + 0 + 0 + 0 + 0 < 2^{-53}$$

□

O.5 5-Round Complexity Analysis

Theorem 22 (Complexity of $\Pi_{r_0}^{\text{5rnd}}$). *The optimized protocol achieves:*

1. **Online rounds:** 5
2. **Online communication:** $O(n \cdot m \cdot \log q)$ bits (unchanged)
3. **Offline preprocessing:** Same as 8-round version

Proof. **Round reduction analysis:**

- Rounds 1-2 → Round 1: Merge share exchange with aggregation (linear operations)
- Rounds 3-4 → Round 2: Combiner-mediated simultaneous release
- Round 5 → Round 3: A2B conversion (unchanged)
- Rounds 6-7-8 → Rounds 4-5: Parallel comparison circuits and AND aggregation execute simultaneously in Round 4 (saving 1 round); output is broadcast in Round 5 (total: 3 original rounds → 2 new rounds)

Communication unchanged: Same data transmitted, just fewer rounds.

Preprocessing unchanged: Same edaBits and Beaver triples required. □

P Complete UC Security Proof for Profile P3+

We provide the complete UC security proof for the P3+ semi-asynchronous protocol. This extends the P3 proof sketch (Section 6.5) to a full proof with explicit handling of the pre-signing and semi-async model.

Table 15: Round comparison between original and optimized P2 protocols.

Component	8-rnd	5-rnd
Share exchange + aggregation	2	1
Masked reveal	2	1
A2B conversion	1	1
Comparison + AND tree	3	2
Total	8	5

P.1 Semi-Asynchronous Security Model

Definition 18 (Semi-Asynchronous Timing Model). The semi-async model consists of four timing phases:

1. **Pre-signing Window** $[t_0, t_1]$: Fully asynchronous. Signers precompute at any time.
2. **Challenge Broadcast** t_2 : Combiner derives and broadcasts challenge.
3. **Response Window** $[t_2, t_2 + \Delta]$: Semi-synchronous. Signers respond within bounded time Δ .
4. **2PC Execution** $[t_3, t_4]$: Synchronous between CPs only.

Definition 19 (Semi-Async Adversary). We adopt the synchronous UC model [Kat07] where all parties share a global clock. The adversary \mathcal{A} can:

- Corrupt up to $T - 1$ signers (static corruption)
- Corrupt at most one of $\{\text{CP}_1, \text{CP}_2\}$
- Control message scheduling within each phase, but *cannot* advance the clock past the signer response deadline Δ
- *Cannot* control the global clock or extend Δ

Theorem 26 applies to any protocol meeting this interface.

P.2 Ideal Functionality for P3+

Definition 20 (Ideal Functionality $\mathcal{F}_{r_0}^{2\text{PC}}$ (UC Proof Compact Form)). The functionality $\mathcal{F}_{r_0}^{2\text{PC}}$ captures a two-party computation of the r0-check predicate. It receives private input $\mathbf{S}_j \in \mathbb{Z}_q^m$ from each computation party CP_j ($j \in \{1, 2\}$), reconstructs $\text{cs}_2 = \mathbf{S}_1 + \mathbf{S}_2 \bmod q$ (private inputs satisfy this additive split; in the concrete protocol, $\mathbf{S}_j = \sum_{i \text{ assigned to } \text{CP}_j} \lambda_i \cdot \text{cs}_{2,i}$), computes $\mathbf{w}' = \mathbf{w} - \text{cs}_2$ (using the public \mathbf{w} agreed upon during challenge derivation), evaluates $\text{result} = \bigwedge_j (|\text{LowBits}(\mathbf{w}'_j, 2\gamma_2)|_\infty < \gamma_2 - \beta)$, and outputs only result (1 bit) and the hint $\mathbf{h} = \text{MakeHint}(\mathbf{w}', \mathbf{w}, 2\gamma_2)$ to the combiner. Neither cs_2 nor \mathbf{w}' is revealed outside $\mathcal{F}_{r_0}^{2\text{PC}}$.

Functionality 23 ($\mathcal{F}_{r_0}^{\text{semi-async}}$ – Semi-Async r0-Check). *Extends* $\mathcal{F}_{r_0}^{2\text{PC}}$ (Definition 20) with *pre-signing and timing*.

Pre-signing Phase:

On receiving (PRESIGN, sid, i , set_id, Com_i) from signer P_i :

1. Store $\text{presigning}[i][\text{set_id}] \leftarrow \text{Com}_i$
2. Send (PRESIGNED, sid, i , set_id) to \mathcal{S}

Challenge Phase:

On receiving (CHALLENGE, sid, signers, set_map, c) from combiner:

1. Verify all signers have pre-signing sets available
2. Set deadline \leftarrow now + Δ
3. Broadcast c to all signers in signers
4. Send (CHALLENGED, sid) to S

Response Phase:

On receiving (RESPOND, sid, i, response_i) from signer P_i:

1. If now > deadline: reject (too late)
2. If P_i \notin signers: reject
3. Store responses[i] \leftarrow response_i
4. If |responses| \geq T: trigger 2PC phase

2PC Phase:

On T responses collected:

1. Aggregate inputs for CPs
2. Execute $\mathcal{F}_{r_0}^{2PC}$ between CP₁, CP₂
3. Return result to combiner

P.3 Real Protocol $\Pi_{r_0}^{P3+}$

Protocol 24 ($\Pi_{r_0}^{P3+}$ – P3+ Semi-Async Protocol). **Offline Phase: Pre-signing**

Each signer P_i:

1. Generate B pre-signing sets:
 - (a) Sample set_id $\xleftarrow{\$}$ $\{0, 1\}^{256}$ (pre-signing set identifier)
 - (b) Sample nonce \mathbf{y}_i with reduced range
 - (c) Compute $\mathbf{w}_i = \mathbf{A} \cdot \mathbf{y}_i$
 - (d) Sample commitment randomness $r_i \xleftarrow{\$}$ $\{0, 1\}^{256}$
 - (e) Compute commitment Com_i = H("com" || \mathbf{y}_i || \mathbf{w}_i || r_i)
2. Send (set_id, \mathbf{w}_i , Com_i) to combiner \triangleright r_i is not sent; kept secret by signer

Offline Phase: GC Precomputation

CP₁:

1. Build r0-check circuit C
2. Generate B garbled circuits $\{\tilde{C}_k\}_{k=1}^B$
3. Prepare OT setup for each circuit

Online Phase 1: Challenge Derivation

Combiner:

1. Receive signing request for message μ

2. Select T signers with available pre-signing sets
3. Aggregate $\mathbf{w} = \sum_i \lambda_i \cdot \mathbf{w}_i$ ▷ Lagrange reconstruction
4. Compute $\mathbf{w}_1 = \text{HighBits}(\mathbf{w}, 2\gamma_2)$
5. Derive $c = \text{SampleChallenge}(H(\text{tr}\|\mu\|\mathbf{w}_1))$
6. Broadcast $(c, \text{set_map})$ to signers

Online Phase 2: Signer Response

Each signer P_i (within Δ):

1. Retrieve nonce DKG share \mathbf{y}_i and commitment \mathbf{w}_i for assigned `set_id`
2. Compute:

$$\begin{aligned} \mathbf{z}_i &= \mathbf{y}_i + c \cdot \mathbf{s}_{1,i} \\ \mathbf{V}_i &= \lambda_i c \mathbf{s}_{2,i} + \mathbf{m}_i^{(s_2)} \end{aligned}$$

where λ_i is the Lagrange coefficient for party i in signing set S

3. Send $(\mathbf{z}_i, \mathbf{V}_i)$ to combiner
4. Mark `set_id` as consumed

Online Phase 3: 2PC Execution

Combiner:

1. Wait for T responses (or timeout)
2. Aggregate response: $\mathbf{z} = \sum_{i \in S} \lambda_i \cdot \mathbf{z}_i$ (Lagrange reconstruction)
3. Split \mathbf{cs}_2 contributions: \mathbf{S}_1 for CP_1 , \mathbf{S}_2 for CP_2
4. Send $(\mathbf{w}, \mathbf{S}_1)$ to CP_1 , (\mathbf{S}_2) to CP_2

CP_1 (Garbler):

1. Select precomputed garbled circuit \tilde{C}
2. Select input wire labels for $(\mathbf{w}, \mathbf{S}_1)$
3. Send $(\tilde{C}, \text{labels}_1)$ to CP_2

CP_2 (Evaluator):

1. Execute OT to obtain labels for \mathbf{S}_2
2. Evaluate \tilde{C} to obtain result
3. Send result to both CPs

Output:

1. If `result = 1`: The 2PC circuit outputs the hint

$$\mathbf{h} = \text{MakeHint}(-ct_0, \mathbf{A}\mathbf{z} - ct_1 \cdot 2^d, 2\gamma_2)$$

(computed inside the circuit using $\mathbf{cs}_2 = \mathbf{S}_1 + \mathbf{S}_2$); the combiner outputs signature $\sigma = (\tilde{c}, \mathbf{z}, \mathbf{h})$

2. If `result = 0`: Retry with fresh pre-signing sets

P.4 Simulator Construction for P3+

Simulator 25 ($\mathcal{S}^{\text{P3+}}$ for $\Pi_{r_0}^{\text{P3+}}$). \mathcal{S} interacts with $\mathcal{F}_{r_0}^{\text{semi-async}}$ and simulates the adversary's view.

Simulating Key DKG:

1. \mathcal{S} receives the corrupted parties' key shares $\{(\mathbf{s}_{1,j}, \mathbf{s}_{2,j})\}_{j \in C}$ from the adversary (via corruption; in P3+ the key DKG is modeled as a trusted-dealer setup phase, so the simulator acts as the trusted dealer and generates all shares directly).
2. \mathcal{S} runs the ideal key-generation functionality on behalf of all honest parties: \mathcal{S} samples a fresh degree- $(T-1)$ Shamir polynomial for each component of $(\mathbf{s}_1, \mathbf{s}_2)$, consistent with the corrupted-party shares received in step 1, and computes the honest-party evaluations $\{(\mathbf{s}_{1,i}, \mathbf{s}_{2,i})\}_{i \notin C}$ directly from these polynomials.
3. \mathcal{S} stores all shares $\{(\mathbf{s}_{1,i}, \mathbf{s}_{2,i})\}_{i=1}^N$ for use in the response simulation.
4. **Justification:** The simulator acts as the DKG simulator, generating the full Shamir polynomials during key setup. It does not infer honest shares post-hoc from \mathbf{t}_1 (which is a lossy commitment and does not uniquely determine $(\mathbf{s}_1, \mathbf{s}_2)$). Rather, the polynomials are fixed at key-generation time by \mathcal{S} 's own choices, and all evaluations $\{(\mathbf{s}_{1,i}, \mathbf{s}_{2,i})\}_{i=1}^N$ are therefore directly available to \mathcal{S} . When $|C| < T-1$, there are multiple polynomials consistent with the corrupted shares; \mathcal{S} uses the one it sampled.

Simulating Pre-signing (Honest Signers):

1. For each honest signer P_i :
 - (a) Sample $\tilde{\mathbf{y}}_i \xleftarrow{\$} \mathcal{R}_q^\ell$ (simulated nonce share)
 - (b) Compute $\tilde{\mathbf{w}}_i = \mathbf{A} \cdot \tilde{\mathbf{y}}_i$ (same computation as real protocol)
 - (c) Sample $\tilde{r}_i \xleftarrow{\$} \{0, 1\}^{256}$ (commitment randomness); program the random oracle so that $H(\text{"com"} \parallel \tilde{\mathbf{y}}_i \parallel \tilde{\mathbf{w}}_i \parallel \tilde{r}_i) := \text{Com}_i$ where $\text{Com}_i \xleftarrow{\$} \{0, 1\}^{256}$; store $(\tilde{\mathbf{y}}_i, \tilde{\mathbf{w}}_i, \tilde{r}_i)$ for potential blame-protocol opening
 - (d) Send $(\text{set_id}, \tilde{\mathbf{w}}_i, \text{Com}_i)$ to adversary
2. **Justification:** Commitment hides \mathbf{y}_i (random oracle). Simulated $\tilde{\mathbf{w}}_i = \mathbf{A} \cdot \tilde{\mathbf{y}}_i$ has the same distribution as the real $\mathbf{w}_i = \mathbf{A} \cdot \mathbf{y}_i$: the real $\mathbf{y}_i = F(i)$ for $i \neq 0$ is \mathcal{R}_q^ℓ -uniform because the degree-1-through- $(T-1)$ coefficients of F are sampled uniformly (Theorem 28), making each non-zero evaluation uniform by linearity; thus $\tilde{\mathbf{y}}_i \xleftarrow{\$} \mathcal{R}_q^\ell$ matches this distribution exactly ($SD = 0$). The stored \tilde{r}_i enables blame-protocol commitment opening.

Simulating Response Phase (Honest Signers):

1. On challenge c from combiner:
 - (a) For each honest signer P_i :
 - (b) Compute $\mathbf{z}_i = \tilde{\mathbf{y}}_i + c \cdot \mathbf{s}_{1,i}$ using the nonce shares $\tilde{\mathbf{y}}_i$ from the simulated pre-signing phase and key shares $\mathbf{s}_{1,i}$ from the simulated key DKG
 - (c) Compute $\mathbf{V}_i = \lambda_i c \mathbf{s}_{2,i} + \mathbf{m}_i^{(s_2)}$ using the simulated key shares and PRF masks
 - (d) Send $(\mathbf{z}_i, \mathbf{V}_i)$ to adversary (via combiner)

2. **Justification:** The simulator computes responses using the same deterministic function as the real protocol, applied to the simulated DKG values. Since the simulated DKG produces values with identical distribution to the real DKG (Lemma 12), the resulting $\mathbf{z}_i = \tilde{\mathbf{y}}_i + c \cdot \mathbf{s}_{1,i}$ is perfectly indistinguishable from the real value ($SD = 0$, since $\tilde{\mathbf{y}}_i$ and \mathbf{y}_i have identical distribution). The masked key-share component $\mathbf{V}_i = \lambda_i c \mathbf{s}_{2,i} + \mathbf{m}_i^{(s2)}$ uses PRF-derived masks $\mathbf{m}_i^{(s2)}$; the simulator uses the actual pairwise PRF seeds established during key setup simulation, computing the same mask values $\mathbf{m}_i^{(s2)} = \text{PRF}(\text{seed}_{h,i}, \text{sid})$ as the real protocol. No PRF replacement is needed; the simulation is bit-for-bit identical to the real protocol for this component. The overall gap is therefore 0.

Simulating 2PC (Corrupt CP_1):

1. Adversary controls garbler CP_1
2. \mathcal{S} extracts \mathbf{S}_1 from adversary's garbled circuit inputs (using garbled-circuit extractability [LP07]); \mathbf{w} is already public (broadcast by the combiner)
3. \mathcal{S} sends \mathbf{S}_1 to $\mathcal{F}_{r_0}^{\text{semi-async}}$
4. Receives result from functionality
5. Simulates honest CP_2 :
 - (a) Execute OT protocol with adversary
 - (b) Return result to adversary
6. **Justification:** Garbled circuit extractability [LP07] allows extraction of garbler's inputs.

Simulating 2PC (Corrupt CP_2):

1. Adversary controls evaluator CP_2
2. \mathcal{S} extracts \mathbf{S}_2 from adversary's OT queries
3. \mathcal{S} sends \mathbf{S}_2 to $\mathcal{F}_{r_0}^{\text{semi-async}}$
4. Receives result from functionality
5. Simulates honest CP_1 :
 - (a) Generate a simulated garbled circuit \tilde{C} together with all input wire labels for $(\mathbf{w}, \mathbf{S}_1)$ (garbler's inputs) and the wire labels for \mathbf{S}_2 selected by CP_2 's OT queries, consistent with the output result, using the BHR12 simulator for the full two-input garbled circuit [BHR12].
6. **Justification:** Garbled circuit simulatability (BHR12 privacy definition): given the output $f(\mathbf{w}, \mathbf{S}_1, \mathbf{S}_2)$ and the evaluator's input labels (for \mathbf{S}_2 , known from OT), the BHR12 simulator produces a simulated circuit \tilde{C} plus all evaluator-side input labels computationally indistinguishable from the real garbled circuit. The garbler's (CP_1 's) input wire labels for $(\mathbf{w}, \mathbf{S}_1)$ are included in the simulated output; these are internally consistent with \tilde{C} by construction.

Simulating 2PC (Both CP s Honest): When both CP_1 and CP_2 are honest, the adversary observes only:

- Pre-signing commitments Com_i (simulated uniformly above, $SD = 0$).

- The broadcast challenge c (determined by the ideal functionality).
- Responses $(\mathbf{z}_i, \mathbf{V}_i)$ for honest $i \notin C$ (simulated above: \mathbf{z}_i with $SD = 0$; \mathbf{V}_i with $SD = 0$ since the simulator uses the actual PRF seeds established during key setup, producing bit-for-bit identical mask values).
- The final result bit (provided by $\mathcal{F}_{r_0}^{\text{semi-async}}$).

The 2PC OT and GC transcripts are exchanged solely between the two honest CPs and are never delivered to the adversary. \mathcal{S} need not simulate these messages; the hybrid sequence $H_0 \rightarrow H_1$ (replace OT) $\rightarrow H_2$ (replace GC) captures the honest-CP case via ideal-functionality substitution.

Simulating Timeout / Abort:

1. If the adversary delays honest signers' responses past the deadline deadline (e.g., by withholding the challenge or blocking network messages):
 - (a) \mathcal{S} detects no challenge delivered to honest signers within $\text{deadline} - \Delta$ rounds.
 - (b) \mathcal{S} sends $(\text{ABORT}, \text{sid})$ to $\mathcal{F}_{r_0}^{\text{semi-async}}$.
 - (c) \mathcal{S} delivers $(\text{abort}, \text{sid})$ to all honest parties in the simulated execution.
2. **Justification:** The functionality enforces “if now > deadline: reject” (see Response Phase, condition 1). When the adversary induces timeout, both ideal and simulated executions abort identically; the simulated abort message matches the real abort, giving indistinguishability.

P.5 Hybrid Argument for P3+

Definition 21 (P3+ Hybrids). • H_0 : Real execution of $\Pi_{r_0}^{\text{P3+}}$

- H_1 : Replace OT with \mathcal{F}_{OT}
- H_2 : Replace GC with \mathcal{F}_{GC}
- H_3 : Simulate pre-signing (sample $\tilde{\mathbf{y}}_i$, compute $\tilde{\mathbf{w}}_i = \mathbf{A}\tilde{\mathbf{y}}_i$)
- H_4 : Simulate responses from $\tilde{\mathbf{y}}_i$ and simulated key shares
- H_5 : Ideal execution with $\mathcal{F}_{r_0}^{\text{semi-async}}$

Lemma 12 (Pre-signing Simulation (ROM)). $\Pr[H_2 = 1] = \Pr[H_3 = 1]$ (perfect indistinguishability in the random oracle model)

Proof. We work in the UC random oracle model: H is modeled as an ideal functionality \mathcal{F}_{RO} (following [Can01, BR93]). The simulator $\mathcal{S}^{\text{P3+}}$ programs \mathcal{F}_{RO} at honest parties' pre-image inputs: when the simulator generates $\tilde{\text{Com}}_i \xleftarrow{\$} \{0, 1\}^{256}$, it programs $H(\tilde{\mathbf{y}}_i \| \mathbf{A}\tilde{\mathbf{y}}_i \| \text{set_id}) := \text{Com}_i$ at the simulated pre-image (the adversary does not know $\tilde{\mathbf{y}}_i$ and cannot query H on this input without knowing the simulation randomness).

Pre-signing values visible to the adversary:

- $\text{Com}_i = H(\mathbf{y}_i \| \mathbf{w}_i \| \text{set_id})$: In the ROM, Com_i is uniform over $\{0, 1\}^{256}$ regardless of \mathbf{y}_i 's distribution, since the adversary does not know \mathbf{y}_i (or $\mathbf{w}_i = \mathbf{A}\mathbf{y}_i$) and cannot query \mathcal{F}_{RO} at the pre-image without knowing the honest party's nonce. (Note: in the real protocol with $T \geq 2$, $\mathbf{y}_i = \mathbf{F}(i)$ is \mathbb{Z}_q -uniform: the high-degree DKG coefficients (degree ≥ 1) are sampled R_q -uniformly, and for evaluation point $i \neq 0$ their contribution is uniform by additive mixing, giving $\mathbf{y}_i \sim \mathbb{Z}_q$ -uniform exactly. When $T = 1$ there are no high-degree terms and $\mathbf{y}_i = \mathbf{y}_0$ is the constant nonce, but

this is a degenerate threshold that is excluded by the protocol requirement $T \geq 2$. The Irwin-Hall distribution applies to the *aggregate* nonce $\mathbf{y} = \mathbf{F}(0) = \sum_k \hat{\mathbf{y}}_k$, not to individual shares $\mathbf{y}_i = \mathbf{F}(i)$. The simulated $\tilde{\mathbf{y}}_i \xleftarrow{\$} \mathbb{Z}_q$ and $\tilde{\text{Com}}_i \xleftarrow{\$} \{0, 1\}^{256}$ therefore match the real distributions exactly ($\text{SD} = 0$).

- $\mathbf{W}_i = \lambda_i \mathbf{w}_i + \mathbf{m}_i^{(w)}$ (masked commitment sent to CP combiner): In P3+, \mathbf{W}_i is transmitted *only* to the CP combiner, not broadcast to other parties. By the 1-of-2 CP honest assumption, at least one CP is honest; in this proof we assume the adversary does not control the combiner's input-aggregation role (if a CP is corrupted, the relevant 2PC simulation case handles it below). Since \mathbf{W}_i never reaches the adversary, *no mask-hiding argument is required*. The value is hidden entirely by the honest combiner. (Note: Lemma 2 applies to the P2 broadcast model where \mathbf{W}_i is sent to all parties; it does not apply here.)

Thus:

$$\Pr[\mathbf{H}_2 = 1] = \Pr[\mathbf{H}_3 = 1]$$

□

Lemma 13 (Response Simulation). $\Pr[\mathbf{H}_3 = 1] = \Pr[\mathbf{H}_4 = 1]$ (*perfect indistinguishability*)

Proof. The simulator computes each honest party's response deterministically from its simulated DKG values, producing an identical distribution to the real protocol:

$$\begin{aligned} \mathbf{z}_i &= \mathbf{y}_i + c \cdot \mathbf{s}_{1,i} \\ \mathbf{V}_i &= \lambda_i c \mathbf{s}_{2,i} + \mathbf{m}_i^{(s2)} \end{aligned}$$

where \mathbf{y}_i are the nonce shares from the simulated nonce DKG (Lemma 12) and $\mathbf{s}_{1,i}, \mathbf{s}_{2,i}$ are the key shares from the simulated key DKG. Since the simulator possesses the actual simulated values (not just their distributions), it computes \mathbf{z}_i and \mathbf{V}_i using the same deterministic function as the real protocol; the resulting joint distribution is identical to the real execution. For \mathbf{V}_i , the simulator computes the masked r0-check share using the simulated key shares and the PRF masks (derived from the same seeds used in earlier hybrids). Perfect indistinguishability follows: $\Pr[\mathbf{H}_3 = 1] = \Pr[\mathbf{H}_4 = 1]$. □

Theorem 26 (P3+ UC Security). *Protocol $\Pi_{r_0}^{\text{P3+}}$ UC-realizes $\mathcal{F}_{r_0}^{\text{semi-async}}$ in the $(\mathcal{F}_{\text{OT}}, \mathcal{F}_{\text{GC}})$ -hybrid model against static malicious adversaries corrupting up to $T - 1$ signers and at most one of $\{\text{CP}_1, \text{CP}_2\}$, with security-with-abort. Key DKG is handled by a trusted dealer (modeled as a trusted setup phase); the simulator acts as the trusted dealer and directly generates all key shares.*

Concretely:

$$|\Pr[\text{REAL} = 1] - \Pr[\text{IDEAL} = 1]| \leq \epsilon_{\text{OT}} + \epsilon_{\text{GC}} + \epsilon_{\text{ext}} < 2^{-\kappa}$$

where κ is the computational security parameter, ϵ_{OT} is the OT error, ϵ_{GC} is the garbled-circuit simulation error (over honest garbler [BHR12]), and $\epsilon_{\text{ext}} \leq 2^{-B/2}$ is the cut-and-choose extraction error when CP_1 is corrupted (LP07 extractability [LP07] with B circuits, $B/2$ opened for verification).

Proof. By the hybrid argument:

$$\begin{aligned} |\Pr[\mathbf{H}_0] - \Pr[\mathbf{H}_5]| &\leq \sum_{i=0}^4 |\Pr[\mathbf{H}_i] - \Pr[\mathbf{H}_{i+1}]| + |\Pr[\mathbf{H}_{2.5,\text{ext}}] - \Pr[\mathbf{H}_3]| \\ &= \epsilon_{\text{OT}} + \epsilon_{\text{GC}} + \epsilon_{\text{ext}} + 0 + 0 + 0 \\ &< 2^{-\kappa} \end{aligned}$$

The hybrid $H_{2.5,\text{ext}}$ (between H_2 and H_3) is the *extraction hybrid*: when CP_1 is corrupted, the simulator uses LP07 cut-and-choose extractability to extract \mathbf{S}_1 from the adversarially-submitted garbled circuit; this succeeds except with probability $\epsilon_{\text{ext}} \leq 2^{-B/2}$ (see the extraction error accounting below). The three subsequent zero terms arise from perfect indistinguishability: pre-signing simulation (Lemma 12), response simulation (Lemma 13), and the transition to the ideal execution.

Hint output and combiner role. The ideal functionality $\mathcal{F}_{r_0}^{2\text{PC}}$ (Definition 20) outputs both the 1-bit result *and* the hint $\mathbf{h} = \text{MakeHint}(\mathbf{w}', \mathbf{w}, 2\gamma_2)$ to the combiner. In both simulator cases, $S^{\text{P3+}}$ receives $(\text{result}, \mathbf{h})$ from $\mathcal{F}_{r_0}^{\text{semi-async}}$ and passes \mathbf{h} to the adversary. The hint \mathbf{h} appears in the public signature $\sigma = (\tilde{c}, \mathbf{z}, \mathbf{h})$ and creates no leakage beyond what σ already reveals; the BHR12 simulator constructs a garbled circuit consistent with output $(\text{result}, \mathbf{h})$ without exposing cs_2 .

Combiner and CP roles. In P3+, CP_1 (the garbler) also acts as the combiner: it aggregates signer responses $(\mathbf{z}_j, \mathbf{V}_j)$, computes the split (S_1, S_2) for the 2PC, and executes the garbled-circuit protocol with CP_2 . Combiner corruption is subsumed by the “ CP_1 is corrupted” case (Simulator 25): the simulator uses LP07 extraction to recover \mathbf{S}_1 from the adversary’s garbled circuit and forwards honest parties’ contributions via the ideal-world channel to $\mathcal{F}_{r_0}^{\text{semi-async}}$.

Extraction error accounting. When CP_1 (garbler) is corrupted, $S^{\text{P3+}}$ uses LP07 extractability to recover \mathbf{S}_1 from the adversarially-submitted garbled circuit. The cut-and-choose protocol (generate B circuits; open $\lfloor B/2 \rfloor$ for verification; use the rest) ensures a cheating garbler is caught with probability $1 - 2^{-\lfloor B/2 \rfloor} \geq 1 - 2^{-B/2}$. For unopened circuits, LP07 extraction succeeds with probability 1 (requires only correct evaluation, guaranteed by cut-and-choose). Thus $\epsilon_{\text{ext}} \leq 2^{-B/2}$; setting $B = 2\kappa$ gives $\epsilon_{\text{ext}} \leq 2^{-\kappa}$. The full bound $\epsilon_{\text{OT}} + \epsilon_{\text{GC}} + 2^{-B/2} < 2^{-\kappa+1}$ holds for standard κ -bit-secure OT and GC. \square

P.6 Security Properties of P3+

Corollary 6 (P3+ Full Security). *Protocol P3+ achieves:*

1. **EUFCMA:** Under Module-SIS (same as P3)
2. **UC Security:** Against malicious adversaries with 1-of-2 CP honest
3. **Privacy:** Nonce shares \mathbf{y}_i enjoy statistical privacy (Theorem 3); key privacy given σ is conjectured to hold computationally under Module-LWE (open problem); commitment and r_0 -check values hidden by pairwise masks if ≥ 2 honest signers
4. **Liveness:** Completes if T signers respond within Δ and both CPs available

Proof. **EUFCMA:** Pre-signing does not change the signature distribution. The commitment binding ensures signers commit to nonces before seeing challenges. Reduction to Module-SIS identical to P3.

UC Security: Theorem 26.

Privacy: By Lemma 13, the simulator computes honest signers’ responses from simulated DKG values (perfect indistinguishability). Nonce shares have high conditional min-entropy (Theorem 3, statistical); key privacy given σ is conjectured to hold computationally under Module-LWE (formal reduction is an open problem, unresolved even in the single-signer setting). The \mathbf{V}_j values are computationally hidden by pairwise masks. The 2PC reveals the result bit and hint \mathbf{h} (both appear in the public signature); \mathbf{h} does not create additional privacy leakage beyond what σ already reveals. Combining: adversary view simulatable from public values + corrupted shares + $(\text{result}, \mathbf{h})$.

Liveness: The protocol has an explicit timeout. If conditions are met, the 2PC completes in bounded time (synchronous between CPs). If not, the protocol aborts (no liveness violation; just unsuccessful signing). \square

P.7 P3+ Round Complexity

Theorem 27 (P3+ Complexity). *P3+ achieves:*

1. **Signer rounds:** 1 (respond within window)
2. **Server rounds:** 1 (2PC between CPs)
3. **Total logical rounds:** 2
4. **Expected retries:** 3.7 ($\approx 27\%$ success rate)
5. **Expected total rounds:** 7.4 (2 rounds \times 3.7 attempts)

Proof. Signer experience: After receiving the challenge, the signer computes a local response and sends it once. No further interaction is required.

Server interaction: CPs execute 2PC in constant rounds (with GC precomputation), effectively 1 round (OT + evaluate).

Retry handling: Each retry requires a fresh pre-signing set and response; the signer daemon handles this automatically.

Total: $2 \times 3.7 \approx 7.4$ expected rounds (vs. $5 \times 3.5 = 17.5$ for P2). \square

Table 16: Round complexity across profiles. \dagger P3: synchronous 2PC variant (5 rounds) before the semi-async optimization; P3+ is the final protocol (Section 6.5).

Profile	Rds/Attempt	Exp. Attempts	Total Rds
P2 (8-round)	8	3.5	28
P2 (5-round)	5	3.5	17.5
P3 \dagger	5	3.5	17.5
P3+	2	3.7	7.4

Q Technical Lemmas

This section provides rigorous proofs of technical lemmas used throughout the paper.

Q.1 Mask Properties

Lemma 14 (Mask Cancellation – Formal Statement). *Let $S \subseteq [N]$ be a signing set with $|S| \geq 2$. For any PRF input $\text{ctx} \in \{0, 1\}^*$ (typically $\text{ctx} = \text{session_id} \parallel \text{dom}$, where session_id is a fresh per-session identifier and dom is a fixed domain label) and PRF $\text{PRF} : \{0, 1\}^{256} \times \{0, 1\}^* \rightarrow R_q^k$ (where $k = 6$ is the module rank; not the dropping-bits parameter $d = 13$), define:*

$$\mathbf{m}_i = \sum_{j \in S: j > i} \text{PRF}(\text{seed}_{i,j}, \text{ctx}) - \sum_{j \in S: j < i} \text{PRF}(\text{seed}_{j,i}, \text{ctx})$$

Then $\sum_{i \in S} \mathbf{m}_i = \mathbf{0} \in R_q^k$.

Proof. We prove this by showing each PRF term appears exactly once with coefficient +1 and once with coefficient -1.

For any pair $(i, j) \in S \times S$ with $i < j$, the term $\text{PRF}(\text{seed}_{i,j}, \text{ctx})$ appears:

1. In \mathbf{m}_i with coefficient +1 (from the sum over $k > i$, taking $k = j$)

2. In \mathbf{m}_j with coefficient -1 (from the sum over $k < j$, taking $k = i$)

Thus:

$$\begin{aligned} \sum_{i \in S} \mathbf{m}_i &= \sum_{i \in S} \left(\sum_{j \in S: j > i} \text{PRF}(\text{seed}_{i,j}, \text{ctx}) - \sum_{j \in S: j < i} \text{PRF}(\text{seed}_{j,i}, \text{ctx}) \right) \\ &= \sum_{\substack{(i,j) \in S \times S \\ i < j}} \text{PRF}(\text{seed}_{i,j}, \text{ctx}) - \sum_{\substack{(i,j) \in S \times S \\ i < j}} \text{PRF}(\text{seed}_{i,j}, \text{ctx}) \\ &= \mathbf{0} \end{aligned}$$

□

Theorem 28 (Statistical Share Privacy – Formal Statement). *Let S be a signing set with $|S| \geq T$, let $C \subset S$ with $|C| \leq T - 1$ be the set of corrupted parties, and let $h \in S \setminus C$ be an honest party. In the Shamir nonce DKG protocol (Algorithm 2), each party samples its constant-term contribution $\hat{\mathbf{y}}_h \stackrel{\$}{\leftarrow} \{-\lfloor \gamma_1/|S| \rfloor, \dots, \lfloor \gamma_1/|S| \rfloor\}^{n\ell}$ and constructs a degree- $(T - 1)$ polynomial with uniform higher-degree coefficients. The honest party’s nonce share $\mathbf{y}_h = \sum_{i \in S} \mathbf{f}_i(h)$ has conditional min-entropy:*

$$H_\infty(\mathbf{y}_h \mid \{\mathbf{f}_j\}_{j \in C}, \{\mathbf{f}_h(j)\}_{j \in C}) \geq n\ell \cdot \log_2(2\lfloor \gamma_1/|S| \rfloor + 1)$$

where the inequality holds directly from the sampling procedure (no rejection conditioning needed): the bounded sampling range for each party’s constant term directly ensures that the honest party’s polynomial \mathbf{f}_h has $\mathbf{f}_h(0) = \hat{\mathbf{y}}_h \in [-\lfloor \gamma_1/|S| \rfloor, \lfloor \gamma_1/|S| \rfloor]^{n\ell}$ by construction (Algorithm 2, Line 2). No computational assumptions are needed for the nonce privacy; it is purely statistical. For ML-DSA-65 with $|S| \leq 17$, this exceeds 20,000 bits—over $5 \times$ the short secret key entropy $H(\mathbf{s}_1) \leq 4058$ bits. (Shamir shares $\mathbf{s}_{1,h}$ for $h \neq 0$ are \mathbb{Z}_q -uniform; the entropy comparison is against the short secret $\mathbf{s}_1 = \mathbf{f}(0)$.)

Note on aggregated nonce $\mathbf{y} = \sum_i \hat{\mathbf{y}}_i$. The aggregated nonce \mathbf{y} (sum of all parties’ constant terms) follows an Irwin-Hall distribution with tails extending beyond $[-\gamma_1, \gamma_1]$. However, the aggregated nonce is never required to lie strictly within this range for the min-entropy bound to hold: the bound applies to individual shares \mathbf{y}_h , not the aggregate. The z -bound check $\|\mathbf{z}\|_\infty < \gamma_1 - \beta$ implicitly rejects sessions where the aggregate $\|\mathbf{y}\|_\infty$ is too large (via $\mathbf{z} = \mathbf{y} + c\mathbf{s}_1$), but this rejection event is already accounted for in the Irwin-Hall tail probability $\epsilon < 10^{-30}$ (Lemma 19); it does not affect the per-share conditional min-entropy.

Key privacy given σ (computational, informal). Even given the public signature σ (from which $\mathbf{z}_h = \mathbf{y}_h + c \cdot \mathbf{s}_{1,h}$ is computable when $|S \setminus C| = 1$), extracting $\mathbf{s}_{1,h}$ requires solving a bounded-distance decoding problem with sparse multiplier c . While not a standard Module-LWE instance, this is at least as hard as key recovery from single-signer ML-DSA signatures; see the discussion in Theorem 3 (Section 4).

Proof. The proof proceeds in three steps, following a null space argument on the honest party’s polynomial.

Reduction to the worst case $|C| = T - 1$. The stated min-entropy lower bound is monotone non-decreasing as $|C|$ decreases: fewer corrupted evaluations give a higher-dimensional null space (dimension $T - |C| > 1$ when $|C| < T - 1$), meaning the adversary is more uncertain about \mathbf{y}_h (higher conditional min-entropy). Hence it suffices to prove the bound for the hardest case $|C| = T - 1$ (minimum uncertainty for the adversary); the case $|C| < T - 1$ gives at least as much privacy and follows a fortiori. We henceforth assume $|C| = T - 1$.

The adversary’s knowledge about the honest party’s polynomial \mathbf{f}_h consists of the evaluations $\{\mathbf{f}_h(j)\}_{j \in C}$ received during the DKG. With $|C| = T - 1$ and \mathbf{f}_h having degree

$T-1$ (hence T coefficients), the adversary has exactly $T-1$ linear equations in T unknowns: the null space of the evaluation map has dimension exactly 1.

Step 1: Null space. The evaluation map $\mathbf{f}_h \mapsto (\mathbf{f}_h(j_1), \dots, \mathbf{f}_h(j_{T-1}))$ (with $|C| = T-1$) has a one-dimensional null space, spanned by the monic polynomial $\mathbf{n}(x) = \prod_{j \in C} (x - x_j)$ of degree $T-1$ and leading coefficient 1. The set of polynomials consistent with the adversary's observations is $\mathbf{f}_h(x) = \mathbf{g}(x) + \mathbf{t} \cdot \mathbf{n}(x)$, where \mathbf{g} is any fixed interpolant through the known points and $\mathbf{t} \in R_q^\ell$ is the unique free parameter.

Step 2: Posterior constraint on \mathbf{t} . In the nonce DKG, each honest party h samples $\hat{\mathbf{y}}_h$ directly from $[-\lceil \gamma_1/|S| \rceil, \lceil \gamma_1/|S| \rceil]^{n\ell}$ and all $T-1$ higher-degree coefficients $\mathbf{a}_{h,1}, \dots, \mathbf{a}_{h,T-1}$ independently and uniformly from R_q^ℓ . In the null-space parameterization, the free parameter is $\mathbf{t} = \mathbf{a}_{h,T-1} - \mathbf{g}_{T-1}$, where \mathbf{g}_{T-1} is the leading coefficient of the fixed interpolant \mathbf{g} . Because $\mathbf{a}_{h,T-1}$ is \mathbb{Z}_q -uniform *a priori*, \mathbf{t} is \mathbb{Z}_q -uniform per coefficient. The constant term $\hat{\mathbf{y}}_h = \mathbf{f}_h(0) = \mathbf{g}(0) + \mathbf{t} \cdot \mathbf{n}(0)$ must satisfy $\hat{\mathbf{y}}_h \in [-\lceil \gamma_1/|S| \rceil, \lceil \gamma_1/|S| \rceil]^{n\ell}$. Since $\mathbf{n}(0) = \prod_{j \in C} (-j) \not\equiv 0 \pmod{q}$ (each $j \in C$ satisfies $1 \leq j \leq N \leq q-1$, so $j \not\equiv 0 \pmod{q}$), and the product of nonzero field elements is nonzero), multiplication by $\mathbf{n}(0)$ is a bijection on \mathbb{Z}_q . Since the Shamir evaluation map acts independently on each of the $n\ell = 1280$ coefficient slots (each coefficient of \mathbf{f}_h follows a separate scalar Shamir sharing over \mathbb{Z}_q), this bijection applies coordinate-by-coordinate across all $n\ell$ slots; the constraint selects exactly $2\lceil \gamma_1/|S| \rceil + 1$ values per coefficient of \mathbf{t} . Because the prior is \mathbb{Z}_q -uniform, conditioning on this subset yields a *uniform* posterior over the valid values.

Step 3: Min-entropy at honest point. The honest party's share is $\mathbf{f}_h(x_h) = \mathbf{g}(x_h) + \mathbf{t} \cdot \mathbf{n}(x_h)$. Since $x_h \notin C$ and q is prime, $\mathbf{n}(x_h) \not\equiv 0 \pmod{q}$, so multiplication by $\mathbf{n}(x_h)$ is a bijection on \mathbb{Z}_q . The evaluation $\mathbf{f}_h(x_h)$ inherits the same per-coefficient support size $2\lceil \gamma_1/|S| \rceil + 1$. The nonce share $\mathbf{y}_h = \sum_{j \in C} \mathbf{f}_j(x_h) + \mathbf{f}_h(x_h)$ shifts by a known constant, preserving support.

Key privacy (computational). Given the public signature σ , the adversary can compute \mathbf{z}_h (when $|S \setminus C| = 1$). The equation $\mathbf{z}_h = \mathbf{y}_h + c \cdot \mathbf{s}_{1,h}$ relates two bounded unknowns. The high min-entropy of \mathbf{y}_h ensures this is a non-trivial bounded-distance decoding instance: extracting $\mathbf{s}_{1,h}$ is computationally hard under the Module-LWE assumption. \square

Lemma 15 (Mask Hiding – Formal Statement (for \mathbf{V}_i and \mathbf{W}_i)). *Let $C \subsetneq S$ be the set of corrupted parties in signing set S , with $|S \setminus C| \geq 2$. For any honest party $j \in S \setminus C$, the masked r_0 -check share $\mathbf{V}_j = \lambda_j c \mathbf{s}_{2,j} + \mathbf{m}_j^{(s2)}$ and masked commitment $\mathbf{W}_j = \lambda_j \mathbf{w}_j + \mathbf{m}_j^{(w)}$ are computationally indistinguishable from uniform, given the adversary's view.*

Note: This lemma applies to the commitment and r_0 -check values, which still use pairwise-canceling masks. The response $\mathbf{z}_j = \mathbf{y}_j + c \cdot \mathbf{s}_{1,j}$ does not require masks: the underlying nonce share \mathbf{y}_j has statistical privacy via the Shamir nonce DKG (Theorem 28), enabling perfect simulation of \mathbf{z}_j from simulated DKG values.

Proof. We prove the result for \mathbf{V}_j ; the argument for \mathbf{W}_j is identical. Decompose the mask $\mathbf{m}_j^{(s2)}$ based on counterparty corruption status:

$$\begin{aligned} \mathbf{m}_j^{(s2)} &= \underbrace{\sum_{\substack{k \in C \cap S \\ k > j}} \text{PRF}(\text{seed}_{j,k}, \text{ctx}) - \sum_{\substack{k \in C \cap S \\ k < j}} \text{PRF}(\text{seed}_{k,j}, \text{ctx})}_{\text{known to } \mathcal{A}} \\ &+ \underbrace{\sum_{\substack{k \in (S \setminus C) \setminus \{j\} \\ k > j}} \text{PRF}(\text{seed}_{j,k}, \text{ctx}) - \sum_{\substack{k \in (S \setminus C) \setminus \{j\} \\ k < j}} \text{PRF}(\text{seed}_{k,j}, \text{ctx})}_{\text{unknown to } \mathcal{A}} \end{aligned}$$

Since $|S \setminus C| \geq 2$, there exists at least one honest party $k' \in (S \setminus C) \setminus \{j\}$ whose PRF seed $\text{seed}_{j,k'}$ is unknown to \mathcal{A} . By PRF security, $\text{PRF}(\text{seed}_{j,k'}, \text{ctx})$ is computationally

indistinguishable from uniform in R_q^k . Since the mask contains at least one such uniform-looking term, and uniform plus fixed equals uniform, $\mathbf{V}_j \stackrel{c}{\approx} \text{Uniform}(R_q^k)$. One unknown PRF term suffices; the distinguishing advantage is bounded by ϵ_{PRF} (or at most $(|S \setminus C| - 1) \cdot \epsilon_{\text{PRF}}$ via a union bound over honest-honest seed pairs). \square

Q.2 Irwin-Hall Distribution Analysis

We provide a self-contained analysis of the security implications of using Irwin-Hall distributed nonces.

Definition 22 (Discrete Irwin-Hall Distribution). Let X_1, \dots, X_n be independent uniform random variables on the discrete interval $\{-B, -B + 1, \dots, B - 1, B\}$. The sum $Y = \sum_{i=1}^n X_i$ follows the *discrete Irwin-Hall distribution* $\text{IH}(n, B)$.

Lemma 16 (Irwin-Hall Moments). For $Y \sim \text{IH}(n, B)$:

1. $\mathbb{E}[Y] = 0$
2. $\text{Var}(Y) = n \cdot \frac{(2B+1)^2 - 1}{12} = n \cdot \frac{B(B+1)}{3}$
3. For large n , Y is approximately Gaussian by the Central Limit Theorem

Proof. Mean: Each X_i has mean $\mathbb{E}[X_i] = 0$ by symmetry. Thus $\mathbb{E}[Y] = \sum_i \mathbb{E}[X_i] = 0$.

Variance: For uniform on $\{-B, \dots, B\}$:

$$\begin{aligned} \text{Var}(X_i) &= \mathbb{E}[X_i^2] = \frac{1}{2B+1} \sum_{k=-B}^B k^2 \\ &= \frac{1}{2B+1} \cdot \frac{2B(B+1)(2B+1)}{6} = \frac{B(B+1)}{3} \end{aligned}$$

By independence, $\text{Var}(Y) = n \cdot \text{Var}(X_1) = n \cdot \frac{B(B+1)}{3}$.

CLT: Standard application of Lindeberg-Lévy. \square

Definition 23 (Rényi Divergence). For distributions P, Q over Ω with $P \ll Q$, the Rényi divergence of order $\alpha > 1$ is:

$$R_\alpha(P\|Q) = \left(\sum_{x \in \Omega} P(x)^\alpha Q(x)^{1-\alpha} \right)^{1/(\alpha-1)}$$

We use the *exponential* (non-log) form throughout, following [BLL⁺15, dPEK⁺24]. In this convention $R_2(P\|Q) = \sum_x P(x)^2/Q(x)$, the product rule $R_2(P_1 \times P_2\|Q_1 \times Q_2) = R_2(P_1\|Q_1) \cdot R_2(P_2\|Q_2)$ holds exactly, and the chi-squared divergence satisfies $\chi^2(P\|Q) = R_2(P\|Q) - 1$.

Definition 24 (Chi-Squared Divergence). The chi-squared divergence between distributions P and Q (with $P \ll Q$) is:

$$\chi^2(P\|Q) = \sum_{x \in \Omega} \frac{(P(x) - Q(x))^2}{Q(x)} = R_2(P\|Q) - 1$$

where the last equality holds by the definition of R_2 (order-2 Rényi divergence).

Definition 25 (Smooth Rényi Divergence [dPEK⁺24]). For $\epsilon \geq 0$, the *one-sided* smooth Rényi divergence is:

$$R_\alpha^\epsilon(P\|Q) = \min_{P'} R_\alpha(P'\|Q), \quad P' : \Delta(P', P) \leq \epsilon$$

where Δ denotes statistical distance. We use the one-sided variant (smoothing over P' only, Q fixed), as required by Lemma 17.

Lemma 17 (Security Reduction via Rényi Divergence [BLL⁺15, dPEK⁺24]). *Let P, Q be distributions such that $R_2^\epsilon(P\|Q) < \infty$ with one-sided smoothing (ϵ -close variant P' of P). For any event E :*

$$P(E) \leq \sqrt{R_2^\epsilon(P\|Q) \cdot Q(E)} + \epsilon$$

where ϵ is the total variation distance between P and its smoothed variant P' . This follows from $P(E) \leq P'(E) + \epsilon \leq \sqrt{R_2(P'\|Q) \cdot Q(E)} + \epsilon$ by Cauchy-Schwarz.

Proof. See [BLL⁺15, Theorem 1] and [dPEK⁺24, Lemma 4.1]. \square

Theorem 29 (Irwin-Hall Security for Threshold ML-DSA). *Let Π_{IH} be threshold ML-DSA with Irwin-Hall nonces (sum of $|S|$ uniforms), and Π_{U} be the hypothetical scheme with uniform nonces. Then for any PPT adversary \mathcal{A} making at most q_s signing queries:*

$$\text{Adv}_{\Pi_{\text{IH}}}^{\text{EUF-CMA}}(\mathcal{A}) \leq (R_2^{\text{vec}})^{q_s/2} \cdot \sqrt{\text{Adv}_{\Pi_{\text{U}}}^{\text{EUF-CMA}}(\mathcal{A})} + q_s \cdot \epsilon$$

where $R_2^{\text{vec}} = (R_2^{\epsilon, \text{coord}})^{n\ell}$ is the full-vector per-session Rényi divergence, and the per-coordinate $R_2^{\epsilon, \text{coord}}, \epsilon$ are computed below. The $(R_2^{\text{vec}})^{q_s/2}$ factor accounts for multi-session composition; see Remark 28. For the direct bound (Corollary 8), this factor is $(1 + \chi_{\text{max}}^2)^{n\ell q_s/2}$ and the security loss grows as $\approx 6.1 \times 10^{-3} q_s$ bits for $|S| = 17$.

Proof. We analyze the distribution of the signature response $\mathbf{z} = \mathbf{y} + \mathbf{cs}_1$.

In Π_{U} (hypothetical): $\mathbf{y} \stackrel{\$}{\leftarrow} \{-\gamma_1, \dots, \gamma_1\}^{n\ell}$ uniform. Thus $\mathbf{z} = \mathbf{y} + \mathbf{cs}_1$ is a shifted uniform.

In Π_{IH} (real): $\mathbf{y} = \sum_{i \in S} \hat{\mathbf{y}}_i$ where each

$$\hat{\mathbf{y}}_i \stackrel{\$}{\leftarrow} \{-\lfloor \gamma_1/|S| \rfloor, \dots, \lfloor \gamma_1/|S| \rfloor\}^{n\ell}$$

is party i 's constant-term contribution in the nonce DKG.

For each coordinate, we compare:

- P : Irwin-Hall distribution shifted by $(\mathbf{cs}_1)_j$
- Q : Uniform distribution shifted by $(\mathbf{cs}_1)_j$

The key insight is that the shift is the same in both cases. We bound $R_2^\epsilon(P\|Q)$.

Applying Lemma 4.2 of [dPEK⁺24]:

The Raccoon signature scheme [dPEK⁺24] faces an analogous problem: threshold signers contribute nonce shares that sum to a non-uniform (Irwin-Hall) distribution, and security requires bounding the statistical distance from uniform. Lemma 4.2 of [dPEK⁺24] provides a Rényi divergence bound for sums of discrete uniforms with bounded shifts. This lemma is directly applicable to our setting because:

1. Both schemes use additive secret sharing of nonces across threshold parties.
2. The shift arises from multiplying the challenge by the secret key share, bounded by $\|\mathbf{cs}_1\|_\infty \leq \beta$.

3. The discrete uniform ranges and modular arithmetic are structurally identical.

Let $m = |S|$ denote the signing set size and $B = 2\lfloor \gamma_1/|S| \rfloor$ the per-party **full** nonce range (distinct from the ring degree $n = 256$ used elsewhere; note B here equals $2\times$ the half-range B' in Definition 22, i.e., $B' = B/2 = \lfloor \gamma_1/|S| \rfloor$). For m uniforms on half-range $B/2$ with shift $\delta = \|(cs_1)_j\|_\infty \leq \beta$ (where c is the challenge polynomial), specializing to $\alpha = 2$ (where the factor $\alpha(\alpha - 1)/2 = 1$):

$$R_2^\epsilon \leq 1 + \frac{m^2\delta^2}{B^2} + O(1/m!)$$

For ML-DSA-65 parameters:

- $\gamma_1 = 2^{19} = 524288$
- $\beta = 196$
- $m = |S|$ (signing set size; note $n = 256$ is the ring degree)

$$\begin{aligned} R_2^\epsilon &\leq 1 + \frac{m^2 \cdot \beta^2}{(2\gamma_1/m)^2} = 1 + \frac{m^4 \cdot \beta^2}{4\gamma_1^2} \\ &= 1 + \frac{|S|^4 \cdot 196^2}{4 \cdot (524288)^2} = 1 + \frac{|S|^4 \cdot 38416}{1.099 \times 10^{12}} \end{aligned}$$

Why this bound is conservative ($\approx |S|^3/12$ looser than the Gaussian CLT): The Raccoon Lemma 4.2 formula $m^2\delta^2/B^2$ uses a moment bound that treats the IH sum as if its worst-case chi-squared scales with m^2/B^2 (reflecting a worst-case uniform-distribution approximation over the aggregate range $mB/2$). The Gaussian CLT-based Fisher information bound: the IH variance is $\text{Var}(Y) = \gamma_1^2/(3m)$ (sum of m i.i.d. uniforms on $[-\gamma_1/m, \gamma_1/m]$ with variance $(\gamma_1/m)^2/3$), giving Fisher information $I_F = 3m/\gamma_1^2$ and $\chi^2 \approx \delta^2 \cdot I_F = 3m\delta^2/\gamma_1^2$. Substituting $\gamma_1 = Bm/2$ (from $B = 2\gamma_1/m$): $\chi^2 = 3m\delta^2/(Bm/2)^2 = 12\delta^2/(mB^2)$ (proportional to m^{-1} , since variance grows as m), while the Raccoon formula gives $m^2\delta^2/B^2$ (proportional to m^2). The ratio is

$$\frac{m^2\delta^2/B^2}{12\delta^2/(mB^2)} = \frac{m^3}{12} \approx \frac{|S|^3}{12},$$

which equals 409 for $|S| = 17$ (the Gaussian approximation; the exact D2 ratio from FFT values is ≈ 441 , cited as $\approx 440\times$ throughout the paper). The Raccoon formula is formally correct as an upper bound; the direct Gaussian-based analysis (Lemma 19) gives the tight bound by using the actual IH variance rather than the aggregate-range worst case.

Concrete values (per-coordinate): Since nonce coordinates are sampled independently *before* rejection sampling, the full-vector Rényi divergence factorizes as $R_2^{\text{vec}} = (R_2^{\text{coord}})^{n\ell}$ where $n\ell = 1280$ for ML-DSA-65 (here $n = 256$ is the ring degree, $\ell = 5$ is the secret dimension). This factorization applies to the pre-rejection distributions P and Q . To handle rejection sampling: the smooth Rényi framework removes the tail region $\{|Y| > \gamma_1 - \beta\}$ from the support of P , producing a restricted distribution P' supported on the same acceptance set $\{|Y| \leq \gamma_1 - \beta\}$ as Q' . Within this support the rejection condition is deterministic (every sample is accepted), so the factorization carries through for the accepted distributions P' and Q' . The ϵ term in the bound accounts for the tail mass removed from P ; see [dPEK⁺24] for the precise smooth Rényi treatment. The resulting bound is:

$ S $	$R_2^{\epsilon, \text{coord}} - 1$	R_2^{vec}	$\sqrt{R_2^{\text{vec}}}$	$\sqrt{R_2^{\text{vec}}} \cdot 2^{-96}$
4	8.9×10^{-6}	≈ 1.011	≈ 1.006	$\approx 2^{-96}$
9	2.3×10^{-4}	≈ 1.34	≈ 1.16	$\approx 2^{-96}$
17	2.9×10^{-3}	$\approx 2^{5.4}$	$\approx 2^{2.7}$	$\approx 2^{-93.3}$
25	1.4×10^{-2}	$\approx 2^{25}$	$\approx 2^{12.5}$	$\approx 2^{-83.5}$
33	4.1×10^{-2}	$\approx 2^{75}$	$\approx 2^{37.5}$	$\approx 2^{-58.5}$

$$(R_2^{\text{vec}} = (R_2^{\text{coord}})^{1280})$$

The tail probability ϵ satisfies [dPEK⁺24, Lemma 4.2] (using $m = |S|$ and $B = 2\lceil\gamma_1/|S|\rceil$):

$$\epsilon < \left(\frac{2e \cdot \beta}{B}\right)^m / \sqrt{2\pi m}$$

For $|S| = 17$: $B = 2\lceil 524288/17 \rceil = 2 \times 30840 = 61680$, so $\epsilon < (2e \cdot 196/61680)^{17} / \sqrt{34\pi} < 10^{-30}$.

Conclusion: Applying Lemma 17 to the joint distribution over q_s independent signing sessions (joint Rényi divergence $(R_2^{\text{vec}})^{q_s}$) and taking a union bound over the smoothing tails:

$$\text{Adv}_{\Pi_{\text{IH}}}^{\text{EUF-CMA}} \leq (R_2^{\text{vec}})^{q_s/2} \cdot \sqrt{\text{Adv}_{\Pi_{\text{U}}}^{\text{EUF-CMA}}} + q_s \cdot \epsilon$$

Security interpretation (direct bound, Corollary 8): Using $R_2^{\text{vec}} \approx (1 + \chi_{\text{direct}}^2)^{1280}$ where χ_{direct}^2 is the directly computed chi-squared divergence (Corollary 8; slightly smaller than the Gaussian approximation $3|S|\beta^2/\gamma_1^2$), the multi-session factor contributes $\approx \frac{q_s \cdot n\ell}{2} \cdot \log_2(1 + \chi_{\text{direct}}^2)$ bits of security loss. For ML-DSA-65 with $\text{Adv}_{\text{U}} \leq 2^{-192}$:

$ S $	χ_{direct}^2	Loss/query (bits)	Max q_s for ≤ 10 -bit loss
4	8.4×10^{-7}	7.7×10^{-4}	$\approx 2^{14}$
17	6.6×10^{-6}	6.1×10^{-3}	≈ 1600
33	1.4×10^{-5}	1.2×10^{-2}	≈ 830

The conservative bound (Raccoon Lemma 4.2, $R_2^{\text{vec}} \approx 2^{5.4}$ for $|S| = 17$) is vacuous for $q_s \gtrsim 36$ queries; the direct bound above should be used for concrete security estimates.

Remark: The per-coordinate composition $(R_2^{\text{coord}})^{n\ell}$ (where $n = 256$ is the ring degree and $\ell = 5$ is the secret dimension, giving $n\ell = 1280$) is a consequence of applying the Rényi game hop at the nonce sampling stage, where coordinates are independent. Tighter reductions for Fiat-Shamir with Aborts [dPEK⁺24] can exploit the rejection sampling structure (which acts on the full vector \mathbf{z}) to potentially avoid this exponential composition. A tighter bound via direct shift-invariance is given in Lemma 19 and Corollary 8; developing an even tighter full-vector bound remains an interesting direction. \square

Remark 28 (Multi-session Rényi Composition). The bound in Theorem 29 involves two distinct costs:

(1) **Rényi hop cost** $(R_2^{\text{vec}})^{q_s}$. When the adversary makes q_s signing queries, each query sees a different nonce drawn from the Irwin-Hall distribution (Game 3) vs. from the uniform distribution (Game 4). Because the nonces are independent across sessions, the *joint* Rényi divergence over the full transcript is

$$R_2^{\text{joint}} = (R_2^{\text{vec}})^{q_s}.$$

This is the quantity that appears in the Rényi probability-preservation lemma applied to the *complete* EUF-CMA experiment. The corresponding security loss (in bits) is

$$\text{loss}(q_s) = \frac{q_s \cdot n\ell}{2} \cdot \log_2(1 + \chi_{\text{direct}}^2(|S|)) \lesssim q_s \cdot \frac{3|S|\beta^2 n\ell}{2\gamma_1^2 \ln 2},$$

where the \lesssim uses the Gaussian upper bound $\chi_{\text{Gauss}}^2 = 3|S|\beta^2/\gamma_1^2 \geq \chi_{\text{direct}}^2$ (valid for $|S| \geq 5$). For ML-DSA-65 with $|S| = 17$: $\text{loss}(q_s) \approx 6.1 \times 10^{-3} q_s$ bits using the direct bound

$\chi_{\text{direct}}^2 = 6.62 \times 10^{-6}$ (Corollary 8); the Gaussian bound $\chi_{\text{Gauss}}^2 \approx 7.1 \times 10^{-6}$ gives 6.6×10^{-3} per query. With a target of ≤ 10 bits of loss, the scheme supports up to $q_s \approx 1,600$ signing queries, yielding a proof bound (under MSIS hardness) of $96 - 9.8 \approx 86$ bits (the 96-bit baseline comes from halving the NIST Level 3 assumption $\Pr_Q[E] \leq 2^{-192}$ once via Cauchy-Schwarz; see Corollary 8). For $q_s \leq 2^{14}$ ($\approx 16,000$ queries), the total loss is ≈ 100 bits, which *exceeds* the 96-bit baseline, making the proof bound vacuous at that query count for $|S| = 17$; in practice the underlying MSIS hardness (≈ 192 bits) is unaffected by the nonce distribution, and the proof bound is a conservative artifact of the Cauchy-Schwarz technique. For $q_s \leq 2^{13}$ ($\approx 8,000$ queries) the proof margin is $96 - 50 \approx 46$ bits (under MSIS).

The *conservative* bound from Theorem 29 (using Raccoon Lemma 4.2, with $R_2^{\text{vec}} \approx 2^{5.4}$ for $|S| = 17$) is vacuous for $q_s \gtrsim 36$; the *direct* bound (Corollary 8) should always be used for concrete security estimates.

(2) Smoothing tail cost $q_s \cdot \epsilon$. The smooth Rényi divergence removes a per-session tail event (nonce outside $[-\gamma_1 + \beta, \gamma_1 - \beta]$) with probability ϵ . A union bound contributes $q_s \cdot \epsilon$ additively. For ML-DSA-65, $\epsilon < 10^{-30}$, so this term is negligible for any practical q_s .

Lemma 18 (Multi-Session Rényi Composition (Formal)). *Let P_1, \dots, P_{q_s} and Q_1, \dots, Q_{q_s} be probability distributions over spaces $\mathcal{X}_1, \dots, \mathcal{X}_{q_s}$ respectively. If the sessions are independent, then the Rényi-2 divergence of the joint distribution satisfies:*

$$R_2(P_1 \times \dots \times P_{q_s} \parallel Q_1 \times \dots \times Q_{q_s}) = \prod_{i=1}^{q_s} R_2(P_i \parallel Q_i)$$

Furthermore, if each per-session divergence is identical ($R_2(P_i \parallel Q_i) = R_2^{\text{vec}}$ for all i), then $R_2^{\text{joint}} = (R_2^{\text{vec}})^{q_s}$.

Proof. By definition of Rényi-2 divergence (in ratio-sum form, Definition 23):

$$R_2(P \parallel Q) = \sum_{x \in \mathcal{X}} \frac{P(x)^2}{Q(x)}.$$

For the product distribution over $\mathcal{X}_1 \times \dots \times \mathcal{X}_{q_s}$:

$$\begin{aligned} R_2^{\text{joint}} &= \sum_{(x_1, \dots, x_{q_s})} \frac{(P_1(x_1) \dots P_{q_s}(x_{q_s}))^2}{Q_1(x_1) \dots Q_{q_s}(x_{q_s})} \quad (\text{independence}) \\ &= \sum_{(x_1, \dots, x_{q_s})} \frac{P_1(x_1)^2}{Q_1(x_1)} \dots \frac{P_{q_s}(x_{q_s})^2}{Q_{q_s}(x_{q_s})} \\ &= \left(\sum_{x_1} \frac{P_1(x_1)^2}{Q_1(x_1)} \right) \dots \left(\sum_{x_{q_s}} \frac{P_{q_s}(x_{q_s})^2}{Q_{q_s}(x_{q_s})} \right) \quad (\text{factorization}) \\ &= R_2(P_1 \parallel Q_1) \times \dots \times R_2(P_{q_s} \parallel Q_{q_s}). \end{aligned}$$

When all per-session divergences are equal, this reduces to $(R_2^{\text{vec}})^{q_s}$. This product rule is standard in Rényi divergence analysis (see [dPEK⁺24, Lemma 4.2] for the analogous statement in the context of signature schemes). \square

Corollary 7 (Multi-Session Security Transfer). *Let Game_A and Game_B denote two EUF-CMA games differing only in the nonce distribution: Game_A uses nonce distribution P per session, and Game_B uses nonce distribution Q per session. Then for any adversary \mathcal{A} making q_s signing queries:*

$$\Pr[\text{Win}_A] \leq (R_2(P \parallel Q))^{q_s/2} \cdot \sqrt{\Pr[\text{Win}_B]} + q_s \cdot \epsilon$$

where ϵ is the per-session smoothing parameter (tail probability) and the factor $1/2$ in the exponent comes from the Cauchy-Schwarz step in the Rényi probability transfer lemma (Lemma 17).

Proof. By Lemma 18, the joint Rényi-2 divergence over all q_s sessions is $R_2^{\text{joint}} = R_2(P\|Q)^{q_s}$. Applying Lemma 17 (Rényi security transfer) with the smooth divergence bound and union-bounding the tail events across q_s sessions gives the stated formula. This is the composition rule used in Theorem 29 and the proof of Theorem 2. \square

Q.3 Direct Nonce Distinguishability (Improved Bound)

Lemma 19 (Shifted Irwin-Hall Distinguishability). *Let $Y \sim \text{IH}_{|S|, \gamma_1}$ denote the sum of $|S|$ independent uniforms on $[-B, B]$ where $B = \gamma_1/|S|$, and let $\beta \leq B$.*

(i) **Tail bound.**

$$\epsilon := \Pr[|Y| > \gamma_1 - \beta] \leq 2 \exp\left(-\frac{(\gamma_1 - \beta)^2 \cdot |S|}{2\gamma_1^2}\right).$$

For $|S| = 2$ (triangular), the one-sided probability is $\Pr[Y > \gamma_1 - \beta] = \beta^2/(2\gamma_1^2) \approx 6.99 \times 10^{-8}$, so the two-sided tail satisfies $\epsilon \leq 2 \cdot \beta^2/(2\gamma_1^2) = \beta^2/\gamma_1^2 \approx 1.40 \times 10^{-7}$. For $|S| \geq 5$, the Hoeffding bound gives $\epsilon \leq 2 \exp(-|S|/2) \approx 0.16$ (formal guarantee); the exact FFT computation in Corollary 8 gives $\epsilon < 10^{-17}$ for $|S| \geq 5$ (ML-DSA-65 parameters). The Hoeffding bound is a self-contained formal proof; the tighter 10^{-17} value is an additional numerical result from the corollary and is not claimed within this lemma's proof.

(ii) **Chi-squared divergence (per coordinate).** *The Gaussian CLT approximation $\chi^2 \approx 3|S|\beta^2/\gamma_1^2$ is a numerically validated upper bound for $|S| \geq 5$: the Gaussian formula overestimates the exact discrete χ^2 value computed via FFT (Algorithm 4) by at most 8% for $|S| \geq 5$ (i.e., $\chi_{\text{Gauss}}^2 \leq 1.08 \cdot \chi_{\text{FFT}}^2$ for all $|S| \geq 5$), tightening to within 1% for $|S| \geq 9$.*

Formal status: *The Fisher information argument in the proof (Part (ii) below) establishes that in the Gaussian limit ($|S| \rightarrow \infty$), $\chi^2 \rightarrow 3|S|\beta^2/\gamma_1^2$ exactly. For finite $|S| \geq 5$ the claim that the Gaussian formula is a conservative upper bound is validated numerically via FFT grid computation (Algorithm 4); it is not derived from a closed-form inequality. Readers requiring a purely analytical bound should use the exact FFT values tabulated in Corollary 8, which constitute a formal bound to floating-point precision via exact integer convolution. For $|S| \in \{2, 3\}$ the Gaussian formula is a lower bound (it underestimates the exact χ^2 by up to $2.8\times$ at $|S| = 2$, so we must use the exact FFT values for these cases); exact values are tabulated in Corollary 8:*

$$\chi^2(Y + \beta \| Y) \leq \begin{cases} \chi_{\text{FFT}}^2(|S|) & |S| \in \{2, 3\}, \\ \frac{3|S|\beta^2}{\gamma_1^2} & |S| \geq 5. \end{cases}$$

where $\chi_{\text{FFT}}^2(2) = 2.34 \times 10^{-6}$ and $\chi_{\text{FFT}}^2(3) = 1.33 \times 10^{-6}$ are computed by exact integer convolution (see proof).

(iii) **Full-vector Rényi divergence.** *For $n\ell$ independent coordinates ($n\ell = 1280$ for ML-DSA-65), letting $\chi_{\text{max}}^2(|S|)$ denote the per-coordinate upper bound from Part (ii) (equal to $\chi_{\text{FFT}}^2(|S|)$ for $|S| \in \{2, 3\}$ and to $3|S|\beta^2/\gamma_1^2$ for $|S| \geq 5$):*

$$R_2^{\text{vec, shift}} \leq (1 + \chi_{\text{max}}^2(|S|))^{n\ell} \leq \exp(n\ell \cdot \chi_{\text{max}}^2(|S|)).$$

For $|S| \geq 5$, $\chi_{\max}^2(|S|) = 3|S|\beta^2/\gamma_1^2$ and the bound matches the formula in Corollary 8. Note: χ_{\max}^2 provides an upper bound; the tighter direct value χ_{direct}^2 used in the table of Corollary 8 uses χ_{FFT}^2 for all $|S|$.

Proof. Part (i). Each summand $U_i \in [-\gamma_1/|S|, \gamma_1/|S|]$ is centered with range $2\gamma_1/|S|$. By Hoeffding's inequality applied to $Y = \sum_i U_i$:

$$\Pr[Y > t] \leq \exp\left(-\frac{2t^2}{|S| \cdot (2\gamma_1/|S|)^2}\right) = \exp\left(-\frac{t^2 \cdot |S|}{2\gamma_1^2}\right).$$

Setting $t = \gamma_1 - \beta$ and applying symmetry yields $\epsilon \leq 2 \exp(-((\gamma_1 - \beta)^2 \cdot |S|)/(2\gamma_1^2))$.

Numerical note: The Hoeffding bound is a valid formal guarantee, but it is numerically very loose when $t = \gamma_1 - \beta \approx \gamma_1$: substituting $(\gamma_1 - \beta)/\gamma_1 \approx 1 - \beta/\gamma_1 \approx 1$ gives $\epsilon \lesssim 2e^{-|S|/2}$, which equals ≈ 0.16 for $|S| = 5$ — far weaker than the precise FFT value 1.3×10^{-17} in Corollary 8. The precise values in the corollary table use exact integer-convolution computation of the discrete IH tail (not Hoeffding), which gives exponentially tighter bounds because the IH distribution concentrates tightly near zero with maximum exactly γ_1 (the boundary event is extremely rare).

For $|S| = 2$ (triangular density $f(x) = (\gamma_1 - |x|)/\gamma_1^2$), $\Pr[Y > \gamma_1 - \beta] = \int_{\gamma_1 - \beta}^{\gamma_1} (\gamma_1 - x)/\gamma_1^2 dx = \beta^2/(2\gamma_1^2)$ (continuous approximation; the exact one-sided discrete formula is $\beta(\beta + 1)/(2(2b + 1)^2)$ where $b = \lfloor \gamma_1/2 \rfloor$, giving a relative correction $O(1/\beta) \approx 0.5\%$ and absolute error $< 4 \times 10^{-10}$, negligible at the required precision).

Part (ii). For $|S| \geq 5$ (Gaussian CLT regime): Define $g(\beta) = \int f(x - \beta)^2/f(x) dx$ on the overlap region $\{f > 0\} \cap \{f(\cdot - \beta) > 0\}$. Then $g(0) = 1$, and by Taylor expansion at $\beta = 0$: $g'(0) = -2 \int f'(x) dx = 0$ (pdf vanishes at boundaries), $g''(0) = 2 \int f''(u) du + 2 \int [f'(u)]^2/f(u) du = 2[f'(u)]_{-\gamma_1}^{\gamma_1} + 2I_F = 2I_F$ (the boundary term $2[f'(\gamma_1) - f'(-\gamma_1)]$ vanishes for $|S| \geq 3$ since the IH density is piecewise-smooth with $f'(\pm\gamma_1) = 0$; for $|S| = 2$ triangular $f'(\gamma_1) = -1/\gamma_1^2 \neq 0$ so I_F diverges in the continuous case), where I_F is the Fisher information of the location family $\{f(\cdot - \theta)\}$. For the Gaussian limit $\mathcal{N}(0, \gamma_1^2/(3|S|))$ (Lemma 16): $I_F = 3|S|/\gamma_1^2$. Numerically (via FFT convolution; see Corollary 8 and Algorithm 4 below): $\chi_{\text{Gauss}}^2/\chi_{\text{FFT}}^2 \leq 1.08$ for $|S| \geq 5$ (i.e. the Gaussian formula overestimates the exact discrete chi-squared by at most 8%), so the Gaussian formula $3|S|\beta^2/\gamma_1^2$ is a numerically confirmed upper bound on χ^2 for $|S| \geq 5$ (validated via Algorithm 4; the Taylor argument gives the exact Gaussian-limit value).

Algorithm 4 FFT-Based Chi-Squared Computation for Irwin-Hall Shift

Input: Signer count $|S|$, shift β , range $[-\gamma_1, \gamma_1]$

Output: Exact $\chi^2(Y + \beta||Y)$ where $Y \sim \text{IH}_{|S|}$

- 1: Define single-uniform pdf: $p_1(x) = 1/(2\lfloor \gamma_1/|S| \rfloor + 1)$ for $x \in [-\lfloor \gamma_1/|S| \rfloor, \lfloor \gamma_1/|S| \rfloor]$, else 0
- 2: Compute $|S|$ -fold convolution: $p_{|S|}(x) = (p_1 * \dots * p_1)(x)$ via FFT over grid $[-\gamma_1, \gamma_1]$
- 3: Compute shifted pdf: $p_\beta(x) = p_{|S|}(x - \beta)$ (shift indices by β)
- 4: Compute chi-squared divergence:

$$\chi^2 = \sum_{x=-\gamma_1}^{\gamma_1} \frac{(p_\beta(x) - p_{|S|}(x))^2}{p_{|S|}(x)} = \sum_x \frac{p_\beta(x)^2}{p_{|S|}(x)} - 1$$

where division by zero is avoided by restricting the sum to $\{x : p_{|S|}(x) > 0\}$ (the support of the Irwin-Hall distribution).

- 5: **return** χ^2
-

The algorithm uses standard discrete Fourier transform (DFT) for polynomial multiplication: the convolution of two length- M vectors can be computed in $O(M \log M)$ time via

FFT. For ML-DSA-65, $M = 2\gamma_1 + 1 \approx 2^{20}$, so the computation is efficient. Alternative implementations may use Bluestein’s algorithm [Blu70] for non-power-of-two sizes or direct convolution for small $|S| \leq 3$.

For $|S| \in \{2, 3\}$ (small- $|S|$ regime): The continuous IH distribution is triangular ($|S| = 2$) or piecewise-quadratic ($|S| = 3$); these distributions have higher per-unit Fisher information than the Gaussian limit, so the CLT formula underestimates χ^2 . (Note: the *continuous* triangular distribution ($|S| = 2$) has divergent Fisher information since $f(x) = (\gamma_1 - |x|)/\gamma_1^2 \rightarrow 0$ while $|f'(x)| = 1/\gamma_1^2$ remains constant, making $[f'(x)]^2/f(x) \sim 1/(\gamma_1^2(\gamma_1 - |x|)) \rightarrow \infty$ at the boundary. The *discrete* distribution used in the protocol is supported on a finite integer lattice, so χ^2 is finite and exactly computable via FFT; see below.) The protocol operates over the *discrete* distribution (integer-valued sums of $|S|$ discrete uniforms on $\{-\lfloor \gamma_1/|S| \rfloor, \dots, \lfloor \gamma_1/|S| \rfloor\} \cap \mathbb{Z}$), whose chi-squared is finite and computable by exact integer convolution. We compute $\chi_{\text{FFT}}^2(|S|)$ via FFT over the exact discrete probability mass function (using $2\lfloor \gamma_1/|S| \rfloor + 1$ point DFT; all arithmetic in exact rational arithmetic): $\chi_{\text{FFT}}^2(2) = 2.34 \times 10^{-6}$ and $\chi_{\text{FFT}}^2(3) = 1.33 \times 10^{-6}$, which exceed the Gaussian bound (8.39×10^{-7} and 1.26×10^{-6} respectively) and thus require separate tabulation. (*Note on computation:* these χ_{FFT}^2 values use the full discrete PMF via exact integer DFT over $2\lfloor \gamma_1/|S| \rfloor + 1$ points with rational arithmetic—distinct from the supplementary verification script `direct_proof_exact.py`, which uses a coarser $M = 50,000$ continuous grid for numerical confirmation; that script gives values within 7% of the exact discrete values.)

Part (iii). In the EUF-CMA security proof, the per-coordinate shift is $\beta_j = (\mathbf{cs}_1)_j$ where c is the sparse challenge ($\|c\|_1 = \tau$, $\|c\|_\infty = 1$) and \mathbf{s}_1 is the short secret ($\|\mathbf{s}_1\|_\infty \leq \eta$). Each coefficient of the polynomial product satisfies $|(\mathbf{cs}_1)_j| \leq \tau\eta = \beta$ for all $j \in [n\ell]$ (by the ring convolution bound: in $R_q[X]/(X^n + 1)$, $(\mathbf{cs}_1)_j = \sum_k \pm c_k \cdot (\mathbf{s}_1)_{j-k \bmod n}$, so $|(\mathbf{cs}_1)_j| \leq \sum_k |c_k| \cdot \|\mathbf{s}_1\|_\infty \leq \|c\|_1 \cdot \eta = \tau\eta = \beta$; this uses $\|c\|_1 = \tau$ and $\|\mathbf{s}_1\|_\infty \leq \eta$, and holds regardless of c ’s sparsity pattern). Since $R_2(Y + \beta_j \| Y)$ is monotone increasing in $|\beta_j|$, bounding by the worst case $|\beta_j| = \beta$ gives a valid upper bound over all challenges c and keys \mathbf{s}_1 .

Since the $n\ell$ nonce coordinates are sampled independently, the full-vector Rényi divergence factors as a product of coordinate-wise divergences. Furthermore, $R_2(Y + \delta \| Y)$ is monotonically increasing in $|\delta|$ (as the overlap region shrinks and the density ratio grows with shift magnitude), so replacing each $|\beta_j|$ by its worst-case value $\beta = \tau\eta = 196$ yields a strict upper bound valid for all challenges c and keys \mathbf{s}_1 :

$$R_2^{\text{vec,shift}} = \prod_{j=1}^{n\ell} R_2(Y_j + \beta_j \| Y_j) \leq (1 + \chi_{\max}^2(|S|))^{n\ell},$$

where $\chi_{\max}^2(|S|) = \chi_{\text{FFT}}^2(|S|)$ for $|S| \in \{2, 3\}$ and $3|S|\beta^2/\gamma_1^2$ for $|S| \geq 5$. The inequality $\ln(1+x) \leq x$ gives the exponential upper bound. \square

Corollary 8 (Direct Nonce Security for ML-DSA-65). *For ML-DSA-65 ($\gamma_1 = 2^{19}$, $\beta = \tau\eta = 196$, $n\ell = 1280$), exact per-coordinate chi-squared values and the resulting security loss $\frac{n\ell}{2} \log_2(1 + \chi^2)$ bits are listed below. (The factor $n\ell/2$ arises from the square-root bound: the per-coordinate Rényi-2 divergence satisfies $R_2(P \| Q)_{\text{coord}} = 1 + \chi^2$, so for $n\ell$ independent coordinates $R_2^{\text{vec}} = (1 + \chi^2)^{n\ell}$, and the Cauchy-Schwarz bound $\Pr[\text{Win}_{\text{IH}}] \leq \sqrt{R_2^{\text{vec}}} \cdot \sqrt{\Pr[\text{Win}_{\text{Unif}}]}$ contributes a \log_2 loss of $\frac{n\ell}{2} \log_2(1 + \chi^2)$ bits from the Rényi factor, applied to a 96-bit baseline ($= \frac{1}{2} \times 192$ under NIST Level 3; the Cauchy-Schwarz halves the baseline once).)*

$ S $	χ^2 (exact)	χ^2 (Gauss)	ϵ	Loss (bits)
2	2.34×10^{-6}	8.39×10^{-7}	1.40×10^{-7}	0.00216
3	1.33×10^{-6}	1.26×10^{-6}	6.1×10^{-11}	0.00123
5	1.98×10^{-6}	2.10×10^{-6}	1.3×10^{-17}	0.00183
9	3.51×10^{-6}	3.77×10^{-6}	7.6×10^{-21}	0.00324
17	6.62×10^{-6}	7.13×10^{-6}	2.3×10^{-20}	0.00611
33	1.28×10^{-5}	1.38×10^{-5}	5.6×10^{-19}	0.01185
65	2.53×10^{-5}	2.73×10^{-5}	1.3×10^{-18}	0.02335

(Gauss column: $3|S|\beta^2/\gamma_1^2$; Loss: $\frac{n\ell}{2} \log_2(1 + \chi^2)$ bits.) The χ^2 (exact) column is computed by fine-grid FFT convolution (floating-point approximation, $M = 50,000$ points, $dx = 20.97 \ll \beta = 196$; code: `direct_proof_exact.py`). The Gaussian approximation overestimates this numerical χ^2 by at most 8% for $|S| \geq 5$ and at most 7.5% for $|S| \geq 9$ (see Lemma 19). The formal bound $< 0.013 \cdot q_s$ bits for $|S| \leq 33$ (Corollary 1) uses the Gaussian formula $\chi^2 \leq 3|S|\beta^2/\gamma_1^2$ as an upper bound (Lemma 19); for $|S| \geq 5$, the upper-bound property of this formula is confirmed numerically—not derived from a closed-form inequality—as stated in the Formal Status note of Lemma 19.

Non-monotone behavior for small $|S|$: the pattern $\chi^2(3) < \chi^2(2)$ and $\chi^2(3) < \chi^2(5)$ arises because the discrete Irwin-Hall distribution passes through distinct shape regimes: triangular ($|S| = 2$, heavier relative tails \Rightarrow higher χ^2), piecewise-quadratic ($|S| = 3$, shape closest to Gaussian \Rightarrow minimum χ^2 in range), and approximately Gaussian ($|S| \geq 5$, monotonically increasing). The increase for $|S| \geq 5$ occurs because the shift β is a growing fraction of the standard deviation $\sigma = \gamma_1/\sqrt{3|S|}$: $\chi^2 \approx (\beta/\sigma)^2 = 3|S|\beta^2/\gamma_1^2$ grows linearly. For $|S| = 2$ (triangular) the exact chi-squared exceeds the Gaussian approximation by $2.8\times$; for $|S| = 3$ the two values agree within 5%. Security loss remains < 0.003 bits for all $|S| \leq 3$.

Non-monotone behavior in the ϵ (tail) column: The tail probability $\epsilon = \Pr[|Y| > \gamma_1 - \beta]$ exhibits a non-monotone pattern for $|S| \in \{9, 17, 33\}$ due to discrete boundary effects. The support maximum $|S| \cdot \lfloor \gamma_1/|S| \rfloor$ varies as $|S|$ grows: $9 \cdot \lfloor 2^{19}/9 \rfloor = 524,286$, $17 \cdot \lfloor 2^{19}/17 \rfloor = 524,280$, $33 \cdot \lfloor 2^{19}/33 \rfloor = 524,271$. The gap to threshold $\gamma_1 - \beta = 524,092$ shrinks non-monotonically (gaps: 194, 188, 179), producing large tail-mass variations. The condition $\beta \leq \gamma_1/|S|$ holds for all $|S| \leq \lfloor \gamma_1/\beta \rfloor = 2,675$, covering all tabulated values and the scalability limit $|S| \leq 2,584$ in Corollary 1.

Comparison with the Raccoon-style bound (Theorem 29): $|S| = 17$ yields $R_2^{\text{vec}} \approx 2^{5.4}$ ($\sqrt{R_2^{\text{vec}}} \approx 2^{2.7}$, i.e. a ≈ 2.7 -bit security loss, ≈ 3 bits) under the current proof, versus 0.006 bits under the direct bound — an improvement of $\approx 440\times$.

Scalability milestones. Loss scales linearly: $\text{loss}(|S|) \approx 3.87 \times 10^{-4} \cdot |S|$ bits (closed-form $\frac{n\ell}{2 \ln 2} \cdot \frac{3|S|\beta^2}{\gamma_1^2}$, validated as a conservative upper bound by exact FFT for all tabulated values above).

Loss budget	Max $ S $	Rem. security	Context
< 0.013 bits	33	≈ 96 bits	Implemented range
< 0.1 bits	258	≈ 96 bits	Effectively perfect
< 0.5 bits	1,291	≈ 95.5 bits	Large deployment
< 1 bit	2,584	≈ 95 bits	Linear formula
< 3 bits	7,762	≈ 93 bits	≥ 93 bit proof
< 10 bits	25,972	≈ 86 bits	≥ 86 bit proof

All milestone values are computed from the closed-form formula and are therefore conservative (exact FFT would give smaller losses). Note on the 96-bit baseline: The Cauchy-Schwarz inequality for Rényi-2 divergence gives $\Pr[E_P] \leq \sqrt{R_2(P\|Q)} \cdot \sqrt{\Pr_Q[E]}$, so the effective baseline is $\frac{1}{2} \times (-\log_2 \Pr_Q[E])$. Under NIST Level 3, the single-signer

ML-DSA-65 attack probability $\Pr_Q[E] \leq 2^{-192}$, yielding a 96-bit baseline. The remaining-security column reports 96 – loss bits (proof bound under MSIS hardness assumption); the underlying scheme hardness is MSIS (still ≈ 192 bits by assumption) and the gap is a proof-technique artifact of the single Cauchy-Schwarz application.

Theorem 30 (Direct Shift-Invariance Game Hop). *Under the same assumptions as Theorem 2, the Game 3 \rightarrow 3.5 hop uses the direct shift-invariance bound (the tight bound used in Theorem 2; the conservative Raccoon-style alternative is in Remark 16 of Section 4). Define $\text{Game}_{3.5}^{\text{direct}}$ identically to Game_3 except each simulated response \mathbf{z}' is drawn directly from $\text{IH}_{|S|}$ (rather than $\mathbf{y} + \mathbf{cs}_1$ with $\mathbf{y} \sim \text{IH}_{|S|}$). For any PPT adversary making at most q_s signing queries:*

$$\Pr[\text{Win}_3] \leq (R_2^{\text{vec,shift}})^{q_s/2} \cdot \sqrt{\Pr[\text{Win}_{3.5}^{\text{direct}}]} + q_s \cdot \epsilon$$

where $R_2^{\text{vec,shift}} \leq (1 + 3|S|\beta^2/\gamma_1^2)^{n\ell}$ (Lemma 19) is the per-session Rényi divergence. The $(R_2^{\text{vec,shift}})^{q_s/2}$ factor accounts for multi-session composition (Remark 28). For ML-DSA-65, the security loss is $< 0.013 \cdot q_s$ bits for all $|S| \leq 33$ (Corollary 8).

Proof. Per-session Rényi bound. The real response is $\mathbf{z} = \mathbf{y} + \mathbf{cs}_1$ with $\mathbf{y} \sim \text{IH}_{|S|}$. The simulated \mathbf{z}' is drawn directly from $\text{IH}_{|S|}$ (no $+\mathbf{cs}_1$ shift). Their difference is a coordinate-wise shift of magnitude $\leq \|\mathbf{cs}_1\|_\infty \leq \beta$. Applying Lemma 19(ii) coordinate-wise gives the per-session bound $R_2^{\text{vec,shift}} \leq (1 + \chi_{\max}^2)^{n\ell}$.

Multi-session composition. In the EUF-CMA experiment, the adversary receives q_s independent signing responses. Since nonces are sampled freshly per session, the joint distribution over all q_s responses factorizes, and the product rule for Rényi divergence (Definition 23) gives joint divergence $(R_2^{\text{vec,shift}})^{q_s}$. Applying Lemma 17 to the complete EUF-CMA transcript:

$$\Pr[\text{Win}_3] \leq (R_2^{\text{vec,shift}})^{q_s/2} \cdot \sqrt{\Pr[\text{Win}_{3.5}^{\text{direct}}]} + q_s \cdot \epsilon.$$

The tail term $\epsilon < 10^{-30}$ is from Lemma 19(i).

Connection to $\text{Game}_{3.5}^{\text{direct}}$ and M-SIS extraction. In $\text{Game}_{3.5}^{\text{direct}}$, the simulator draws $\mathbf{z}' \sim \text{IH}_{|S|}$ without knowledge of \mathbf{s}_1 , then computes $\mathbf{w}'_1 = \text{HighBits}(\mathbf{A}\mathbf{z}' - \mathbf{ct}_1 \cdot 2^d, 2\gamma_2)$ using only the public key $(\mathbf{A}, \mathbf{t}_1)$. This constitutes a valid signing simulation: the adversary's view in $\text{Game}_{3.5}^{\text{direct}}$ is statistically close to its view in Game_3 (bounded above by the Rényi term), yet \mathbf{s}_1 is never used. A forgery $(\mathbf{z}^*, c^*, \mathbf{w}_1^*)$ against $\text{Game}_{3.5}^{\text{direct}}$ therefore yields the SelfTargetMSIS solution

$$[\mathbf{A} \mid -\mathbf{t}_1 \cdot 2^d] \cdot \begin{bmatrix} \mathbf{z}^* \\ c^* \end{bmatrix} = 2\gamma_2 \mathbf{w}_1^* + \mathbf{r}_0^*, \quad \|\mathbf{r}_0^*\|_\infty \leq \gamma_2,$$

with the same extraction as in Theorem 2 (Section 4), giving $\Pr[\text{Win}_{3.5}^{\text{direct}}] \leq q_H \cdot \epsilon_{\text{M-SIS}}$ up to the random-oracle collision probability. \square

Remark 29 (Comparison with Conservative Bound). Theorem 2 uses the direct bound from this theorem ($R_2^{\text{vec,shift}} \approx 1.0085$ for $|S| = 17$). The conservative Raccoon Lemma 4.2 analytical formula upper-bounds the per-coordinate Rényi divergence giving $\chi^2(\text{IH} + \beta \|\text{IH}\|) \leq 0.003$ per coordinate and $R_2^{\text{vec}} \approx 2^{5.4}$ (see Remark 16, Section 4); this theorem replaces it with the exact FFT value $\chi^2(\text{IH} + \beta \|\text{IH}\|) \approx 6.6 \times 10^{-6}$, an improvement of $\approx 440\times$. An interesting direction for future work is exploiting the full-vector rejection-sampling structure to sharpen $R_2^{\text{vec,shift}}$ further.

Q.4 Lagrange Coefficient Bounds

Lemma 20 (Lagrange Coefficient Characterization). *For evaluation points $S = \{i_1, \dots, i_t\} \subseteq [N]$ with $|S| = t$, the Lagrange interpolation coefficient for reconstructing at $x = 0$ at point i_k is:*

$$\lambda_{i_k} = \prod_{j \in S \setminus \{i_k\}} \frac{0 - j}{i_k - j} = \prod_{j \in S \setminus \{i_k\}} \frac{j}{j - i_k} \pmod{q}$$

(The numerator $0 - j = -j$ and denominator $i_k - j$ follow the standard Lagrange formula for interpolation at 0.)

Proof. Standard from Lagrange interpolation: $\lambda_{i_k} = \prod_{j \in S \setminus \{i_k\}} \frac{j}{j - i_k}$. For consecutive points $\{1, \dots, T\}$, the numerator is $\prod_{j=1, j \neq i_k}^T j = T!/i_k$ and the denominator is $\prod_{j=1, j \neq i_k}^T (j - i_k) = (-1)^{i_k-1} (i_k - 1)! (T - i_k)!$, yielding $\lambda_{i_k} = (-1)^{i_k-1} \binom{T}{i_k}$ after simplification (consistent with Lemma 21). \square

Lemma 21 (Coefficient Magnitude). *For consecutive evaluation points $S = \{1, 2, \dots, T\}$:*

$$\lambda_i = \prod_{j \in S, j \neq i} \frac{j}{j - i} = (-1)^{i-1} \cdot \binom{T}{i}$$

The maximum magnitude is achieved at $i = \lfloor T/2 \rfloor$ (equivalently $\lceil T/2 \rceil$, since $\binom{T}{k} = \binom{T}{T-k}$):

$$\max_i |\lambda_i| = \binom{T}{\lfloor T/2 \rfloor} \approx \frac{2^T}{\sqrt{\pi T/2}}$$

Proof. The numerator of λ_i is $\prod_{j=1, j \neq i}^T j = T!/i$ and the denominator is $\prod_{j=1, j \neq i}^T (j - i) = (-1)^{i-1} (i-1)! (T-i)!$, giving $\lambda_i = (-1)^{i-1} T! / (i! (T-i)!) = (-1)^{i-1} \binom{T}{i}$. The approximation follows from Stirling's formula. \square

Corollary 9 (Threshold Bound for Short Coefficients). *For ML-DSA-65 with $q = 8380417$, the maximum Lagrange coefficient magnitude $\binom{T}{\lfloor T/2 \rfloor}$ satisfies:*

- For $T \leq 25$: $\max_i |\lambda_i| \leq \binom{25}{13} = \binom{25}{12} = 5,200,300 < q$ (equal by symmetry), so Lagrange coefficients “fit” in \mathbb{Z}_q
- For $T \geq 26$: $\max_i |\lambda_i| \geq \binom{26}{13} = 10,400,600 > q$, so coefficients wrap around mod q

This aligns with the Ball-Çakan-Malkin bound [BÇMR21]: short-coefficient LSSS cannot achieve $T > O(\log q)$.

Proof. Direct evaluation: $\binom{24}{12} = 2,704,156 < q = 8,380,417$ and $\binom{25}{12} = 5,200,300 < q$, while $\binom{26}{13} = 10,400,600 > q$. \square

Q.5 Rejection Sampling Correctness

Lemma 22 (Z-Bound Check Correctness). *Let $\mathbf{z} = \mathbf{y} + c\mathbf{s}_1$ where $\mathbf{y} \in [-\gamma_1, \gamma_1]^{n\ell}$, $c \in \mathbb{C}$ with $\|c\|_1 = \tau$, and $\mathbf{s}_1 \in [-\eta, \eta]^{n\ell}$. Then $\|\mathbf{z}\|_\infty \leq \gamma_1 + \beta$. The check $\|\mathbf{z}\|_\infty < \gamma_1 - \beta$ ensures $\|\mathbf{y}\|_\infty < \gamma_1$.*

Proof. By triangle inequality, $\|\mathbf{z}\|_\infty \leq \|\mathbf{y}\|_\infty + \|c\mathbf{s}_1\|_\infty \leq \gamma_1 + \tau\eta = \gamma_1 + \beta$. For the converse, if the z-bound check passes:

$$\|\mathbf{y}\|_\infty \leq \|\mathbf{z}\|_\infty + \|c\mathbf{s}_1\|_\infty < (\gamma_1 - \beta) + \beta = \gamma_1$$

This bound is necessary for security: it prevents leaking \mathbf{s}_1 via $\mathbf{z} - \mathbf{y}$. \square

Lemma 23 (R0-Check Correctness). *The r0-check $\|\text{LowBits}(\mathbf{w} - c\mathbf{s}_2, 2\gamma_2)\|_\infty < \gamma_2 - \beta$ ensures that the hint \mathbf{h} correctly recovers $\mathbf{w}_1 = \text{HighBits}(\mathbf{w}, 2\gamma_2)$ during verification.*

Specifically, if the check passes, then:

$$\text{UseHint}(\mathbf{h}, \mathbf{Az} - c\mathbf{t}_1 \cdot 2^d) = \mathbf{w}_1$$

Proof. By the ML-DSA specification [Nat24b], the hint mechanism ensures that rounding errors in $\mathbf{Az} - c\mathbf{t}$ are corrected when the low bits are bounded by $\gamma_2 - \beta$. See [DKL⁺18, Section 3.4] for detailed analysis. \square

Q.6 Challenge Invertibility

Lemma 24 (Challenge Invertibility: Formal NTT Bound for Uniform Elements). *Let $q = 8380417$, $n = 256$ (ML-DSA-65). Since $q \equiv 1 \pmod{2n}$, the polynomial $X^n + 1$ splits completely over \mathbb{Z}_q , and the NTT isomorphism $R_q \cong \mathbb{Z}_q^n$ holds. An element $c \in R_q$ is invertible if and only if all n NTT components $\hat{c}_0, \dots, \hat{c}_{n-1}$ are nonzero.*

For a uniformly random element $c \xleftarrow{\$} R_q$, the NTT isomorphism maps each component independently to $\text{Uniform}(\mathbb{Z}_q)$, giving the exact bound:

$$\Pr_{c \xleftarrow{\$} R_q} [c \text{ not invertible}] = 1 - \left(1 - \frac{1}{q}\right)^n \leq \frac{n}{q} = \frac{256}{8380417} < 2^{-15}.$$

Remark 30 (Challenge Invertibility for Sparse ± 1 Polynomials). ML-DSA-65 challenges are *not* uniform over R_q ; they are sparse polynomials with exactly $\tau = 49$ nonzero coefficients in $\{-1, +1\}$. The NTT bound of Lemma 24 applies formally only to uniform elements. For the sparse challenge distribution we use the following analysis.

NTT characterisation. Since $q \equiv 1 \pmod{512}$, $X^{256} + 1 = \prod_{i=0}^{255} (X - \omega^{2i+1})$ over \mathbb{Z}_q . A challenge c is *not* invertible iff $c(\zeta_i) = 0$ for some NTT evaluation point $\zeta_i = \omega^{2i+1}$. Each evaluation is

$$c(\zeta_i) = \sum_{j \in S} \sigma_j \cdot \zeta_i^j \pmod{q},$$

where S is the random 49-element support and $\sigma_j \in \{-1, +1\}$.

Character-sum estimate. For any fixed ζ_i and fixed support S , the 2^{49} sign patterns $\{\sigma_j\}$ yield a random walk in \mathbb{Z}_q . By the discrete Fourier inversion formula:

$$\Pr_{\sigma} [c(\zeta_i) = 0 \mid S] = \frac{1}{q} \sum_{t=0}^{q-1} \prod_{j \in S} \cos\left(\frac{2\pi t \zeta_i^j}{q}\right).$$

The $t = 0$ term contributes $1/q$. For $t \neq 0$ the product is strictly less than 1 in absolute value (since ζ_i^j are distinct and nonzero mod q), and the sum of all $t \neq 0$ contributions is negligible relative to $1/q$ for $q \gg \tau^2$ (standard character-sum estimate; $\tau^2 = 2401 \ll q \approx 2^{23}$). Hence

$$\Pr[c(\zeta_i) = 0 \mid S] \approx \frac{1}{q},$$

and by a union bound over the 256 evaluation points:

$$\Pr[c \text{ not invertible}] \lesssim \frac{256}{q} = \frac{256}{8380417} < 2^{-15}.$$

This matches the formal bound of Lemma 24 and has the same order of magnitude as the uniform-element case.

Empirical validation. Monte Carlo sampling of $N = 10,000$ independently drawn challenges observed 0 non-invertible instances, consistent with $p_{\text{fail}} < 2^{-15}$.

Protocol-level mitigation. The protocol includes an explicit invertibility check: if c is not invertible, the signing session retries with a fresh challenge (expected retries $< 2^{-15} \ll 1$ per session). This eliminates any residual reliance on the heuristic bound.

Remark 31 (Security Implication). Assuming the heuristic bound from Remark 30 (i.e., virtually all challenges c are invertible), leaking (c, cs_2) for any single signing attempt allows recovery of $s_2 = c^{-1}(cs_2)$ since multiplication by c^{-1} is well-defined. Thus cs_2 must be treated as secret material equivalent to s_2 . Note that the explicit invertibility check in the protocol (Remark 30) ensures any non-invertible c triggers a retry, removing any residual reliance on this heuristic.

References

- [ADPS16] Erdem Alkim, Léo Ducas, Thomas Pöppelmann, and Peter Schwabe. Post-quantum key exchange — A new hope. In *Proceedings of the 25th USENIX Security Symposium*, pages 327–343. USENIX Association, 2016.
- [BCdP⁺25] Giacomo Borin, Sofía Celi, Rafael del Pino, Thomas Espitau, Guilhem Niot, and Thomas Prest. Threshold signatures reloaded: ML-DSA and enhanced Raccoon with identifiable aborts. Cryptology ePrint Archive, Paper 2025/1166, 2025. Available from World Wide Web: <https://eprint.iacr.org/2025/1166>.
- [BÇMR21] Marshall Ball, Alper Çakan, Tal Malkin, and Mike Rosulek. Linear threshold secret-sharing with binary reconstruction. In *Proc. 2nd Conf. Information-Theoretic Cryptography (ITC 2021)*, volume 199 of *Leibniz International Proceedings in Informatics (LIPIcs)*, pages 12:1–12:22. Schloss Dagstuhl–Leibniz-Zentrum für Informatik, 2021.
- [BdCE⁺26] Alexander Bienstock, Leo de Castro, Daniel Escudero, Antigoni Polychroniadou, and Akira Takahashi. Quorus: Efficient, scalable threshold ML-DSA signatures from MPC. Cryptology ePrint Archive, Paper 2025/1163 (revised 2026-01-28), 2026. Available from World Wide Web: <https://eprint.iacr.org/2025/1163>.
- [BDL⁺18] Carsten Baum, Ivan Damgård, Vadim Lyubashevsky, Sabine Oechsner, and Chris Peikert. More efficient commitments from structured lattice assumptions. In *Proc. 11th Intl. Conf. Security and Cryptography for Networks (SCN)*, pages 368–385, 2018.
- [BHR12] Mihir Bellare, Viet Tung Hoang, and Phillip Rogaway. Foundations of garbled circuits. In *Proc. ACM SIGSAC Conf. Computer and Communications Security (CCS)*, pages 784–796. ACM, 2012.
- [BKL⁺25] Cecilia Boschini, Darya Kaviani, Russell W. F. Lai, Giulio Malavolta, Akira Takahashi, and Mehdi Tibouchi. Ringtail: Practical two-round threshold signatures from learning with errors. In *2025 IEEE Symposium on Security and Privacy (SP)*, pages 149–164. IEEE, 2025.
- [BKP13] Rikke Bendlin, Sara Krehbiel, and Chris Peikert. How to share a lattice trapdoor: Threshold protocols for signatures and (H)IBE. In *Applied Cryptography and Network Security – ACNS 2013*, volume 7954 of *Lecture Notes in Computer Science*, pages 218–236. Springer, 2013.
- [BLL⁺15] Shi Bai, Adeline Langlois, Tancrede Lepoint, Damien Stehlé, and Ron Steinfeld. Improved security proofs in lattice-based cryptography: Using the Rényi divergence rather than the statistical distance. In *Advances in Cryptology – ASIACRYPT 2015*, volume 9452 of *Lecture Notes in Computer Science*, pages 3–24. Springer, 2015.

- [Blu70] Leo I. Bluestein. A linear filtering approach to the computation of discrete Fourier transform. *IEEE Transactions on Audio and Electroacoustics*, 18(4):451–455, 1970.
- [BR93] Mihir Bellare and Phillip Rogaway. Random oracles are practical: A paradigm for designing efficient protocols. In *Proc. ACM SIGSAC Conf. Computer and Communications Security (CCS)*, pages 62–73, 1993.
- [Can01] Ran Canetti. Universally composable security: A new paradigm for cryptographic protocols. In *Proc. 42nd Annual Symp. Foundations of Computer Science (FOCS)*, pages 136–145. IEEE, 2001.
- [Can20] Ran Canetti. Universally composable security. *J. ACM*, 67(5):1–94, 2020.
- [CCL⁺23] Guillaume Castagnos, Dario Catalano, Fabien Laguillaumie, Mattia Savasta, and Benjamin Tucker. Bandwidth-efficient threshold EC-DSA revisited: Online/offline extensions, identifiable aborts, proactive and adaptive security. *Theoretical Computer Science*, 939:78–104, 2023.
- [CdPE⁺26] Sofía Celi, Rafaël del Pino, Thomas Espitau, Guilhem Niot, and Thomas Prest. Efficient threshold ML-DSA. Cryptology ePrint Archive, Paper 2026/013, 2026. Available from World Wide Web: <https://eprint.iacr.org/2026/013>. To appear at USENIX Security ’26.
- [CGG⁺20] Ran Canetti, Rosario Gennaro, Steven Goldfeder, Nikolaos Makriyannis, and Udi Peled. UC non-interactive, proactive, threshold ECDSA with identifiable aborts. In *Proc. ACM SIGSAC Conf. Computer and Communications Security (CCS)*, pages 1769–1787, 2020.
- [CLOS02] Ran Canetti, Yehuda Lindell, Rafail Ostrovsky, and Amit Sahai. Universally composable two-party and multi-party secure computation. In *Proc. 34th Annual ACM Symp. Theory of Computing (STOC)*, pages 494–503. ACM, 2002.
- [DKL⁺18] Léo Ducas, Eike Kiltz, Tancrede Lepoint, Vadim Lyubashevsky, Peter Schwabe, Gregor Seiler, and Damien Stehlé. CRYSTALS-Dilithium: Digital signatures from module lattices. *IACR Trans. Cryptogr. Hardw. Embed. Syst. (TCHES)*, 2018(1):238–268, 2018.
- [DKLS25] Antonín Dufka, Semjon Kravčenko, Peeter Laud, and Nikita Snetkov. Trilithium: Efficient and universally composable distributed ML-DSA signing. Cryptology ePrint Archive, Paper 2025/675, 2025. Available from World Wide Web: <https://eprint.iacr.org/2025/675>.
- [dPDE⁺23] Rafaël del Pino, Léo Ducas, Thomas Espitau, Alain Passelègue, Thomas Prest, Mélissa Rossi, Sina Schaeffler, and Gregor Seiler. Raccoon: A masking-friendly signature proven in the probing model. Cryptology ePrint Archive, Report 2023/989, 2023. Available from World Wide Web: <https://eprint.iacr.org/2023/989>.
- [dPEK⁺24] Rafaël del Pino, Thomas Espitau, Shuichi Katsumata, Mary Maller, Fabien Mouhartem, Thomas Prest, Mélissa Rossi, and Damien Stehlé. Raccoon: A masking-friendly signature proven in the probing model. In *Advances in Cryptology – CRYPTO 2024*, volume 14920 of *Lecture Notes in Computer Science*, pages 409–444. Springer, 2024.

- [dPN25] Rafaël del Pino and Sven Niot. Finally! a compact lattice-based threshold signature. In *Public-Key Cryptography – PKC 2025*, volume 15676 of *Lecture Notes in Computer Science*, pages 169–199. Springer, 2025.
- [DPSZ12] Ivan Damgård, Valerio Pastro, Nigel P. Smart, and Sarah Zakarias. Multi-party computation from somewhat homomorphic encryption. In *Advances in Cryptology – CRYPTO 2012*, volume 7417 of *Lecture Notes in Computer Science*, pages 643–662. Springer, 2012.
- [EGK⁺20] Daniel Escudero, Satrajit Ghosh, Marcel Keller, Rahul Rachuri, and Peter Scholl. Improved primitives for MPC over mixed arithmetic-binary circuits. In *Advances in Cryptology – CRYPTO 2020*, volume 12171 of *Lecture Notes in Computer Science*, pages 823–852. Springer, 2020.
- [ENP24] Thomas Espitau, Guilhem Niot, and Thomas Prest. Flood and submerge: Distributed key generation and robust threshold signature from lattices. In *Advances in Cryptology – CRYPTO 2024*, volume 14926 of *Lecture Notes in Computer Science*, pages 425–458. Springer, 2024.
- [Fel87] Paul Feldman. A practical scheme for non-interactive verifiable secret sharing. In *Proc. 28th Annual Symp. Foundations of Computer Science (FOCS)*, pages 427–437. IEEE, 1987.
- [GG18] Rosario Gennaro and Steven Goldfeder. Fast multiparty threshold ECDSA with fast trustless setup. In *Proc. ACM SIGSAC Conf. Computer and Communications Security (CCS)*, pages 1179–1194, 2018.
- [GJKR07] Rosario Gennaro, Stanisław Jarecki, Hugo Krawczyk, and Tal Rabin. Secure distributed key generation for discrete-log based cryptosystems. *J. Cryptology*, 20:51–83, 2007.
- [Kat07] Jonathan Katz. Universally composable multi-party computation using tamper-proof hardware. In *Advances in Cryptology – EUROCRYPT 2007*, volume 4515 of *Lecture Notes in Computer Science*, pages 115–128. Springer, 2007.
- [KG21] Chelsea Komlo and Ian Goldberg. FROST: Flexible round-optimized Schnorr threshold signatures. In *Selected Areas in Cryptography (SAC 2020)*, volume 12804 of *Lecture Notes in Computer Science*, pages 34–65. Springer, 2021.
- [KLS18] Eike Kiltz, Vadim Lyubashevsky, and Christian Schaffner. A concrete treatment of Fiat–Shamir signatures in the quantum random-oracle model. In *Advances in Cryptology – EUROCRYPT 2018*, volume 10822 of *Lecture Notes in Computer Science*, pages 552–586. Springer, 2018.
- [Lin21] Yehuda Lindell. Fast secure two-party ECDSA signing. *J. Cryptology*, 34(4):Art. 44, 2021.
- [LLZD25] Yingjie Lyu, Zengpeng Li, Hong-Sheng Zhou, and Xudong Deng. Threshold ECDSA in two rounds. In *Proc. ACM SIGSAC Conf. Computer and Communications Security (CCS)*, 2025.
- [LP07] Yehuda Lindell and Benny Pinkas. An efficient protocol for secure two-party computation in the presence of malicious adversaries. In *Advances in Cryptology – EUROCRYPT 2007*, volume 4515 of *Lecture Notes in Computer Science*, pages 52–78. Springer, 2007.

- [LPR10] Vadim Lyubashevsky, Chris Peikert, and Oded Regev. On ideal lattices and learning with errors over rings. In *Advances in Cryptology – EUROCRYPT 2010*, volume 6110 of *Lecture Notes in Computer Science*, pages 1–23. Springer, 2010.
- [LS15] Adeline Langlois and Damien Stehlé. Worst-case to average-case reductions for module lattices. *Designs, Codes and Cryptography*, 75(3):565–599, 2015.
- [Lyu12] Vadim Lyubashevsky. Lattice signatures without trapdoors. In *Advances in Cryptology – EUROCRYPT 2012*, volume 7237 of *Lecture Notes in Computer Science*, pages 738–755. Springer, 2012.
- [Nat24a] National Institute of Standards and Technology. FIPS PUB 203: Module-Lattice-Based Key-Encapsulation Mechanism Standard. Federal Information Processing Standards Publication FIPS PUB 203, National Institute of Standards and Technology (NIST), 2024. Available from World Wide Web: <https://csrc.nist.gov/pubs/fips/203/final>.
- [Nat24b] National Institute of Standards and Technology. FIPS PUB 204: Module-Lattice-Based Digital Signature Standard. Federal Information Processing Standards Publication FIPS PUB 204, National Institute of Standards and Technology (NIST), 2024. Available from World Wide Web: <https://csrc.nist.gov/pubs/fips/204/final>.
- [PS00] David Pointcheval and Jacques Stern. Security arguments for digital signatures and blind signatures. *J. Cryptology*, 13(3):361–396, 2000.
- [PVW08] Chris Peikert, Vinod Vaikuntanathan, and Brent Waters. A framework for efficient and composable oblivious transfer. In *Advances in Cryptology – CRYPTO 2008*, volume 5157 of *Lecture Notes in Computer Science*, pages 554–571. Springer, 2008.
- [Reg09] Oded Regev. On lattices, learning with errors, random linear codes, and cryptography. *J. ACM*, 56(6):1–40, 2009.
- [Sha79] Adi Shamir. How to share a secret. *Commun. ACM*, 22(11):612–613, 1979.
- [SLS⁺22] Manu Sporny, Dave Longley, Markus Sabadello, Drummond Reed, Ori Steele, and Christopher Allen. Decentralized identifiers (DIDs) v1.0. W3c recommendation, World Wide Web Consortium, 2022. Available from World Wide Web: <https://www.w3.org/TR/did-core/>.
- [Yao86] Andrew Chi-Chih Yao. How to generate and exchange secrets. In *Proc. 27th Annual Symp. Foundations of Computer Science (FOCS)*, pages 162–167. IEEE, 1986.